



Cite this: DOI: 10.1039/d6sc00384b

# Engineering porous organic polymers for enhanced CO<sub>2</sub> capture: from synthesis to implementation

Mohammed G. Kotp and Shiao-Wei Kuo \*

The escalating concentration of atmospheric carbon dioxide (CO<sub>2</sub>) necessitates the development of efficient and scalable carbon capture technologies. Porous organic polymers (POPs) have emerged as a leading class of solid-state adsorbents, offering an exceptional combination of high surface area, tuneable porosity, and robust chemical stability. This review provides a comprehensive analysis of the engineering of POPs for enhanced CO<sub>2</sub> capture, traversing the journey from molecular design to implementation. We show the fundamental characteristics of POPs, including their classification and unique structure–property relationships that govern adsorption performance. The core of the review critically examines diverse synthetic strategies for creating POPs, with a focus on tailoring pore architecture and chemical functionality—such as amine incorporation and heteroatom doping—to optimize CO<sub>2</sub> capacity, selectivity, and regeneration kinetics. We further assess the performance of POPs under realistic conditions, analysing the critical impact of humidity, co-adsorbates, and long-term cycling on their practical viability. The economic and environmental prospects of POP-based capture are evaluated through techno-economic assessments. Finally, we highlight emerging trends of multi-functional POPs, and outline a roadmap for future research. The review concludes that while challenges in scalability and cost remain, POPs hold immense promise as next-generation adsorbents, with the potential to play a pivotal role in achieving a sustainable and net-zero future.

Received 14th January 2026  
Accepted 5th April 2026

DOI: 10.1039/d6sc00384b

rsc.li/chemical-science

Department of Materials and Optoelectronic Science, Center for Functional Polymers and Supramolecular Materials, National Sun Yat-sen University, Kaohsiung 804, Taiwan. E-mail: kuosw@faculty.nsysu.edu.tw



Mohammed G. Kotp

Mohammed Gamal Kotp earned his PhD in Chemical Engineering from National Sun Yat-sen University, Taiwan, in 2024. He previously obtained his MSc degree in 2017 and his BSc degree in 2012 in Chemistry from Tanta University, Egypt. His research centers on the design, synthesis, and functionalization of porous polymers and nanocomposites for applications in energy storage, environmental remediation, and chemical

sensing. Between 2018 and 2020, he held academic and research appointments at Kuwait University and the American International University (Kuwait). He early conducted postdoctoral research under the support of the National Science and Technology Council (Taiwan). He is currently a Postdoctoral Fellow at the Interdisciplinary Research Center for Advanced Materials (ARC-AM), King Fahd University of Petroleum & Minerals (Saudi Arabia). Before pursuing an academic career, he acquired industrial experience in polyamide dyeing and polyurethane foam manufacturing from 2012 to 2018.



Shiao-Wei Kuo

Shiao-Wei Kuo received his PhD in applied chemistry from National Chiao Tung University in Taiwan (2002). He continued his research work at Chiao Tung University as a postdoctoral researcher during 2002–2007 and also worked at the University of Akron as a postdoctoral researcher during 2005–2006. In 2007, he became an assistant professor in the Department of Materials and Optoelectronic Science, National Sun Yat-sen

University, Taiwan. In 2022, he became a chair professor at National Sun Yat-sen University, Taiwan. His research interests include polymer interactions, mesoporous materials, POSS nanocomposites, polybenzoxazine, and porous organic polymers.



# 1 Introduction

The relentless increase in atmospheric carbon dioxide (CO<sub>2</sub>) concentration, primarily driven by anthropogenic fossil fuel combustion, represents one of the most pressing challenges of our time.<sup>1–3</sup> This accumulation of CO<sub>2</sub> is the principal driver of global climate change, manifesting in rising global temperatures, ocean acidification, and an increased frequency of extreme weather events.<sup>4</sup> The urgency of this crisis is underscored by international efforts, such as the Paris Agreement, which aim to limit global warming to well below 2 °C above pre-industrial levels.<sup>5–7</sup> Achieving this ambitious goal necessitates a multi-pronged strategy that not only transitions to renewable energy sources but also actively deploys technologies for carbon capture, utilization, and storage (CCUS). Notably, beyond its role as a greenhouse gas, CO<sub>2</sub> has emerged as a valuable C1 building block for polymerization and advanced materials development. Within this framework, developing efficient and scalable methods for capturing CO<sub>2</sub> from point sources like flue gas, or directly from the atmosphere, is a critical scientific and engineering imperative to mitigate the most severe consequences of climate change and ensure a sustainable future.<sup>8</sup> In response to this urgent need, a portfolio of carbon capture technologies has been developed, primarily categorized by their separation mechanism.<sup>9</sup> The current benchmark, aqueous amine scrubbing, relies on chemisorption where amines react with CO<sub>2</sub> to form carbamates.<sup>10</sup> While effective, this process is energy-intensive, requiring high temperatures for sorbent regeneration, and suffers from solvent corrosion and degradation.<sup>11</sup> Alternative approaches, such as cryogenic distillation and membrane separation, offer different trade-offs between selectivity and energy demand.<sup>12</sup> This landscape has thus spurred intensive research into solid adsorbents as a promising alternative, with materials like zeolites, metal–organic frameworks (MOFs), and activated carbons being widely investigated.<sup>13</sup> These materials primarily operate through physisorption, which generally offers lower regeneration energies. However, challenges remain in balancing capacity, selectivity, stability, and cost-effectiveness, driving the search for next-generation materials with tailored properties.

Amidst the search for advanced solid adsorbents, porous organic polymers (POPs) have emerged as a particularly promising class of materials to address the limitations of existing technologies.<sup>14–28</sup> POPs are a diverse family of covalently linked amorphous or semi-crystalline frameworks that boast an exceptional degree of synthetic tunability (Fig. 1) including covalent triazine frameworks (CTFs), conjugated microporous polymers (CMPs), hyper-crosslinked polymers (HCPs), covalent organic frameworks (COFs), polyaromatic frameworks (PAFs), and polymers of intrinsic microporosity (PIMs).

Most critically, this allows for the precise engineering of their pore architecture, surface area, and chemical functionality to enhance CO<sub>2</sub> affinity and selectivity. Unlike many benchmark materials, POPs are typically composed of lightweight, robust elements (*e.g.*, C, H, N, O, and B), granting them high physicochemical stability and low regeneration energy requirements.

Their fully organic nature also often confers superior hydrothermal stability compared to MOFs, a crucial advantage for processing humid flue gases.<sup>29,30</sup> Clearly, while MOFs offer high crystallinity and tunable coordination environments, their performance can be limited under humid conditions due to moisture sensitivity and, in some cases, potential metal leaching. Zeolites exhibit excellent thermal and mechanical stability; however, their rigid inorganic frameworks restrict structural tunability and functional diversity. Activated carbons are economically attractive but generally lack precise control over pore architecture and surface chemistry. In contrast, POPs combine high chemical and thermal stability with metal-free, purely covalent frameworks that allow extensive synthetic flexibility. Their modular design enables controlled pore engineering and heteroatom functionalization to enhance CO<sub>2</sub> affinity while maintaining structural robustness. These advantages make POPs particularly promising candidates for adsorption-based CO<sub>2</sub> capture under a wide range of operating conditions.

Capitalizing on the immense design versatility of POPs outlined above, this review provides a comprehensive and forward-looking analysis of the engineering evolution of POPs for efficient CO<sub>2</sub> capture, bridging molecular-level design with practical implementation. Unlike previous reviews that primarily summarize material performance, this work integrates synthetic strategies, pore environment engineering, and binding-site modulation into a unified structure–property–application framework. We systematically elucidate the fundamental design principles and synthetic methodologies used to construct POPs with tailored porosity and enhanced CO<sub>2</sub> affinity.

Beyond evaluating CO<sub>2</sub> adsorption capacities across different POP families, we critically analyse structure–property relationships and adsorption mechanisms to extract generalizable design guidelines. Importantly, while several excellent reviews have recently examined POPs for CO<sub>2</sub> capture—focusing on synthetic methodologies, individual POP subclasses, or performance metrics—a comprehensive framework that systematically connects molecular design principles with practical implementation challenges remains lacking. This review addresses this gap by uniquely integrating three critical dimensions: (i) the relationship between synthetic strategies and pore engineering outcomes across major POP families (CMPs, COFs, CTFs, and HCPs); (ii) the derivation of generalizable structure–function correlations that guide the rational design of high-performance adsorbents; and (iii) an in-depth analysis of real-world deployment factors—including stability under realistic conditions, shaping and pelletization, mechanical integrity, technological feasibility, and Technology Readiness Level (TRL) positioning. By bridging fundamental materials chemistry with engineering considerations, this review provides a holistic roadmap for advancing POPs from laboratory discoveries toward scalable carbon capture technologies. Furthermore, we assess the suitability of POPs across various capture scenarios (post-combustion, pre-combustion, and direct air capture (DAC)) and identify the key scientific and engineering challenges that must



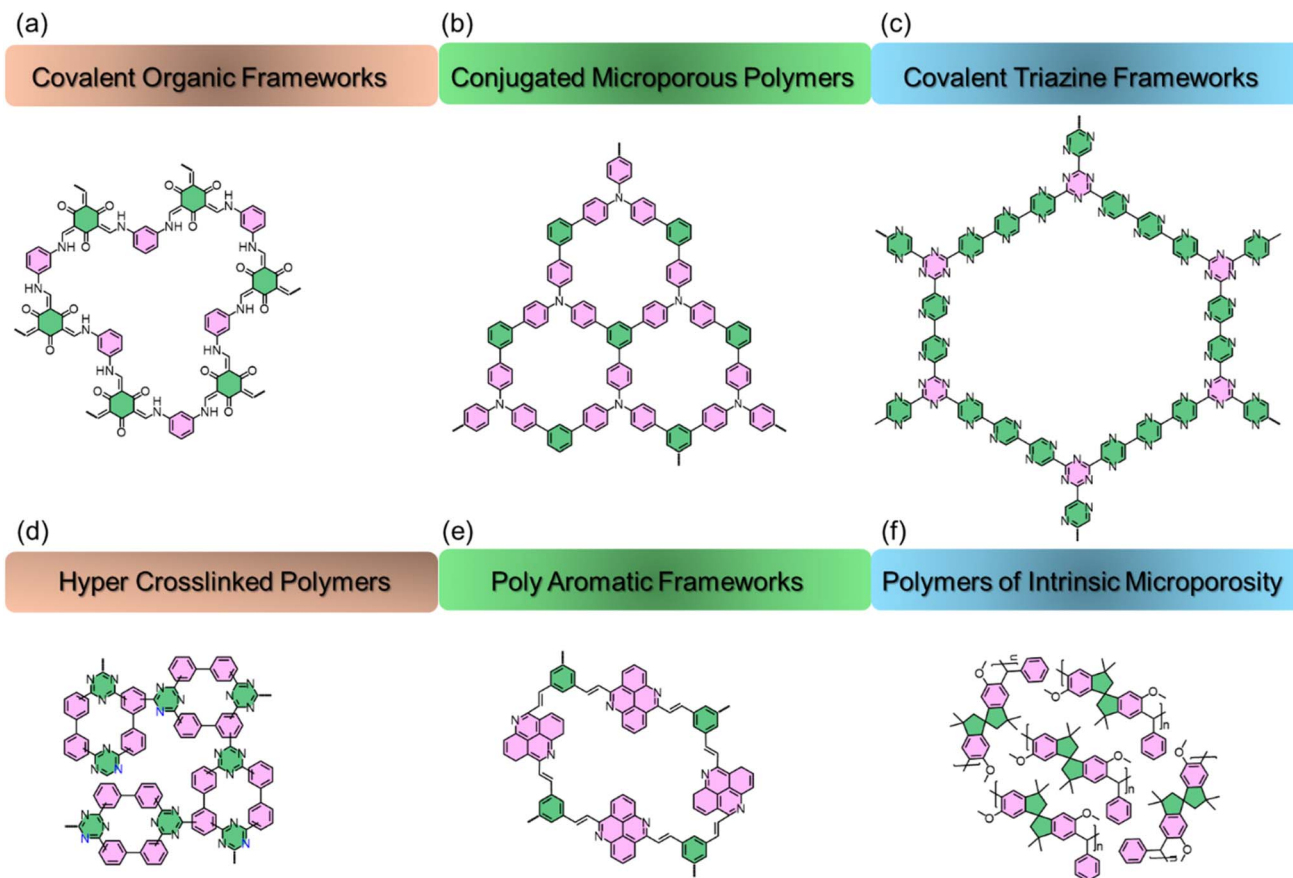


Fig. 1 Representative molecular architectures and structural motifs of porous organic polymers (POPs) including (a) covalent organic frameworks (COFs), (b) conjugated microporous polymers (CMPs), (c) covalent triazine frameworks (CTFs), (d) hyper-crosslinked polymers (HCPs), (e) polyaromatic frameworks (PAFs), and (f) polymers of intrinsic microporosity (PIMs) for CO<sub>2</sub> capture.

be overcome to translate laboratory advances into real-world carbon capture technologies.

By combining molecular insight with application-oriented evaluation, this review aims to provide a strategic roadmap for the rational design and industrial advancement of next-generation POP-based CO<sub>2</sub> adsorbents.

## 2 Implementation contexts for CO<sub>2</sub> capture

POPs can be strategically engineered for CO<sub>2</sub> capture implementation in various contexts including post-combustion, pre-combustion, and DAC, as shown in Fig. 2. In pre-combustion capture from high-pressure syngas (H<sub>2</sub>-rich streams), the focus shifts to POPs with high volumetric surface area and robust frameworks to maximize CO<sub>2</sub> uptake through physisorption.<sup>31</sup> For the challenging task of DAC, where CO<sub>2</sub> concentrations are extremely dilute, POPs require ultra-strong chemisorption sites, such as alkylamines, to effectively bind CO<sub>2</sub> molecules from the atmosphere, while maintaining stability for repeated capture-release cycles.<sup>32–34</sup> Notably, for post-combustion capture from flue gas (N<sub>2</sub>-rich streams), POPs are designed with high CO<sub>2</sub>/N<sub>2</sub> selectivity, often achieved by incorporating nitrogen-containing groups like amines for

chemisorption or tuning pore sizes for enhanced physisorption.<sup>35,36</sup>

### 2.1 Pre-combustion capture

Pre-combustion capture occurs upstream of combustion, targeting a high-pressure synthesis gas (“syngas”) produced from the gasification of fossil fuels or biomass.<sup>37,38</sup> This stream presents a distinct separation challenge, containing a high concentration of CO<sub>2</sub> (typically 15–60%) mixed with a valuable H<sub>2</sub> product, all under significantly elevated pressures (Fig. 2(a)).<sup>39,40</sup> In the pre-combustion capture scenario, the role of POPs shifts towards maximizing performance under high-pressure conditions.<sup>41,42</sup> The critical properties become a combination of high CO<sub>2</sub>/H<sub>2</sub> selectivity and high working capacity. Selectivity is essential to ensure the purification of the valuable H<sub>2</sub> fuel stream by efficiently separating out CO<sub>2</sub>. Simultaneously, the material must possess a high working capacity to make the process efficient and economically viable. The focus is on designing POPs that can capture a significant mass of CO<sub>2</sub> directly from the high-pressure syngas mixture, leveraging the elevated partial pressure of CO<sub>2</sub> to drive high uptake within the polymer’s pores.

Under the high-pressure conditions characteristic of pre-combustion streams, the adsorption mechanism in POPs



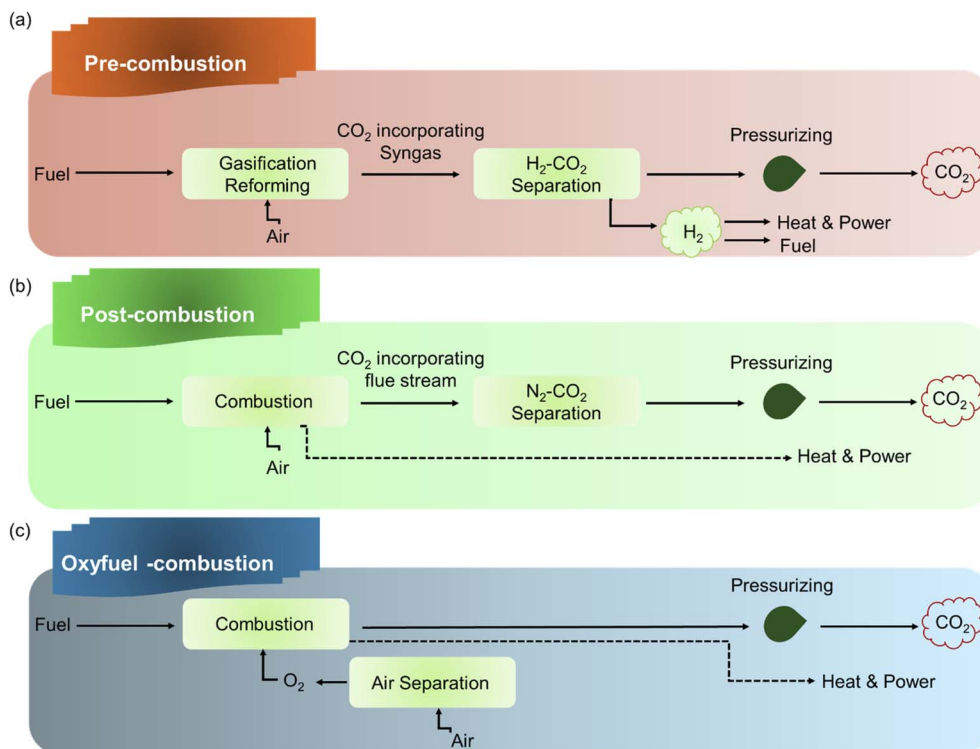


Fig. 2 Different approaches used for CO<sub>2</sub> capture including (a) pre-combustion capture, (b) post-combustion capture, and (c) oxy-fuel combustion.

relies predominantly on physisorption.<sup>43</sup> The elevated CO<sub>2</sub> partial pressure favours this type of interaction, as it drives a large amount of gas into the pores. Consequently, the design goal for POPs in this application is twofold: (i) to achieve a high volumetric surface area to create ample space for gas confinement and (ii) to incorporate a high density of CO<sub>2</sub>-philic sites (such as polar functional groups) within the pores. This synergistic design maximizes the working capacity by ensuring that a significant volume of CO<sub>2</sub> can be captured per cycle through enhanced van der Waals and dipole-quadrupole interactions, while still allowing for relatively low-energy regeneration. A defining advantage of POPs in pre-combustion capture is their inherent robustness under harsh operational conditions.<sup>44</sup> The syngas environment is often at high pressure and can contain significant moisture, which can degrade less stable materials.<sup>45</sup> The extensive covalent bonds forming the backbone of POPs grant them exceptional thermal and mechanical stability, allowing them to withstand high-pressure cycling without structural collapse.<sup>46</sup> Furthermore, many classes of POPs demonstrate remarkable hydrothermal stability, resisting degradation in the presence of water vapor.<sup>47,48</sup> This durability ensures a long operational lifespan and consistent performance, which is a critical advantage over other adsorbents that may swell, decompose, or lose activity under similar demanding conditions.

## 2.2 Post-combustion capture

Post-combustion capture targets the removal of CO<sub>2</sub> from flue gas, the exhaust produced by burning fossil fuels in power

plants and industrial facilities.<sup>49,50</sup> This gas stream is primarily composed of N<sub>2</sub> and contains a relatively dilute concentration of CO<sub>2</sub> at near-ambient pressure and temperature (Fig. 2(b)).<sup>51</sup> The central role of POPs in post-combustion capture is to function as molecular sieves that preferentially adsorb CO<sub>2</sub> over N<sub>2</sub>.<sup>52</sup> Given the massive abundance of N<sub>2</sub> in the flue gas, the most critical performance metric is high CO<sub>2</sub>/N<sub>2</sub> selectivity. POPs are therefore strategically engineered to exhibit a strong thermodynamic affinity for CO<sub>2</sub> molecules, ensuring selective capture from the mixed gas stream.<sup>53</sup> Actually, this high CO<sub>2</sub>/N<sub>2</sub> selectivity is achieved through two primary adsorption mechanisms, which can be engineered independently or synergistically within the POP framework.<sup>54,55</sup> Physisorption relies on weak van der Waals forces. It is optimized by designing POPs with precise ultra-microporosity, where pore diameters are tuned to be less than 1 nm. At this scale, pores closely fit the kinetic diameter of the CO<sub>2</sub> molecule, creating a confined environment that significantly enhances the physical interaction energy between the pore wall and CO<sub>2</sub>, leading to selective adsorption.<sup>56–58</sup> On the other hand, chemisorption involves a stronger, more specific chemical reaction. It is facilitated by the strategic incorporation of nitrogen-rich functional groups such as amines, azo groups, and triazine rings into the polymer backbone or as pendant groups.<sup>59,60</sup> These nitrogen sites act as Lewis bases, which directly and reversibly chemisorb the acidic CO<sub>2</sub> molecule.<sup>61</sup> This creates a much stronger binding affinity than physisorption, dramatically increasing selectivity, particularly under low-concentration conditions. A pivotal advantage of POPs in post-combustion capture lies in their robust material



properties, which offer significant practical benefits over conventional liquid amine scrubbers.<sup>62</sup> As solid adsorbents, POPs circumvent critical operational drawbacks associated with amine solutions, such as solvent evaporation, equipment corrosion, and solvent degradation.<sup>63</sup> Furthermore, the covalent bonds within the porous polymer framework provide high thermal and chemical stability, allowing them to withstand the demanding conditions of capture and regeneration cycles.<sup>64,65</sup> This intrinsic stability, combined with the typically lower binding energy of physisorptive POPs, often leads to a substantially lower energy for regeneration, directly addressing one of the primary economic and efficiency challenges in large-scale carbon capture.<sup>66</sup>

### 2.3 Oxy-fuel combustion

The oxy-fuel combustion protocol represents a distinct pre-combustion strategy where the primary separation involves oxygen rather than CO<sub>2</sub>.<sup>67</sup> In this process, fossil fuels are burned in a mixture of high-purity oxygen and recycled flue gas, rather than air. This eliminates the large volume of nitrogen from the system, resulting in a flue gas stream that is primarily composed of CO<sub>2</sub> and water vapor, which are easily separated by condensation. The central challenge, therefore, shifts to the energy-intensive air separation step to produce the required pure oxygen (Fig. 2(c)). While the application of POPs in oxy-fuel combustion is less explored than in other capture scenarios, their potential role is significant. POPs can be engineered as high-performance O<sub>2</sub>/N<sub>2</sub> adsorbents for oxygen production.<sup>68</sup> The focus here is on designing frameworks with ultra-high O<sub>2</sub>/N<sub>2</sub> selectivity, potentially leveraging the paramagnetic nature of O<sub>2</sub> to enhance separation from diamagnetic N<sub>2</sub>. By enabling more efficient, lower-energy air separation units, POPs could directly address the major cost and efficiency bottleneck of the oxy-fuel process, facilitating the generation of the high-purity CO<sub>2</sub> stream that is its ultimate goal.<sup>69</sup>

### 2.4 CH<sub>4</sub> purification (natural gas/biogas upgrading)

Beyond flue gas treatments, POPs demonstrate significant utility in the critical energy-related process of methane (CH<sub>4</sub>) purification, often referred to as natural gas or biogas upgrading. Raw natural gas and biogas extracted from landfills or anaerobic digesters contain CO<sub>2</sub> as a primary impurity, which reduces the fuel's energy density and promotes pipeline corrosion. The separation challenge here involves isolating CO<sub>2</sub> from a mixture where CH<sub>4</sub> is the valuable product, a task complicated by the similar kinetic diameters and non-polar nature of the two molecules. In this scenario, the role of POPs is to act as highly selective sieves for CO<sub>2</sub>/CH<sub>4</sub> separation. The key properties are high CO<sub>2</sub>/CH<sub>4</sub> selectivity and high CO<sub>2</sub> working capacity, often at medium to high pressures. This selectivity is engineered by leveraging the differences in molecular properties; CO<sub>2</sub> has a significant quadrupole moment and higher polarizability compared to the more inert CH<sub>4</sub>. POPs can be designed with ultra-microporous pores that preferentially interact with the CO<sub>2</sub> molecule through enhanced van der Waals forces or by incorporating polar functional groups (*e.g.*, nitrogen sites or

oxygen groups) that engage in dipole–quadrupole interactions with CO<sub>2</sub>.<sup>56,70</sup> By selectively removing CO<sub>2</sub>, POPs facilitate the production of high-purity, pipeline-quality methane, enhancing fuel efficiency and reducing greenhouse gas emissions from fuel sources.

### 2.5 DAC

DAC represents the most thermodynamically challenging carbon capture methodology. It involves adsorbing CO<sub>2</sub> directly from the ambient atmosphere, where it is present at an extremely dilute concentration of approximately 400 ppm. This ultra-dilute nature is the fundamental source of the challenge. This translates to a very low partial pressure of CO<sub>2</sub> (around 0.04 kPa), which significantly reduces the driving force for adsorption compared to flue gas streams (where CO<sub>2</sub> partial pressure can be 100–1000 times higher). Consequently, the primary hurdle in DAC is not just the capacity to hold CO<sub>2</sub>, but the affinity required to selectively bind these scarce molecules against a vast background of nitrogen, oxygen, and water vapor.<sup>71</sup> This demands sorbents with exceptionally strong and selective binding sites that can effectively capture CO<sub>2</sub> at this minimal concentration.<sup>72</sup> Furthermore, the energy input required to release the captured CO<sub>2</sub> and regenerate the sorbent is intrinsically tied to the strength of this initial binding, creating a critical trade-off between capture efficiency and regeneration cost that is far more acute in DAC than in any other capture technology. Actually, the paramount requirement for POPs in DAC is an ultra-high affinity for CO<sub>2</sub>. The exceptionally low partial pressure of CO<sub>2</sub> in ambient air (~0.04 kPa) provides a minimal driving force for adsorption, rendering conventional physisorption—which relies on weak van der Waals forces—largely ineffective for the initial capture step. At such extreme dilution, the interaction energy provided by physisorption is often insufficient to overcome the entropy penalty of confining a single CO<sub>2</sub> molecule from a vast reservoir of air.<sup>73</sup>

Therefore, POPs engineered for DAC must be functionalized to facilitate strong chemisorption. This is typically achieved by incorporating strong Lewis base sites, such as primary or secondary amines (–NH<sub>2</sub> or –NH), into the porous framework.<sup>74</sup> These amine groups react reversibly with CO<sub>2</sub> to form stable carbamate or bicarbonate species, a chemical reaction that provides the substantial binding energy required to selectively “trap” CO<sub>2</sub> molecules even when they are vastly outnumbered by other gases. This chemisorptive mechanism is non-negotiable for achieving meaningful CO<sub>2</sub> uptake from the atmosphere, as it creates a sufficiently deep energy well to overcome the thermodynamic limitations of the ultra-dilute source. The central challenge in designing POPs for DAC lies in resolving a fundamental thermodynamic contradiction: the material must possess ultra-high affinity to effectively capture CO<sub>2</sub> at trace concentrations, yet it must also allow for low-energy regeneration to release the purified CO<sub>2</sub> and recycle the sorbent. This creates a critical trade-off, as the strong chemisorptive bonds (*e.g.*, carbamate formation) necessary for efficient capture from air typically require significant energy input—often in the form



of high-temperature steam or vacuum—to break, thereby increasing the overall cost and energy penalty of the process. Consequently, the focus of studies is on creating smart POPs that strike a delicate balance. The objective is to engineer binding sites that are strong enough to sequester CO<sub>2</sub> from a 400 ppm source, but weak enough to facilitate release under relatively mild conditions. This involves sophisticated molecular design, such as tuning the alkalinity of amine groups, incorporating cooperative binding effects, or creating humidity-swing mechanisms that use moisture instead of heat to trigger CO<sub>2</sub> release. Furthermore, exceptional hydrolytic stability is non-negotiable, as the POPs will be continuously exposed to ambient humidity, which can degrade many organic functional groups and lead to significant performance loss over time. The ideal DAC sorbent is thus a stable, precisely tuned platform where binding strength is optimized not for maximum capture alone, but for the optimal balance between capture efficiency and regeneration economics.

### 3 Fundamental concepts and metrics in carbon capture

To critically evaluate the performance of POPs for CO<sub>2</sub> capture, it is essential to understand the key metrics and terminologies used in the field.

#### 3.1 Surface area, porosity, and CO<sub>2</sub> capacity

**3.1.1 Surface area.** Typically measured using the Brunauer–Emmett–Teller (BET) method from nitrogen adsorption isotherms at 77 K, this parameter (expressed in m<sup>2</sup> g<sup>-1</sup>) quantifies the total accessible area of a material. A high surface area is generally desirable as it provides more sites for gas molecules to adsorb.<sup>75,76</sup>

**3.1.2 Porosity.** This refers to the pore structure of the material, encompassing pore volume and pore size distribution. Pores classified as micropores (<2 nm) are crucial for CO<sub>2</sub> capture at low pressures, as the proximity of pore walls creates strong adsorption potentials. On the other hand, mesopores (2–50 nm) facilitate gas transport but contribute less to low-pressure uptake. Finally, macropores (>50 nm) act primarily as diffusion pathways.

**3.1.3 CO<sub>2</sub> capacity.** CO<sub>2</sub> capacity is the amount of CO<sub>2</sub> adsorbed by the material under specific conditions of pressure and temperature, usually reported in mmol g<sup>-1</sup> or cm<sup>3</sup> g<sup>-1</sup> (at STP). It is directly measured from CO<sub>2</sub> adsorption isotherms. The working capacity, defined as the difference in uptake between adsorption and desorption conditions, is a more practical metric for cyclic processes.

#### 3.2 Enthalpy of adsorption ( $\Delta H_{\text{ads}}$ or $Q_{\text{st}}$ )

$Q_{\text{st}}$  is a critical thermodynamic parameter that describes the strength of the interaction between the CO<sub>2</sub> molecule and the adsorbent surface. It is a measure of the heat released during adsorption. Lower  $\Delta H_{\text{ads}}$  (typically 20–40 kJ mol<sup>-1</sup>) suggests physisorption, dominated by weak van der Waals forces. This is advantageous for low-energy regeneration but may result in low

selectivity and capacity under dilute conditions.<sup>77</sup> Higher  $\Delta H_{\text{ads}}$  (typically 50–100 kJ mol<sup>-1</sup>) indicates chemisorption, involving strong covalent or ionic bonds (*e.g.*, with amine groups). While this provides high selectivity and capacity at low CO<sub>2</sub> concentrations, it necessitates higher energy input for sorbent regeneration.<sup>78</sup>

#### 3.3 Selectivity

Selectivity quantifies the ability of an adsorbent to preferentially capture one gas (CO<sub>2</sub>) over another (*e.g.*, N<sub>2</sub> or CH<sub>4</sub>).

**3.3.1 Henry's law selectivity.** This is the ratio of Henry's constants ( $K_{\text{H}}$ ) for different gases, calculated from the initial, linear region of the low-pressure adsorption isotherm. It reflects the intrinsic affinity of the adsorbent for one gas over another in an ideal and dilute system.<sup>79</sup>

**3.3.2 The ideal adsorbed solution theory (IAST) selectivity.** IAST is a more rigorous and widely used method for predicting mixture adsorption from single-component isotherms. IAST selectivity accounts for competitive adsorption at higher loadings and pressures, providing a more realistic performance metric for actual operating conditions than the Henry model.<sup>80</sup>

#### 3.4 Recyclability and stability

Mostly, for any CO<sub>2</sub> adsorbent to be viable for industrial applications, it must demonstrate long-term recyclability and stability.<sup>81,82</sup> This is evaluated through multiple adsorption–desorption cycles, where the material is exposed to repeated capture and regeneration conditions. First, recyclability is confirmed if the CO<sub>2</sub> capacity remains high over numerous cycles (*e.g.*, >10–20 cycles with minimal loss). Furthermore, the material must exhibit sufficient thermal stability to withstand regeneration temperatures, as well as chemical stability against moisture, acidic gases (SO<sub>x</sub> and NO<sub>x</sub>), and other flue gas contaminants. These properties are essential for maintaining performance over numerous adsorption–desorption cycles, rendering the material robust and economically viable.

## 4 Evolution of POPs for carbon dioxide capture

The quest for efficient carbon capture has driven the exploration and development of a wide array of porous materials, each with distinct advantages and limitations. The journey often begins with traditional adsorbents, such as zeolites and activated carbons, which primarily rely on physisorption. Zeolites, with their highly ordered, ionic structures, offer high initial CO<sub>2</sub> uptake and selectivity under dry conditions but suffer from significant sensitivity to moisture and high regeneration energy.<sup>9,83–85</sup> Activated carbons, prized for their high surface area, low cost, and hydrophobicity, typically exhibit lower CO<sub>2</sub> selectivity due to their broad pore size distribution.<sup>86–88</sup> The landscape advanced with the rise of MOFs. These materials represented a paradigm shift due to their extraordinary surface areas, unparalleled tunability, and precise pore chemistry.<sup>89–91</sup> MOFs demonstrated record-breaking CO<sub>2</sub> capacities, particularly under high-pressure conditions, and their structures could



be post-synthetically modified with amines to enhance selectivity.<sup>92,93</sup> However, challenges related to their hydrothermal stability, the cost of metal precursors, and long-term degradation under real flue gas conditions have prompted the search for more robust alternatives.

This pursuit has firmly established POPs as a leading-edge class of materials in the carbon capture field. POPs uniquely combine the high surface areas and tunability of MOFs with the robust stability of traditional carbon-based materials.<sup>94–96</sup> Constructed entirely from strong covalent bonds between light organic elements, they exhibit exceptional thermal and chemical stability, resisting moisture and corrosive environments.<sup>97</sup> Their purely organic nature allows for unparalleled synthetic design, enabling the precise incorporation of CO<sub>2</sub>-philic functional groups—such as amines, azo groups, or triazines—directly into the polymer backbone.<sup>98</sup> This synergy of permanent porosity, structural resilience, and molecular-level design freedom positions POPs as a versatile and highly promising platform, capable of being engineered for the specific demands of post-combustion, pre-combustion, and DAC scenarios.

#### 4.1 Fundamentals of POPs

Basically, POPs are a class of advanced materials characterized by rigid, covalently linked organic subunits that create a permanent and well-defined network of pores.<sup>75,99</sup> Their defining feature is their composition, being constructed solely from light, non-metallic elements (*e.g.*, C, H, O, N, and S), which results in high thermal and chemical stability.<sup>64,65,100–103</sup> POPs are primarily classified based on the nature of their chemical bonds and synthesis strategies. The main categories include HCPs, which feature extensive covalent linkages; PIMs, which have rigid and contorted backbones that cannot pack efficiently; COFs, which are highly crystalline structures with ordered pores; and CMPs, which incorporate  $\pi$ -conjugated electronic structures.<sup>104</sup> This diversity in bonding and structure allows for precise tuning of their physical and chemical properties for specific applications like CO<sub>2</sub> capture.<sup>17</sup>

**4.1.1 COFs.** COFs represent a pinnacle of structural precision in the domain of POPs. They are distinguished by their highly crystalline, two-dimensional (2D) or three-dimensional (3D) porous structures, which are formed through reversible covalent bond formation between pre-designed organic building blocks.<sup>105–108</sup> This synthetic approach, often involving condensation reactions under thermodynamic control, allows for the error-correction necessary to form long-range ordered frameworks.<sup>109</sup> The defining characteristic of COFs is their pre-designable and uniform pore architecture. By carefully selecting the geometry and connectivity of symmetric molecular linkers (*e.g.*, boronic acids, aldehydes, and amines), researchers can engineer COFs with precise pore size, shape, and periodicity. This results in moieties with exceptionally high surface areas and well-defined, permanent porosity.<sup>110</sup> For CO<sub>2</sub> capture, this crystallinity and tunability offer unique advantages. The ordered pore channels can be functionalized with atomic-level precision to incorporate specific binding sites, enhancing CO<sub>2</sub> affinity and selectivity. Jiang *et al.*<sup>111</sup> demonstrated how the

intrinsic crystallinity and structural regularity of COFs can be strategically exploited to enhance CO<sub>2</sub> capture performance. By utilizing an ion-exchange approach, facilitated-transport carriers were uniformly distributed within a cationic COF membrane—overcoming the major limitation of conventional, disordered membrane materials where carrier distribution is difficult to control. The ordered pore channels of the COF, combined with their tunable chemistry, provide precise and predictable locations for carrier incorporation, enabling stronger CO<sub>2</sub> affinity and improved selective transport pathways. Furthermore, the incorporation of a small amount of graphene oxide effectively eliminated inter-sheet defects, resulting in ultrathin, defect-free membranes. Together, these structural advantages synergistically enhanced both diffusion-selective and facilitated-transport mechanisms, resulting in high CO<sub>2</sub> permeance and excellent CO<sub>2</sub>/CH<sub>4</sub> selectivity. These findings highlight the unique advantages of crystalline, atomically tunable porous frameworks and emphasize their potential as next-generation platforms for highly efficient CO<sub>2</sub> separation and related gas purification technologies (Fig. 3).

Very recently, by introducing mesoporous silica templates, Kao *et al.*<sup>112</sup> successfully produced COFs with markedly improved pore ordering, higher surface areas, and more defined channel architectures. These ordered pore systems facilitated more efficient molecular diffusion while enabling precise spatial arrangement of functional groups, ultimately resulting in higher CO<sub>2</sub> uptake (3.46 mmol g<sup>-1</sup> at 273 K) compared to non-templated analogues. This directly supports the idea that COFs with well-defined, crystalline pore channels provide a platform for atomic-level tenability, allowing targeted incorporation of binding sites that strengthen CO<sub>2</sub> interactions and improve selectivity. The superior performance of the templated COFs in CO<sub>2</sub> adsorption demonstrates how structural regularity and controllable pore environments amplify adsorption efficiency, aligning with the central claim of this review that ordered and tuneable COF architectures offer unique advantages for high-performance CO<sub>2</sub> capture applications as displayed in Fig. 4.

Furthermore, the combination of high surface area for substantial physisorption capacity and the ability to integrate Lewis basic sites (like nitrogen-rich triazine or imine linkages) directly into the scaffold walls makes COFs compelling candidates for creating highly efficient and selective adsorbents. Their robust covalent bonds, typically boroxine, imine, or triazine linkages, further ensure the thermal and chemical stability required for cyclic capture and regeneration processes. Yu and his group demonstrated that amine-functionalized TaTp-COF achieves exceptional CO<sub>2</sub> capture performance by combining high surface area with uniformly distributed secondary amines formed *via* enol-to-ketoamine tautomerization. The material shows strong CO<sub>2</sub> binding, high CO<sub>2</sub>/N<sub>2</sub> selectivity, and excellent stability even under low-concentration flue-gas conditions, confirming the power of integrating Lewis basic sites directly into a porous COF framework. Their results support our claim that merging large physisorption capacity with built-in nitrogen-rich functionalities yields highly efficient and selective CO<sub>2</sub> adsorbents (Fig. 5).<sup>113</sup>



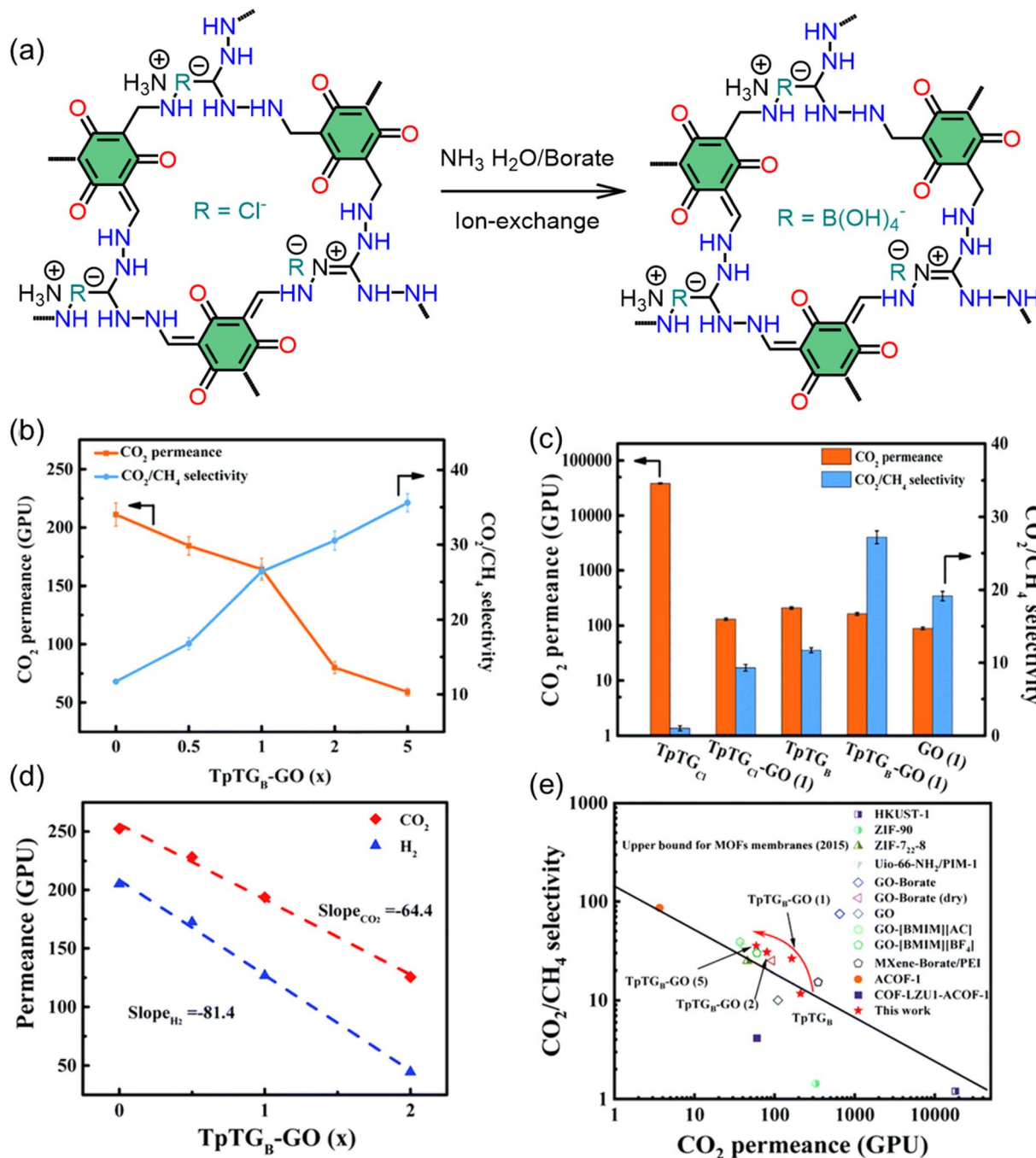


Fig. 3 (a) Synthetic route for TpTGCl and its conversion to TpTGB via ion exchange, (b) gas separation records for TpTGB-GO membranes, (c) TpTGB-GO (1) versus control membranes, (d) linear fit showing the relationship between gas permeance and GO content, and (e) comparison of this work's membrane performance with notable 2D and framework membranes.<sup>111</sup> Adapted with authorization of the Royal Society of Chemistry.

Our assertion that COFs provide a versatile platform for designing selective adsorbents is strongly supported by recent foundational work from the recent Nobel Prize winner Yaghi and colleagues, which also delineates a critical path for optimization.<sup>114</sup> In a seminal study combining advanced simulations and experiments on amine-functionalized COF-999-NH<sub>2</sub>, they confirmed the platform's designability but uncovered a key challenge for DAC applications. While the modular structure

allowed for the precise integration of amine sites (in this case, via reduction of a nitro-functionalized COF), the simulations revealed that water molecules are persistently retained in the pores, forming hydrogen-bonded networks with the nitrile and amine groups. This retained water initiates unwanted side reactions and, crucially, competes directly with CO<sub>2</sub> for adsorption sites, undermining the theoretical uptake capacity. The profound insight from this work is that simply adding



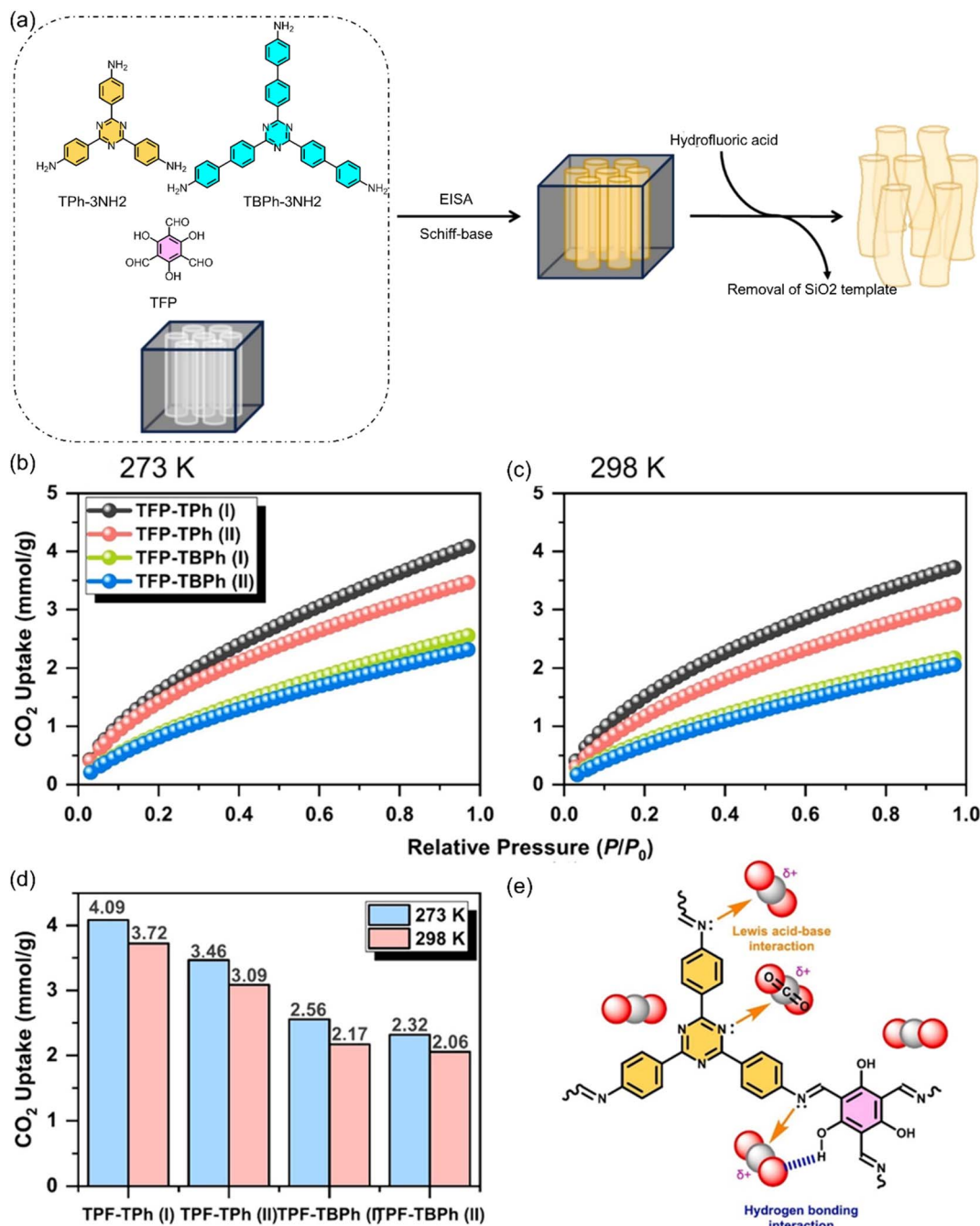


Fig. 4 (a) Preparation of TFP-TPH COFs and TFP-TBPh COFs using silica as a template and CO<sub>2</sub> adsorption curves of TFP COFs at (b) 273 K and (c) 298 K, with (d) a summary of their CO<sub>2</sub> uptake capacities. (e) Suggested adsorption mechanism of CO<sub>2</sub> in TFP-based COFs.<sup>112</sup> Adapted with authorization of Elsevier.

amine functionalities is insufficient for optimal DAC performance. Instead, Yaghi's group proposes a decisive design rule: to maximize CO<sub>2</sub> capture efficiency from humid air, COFs must be engineered with inherently hydrophobic pore environments that actively exclude water while preserving the targeted CO<sub>2</sub>-binding sites. This work exemplifies the sophisticated structure–property understanding achievable with COFs and directly informs the next generation of designs, moving beyond mere functionalization to the holistic engineering of the pore atmosphere for unparalleled selectivity in the presence of humidity.

Furthermore, this inherent designability of COFs, combining high surface area with integrated functionality, is powerfully validated by recent pioneering work. Yaghi and colleagues addressed the stringent requirements of DAC by synthesizing COF-999, a crystalline framework constructed with robust olefin linkages to ensure stability.<sup>115</sup> They then executed a precise post-synthetic modification, covalently grafting amine initiators to grow polyamine chains within its pores—directly integrating high-density Lewis basic sites deriving COF-999-NH<sub>2</sub> (Fig. 6). This engineered material exhibits a substantial



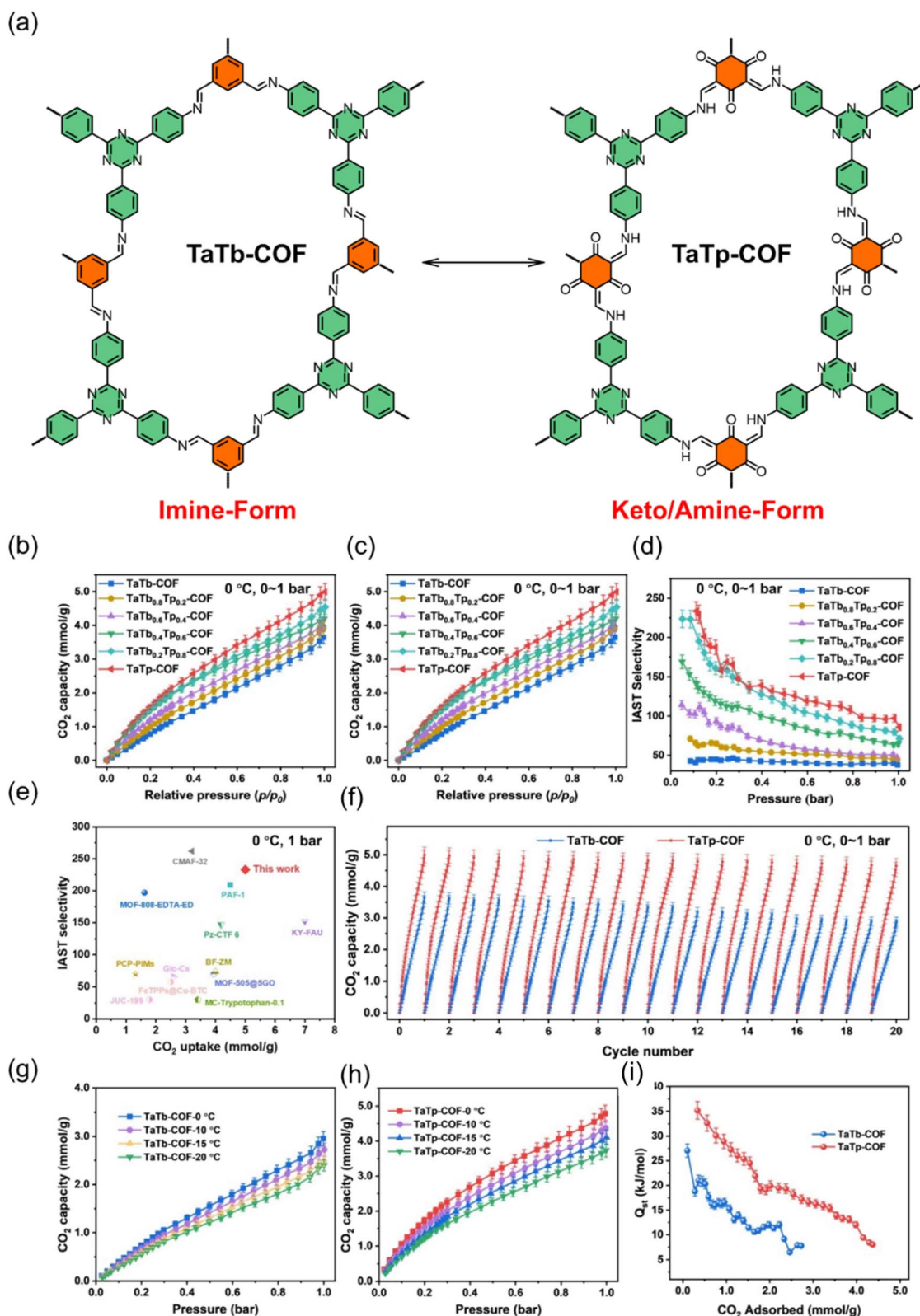


Fig. 5 (a) Synthesis and structures of TaTb-COF and TaTp-COF, (b and c)  $\text{N}_2$  adsorption and  $\text{CO}_2$  adsorption performance, (d) IAST-calculated  $\text{CO}_2/\text{N}_2$  selectivity at 273 K, (e) comparison of  $\text{CO}_2$  uptake and selectivity with benchmark materials, (f)  $\text{CO}_2$  cycling stability, (g and h) temperature-dependent  $\text{CO}_2$  adsorption, and (i) isosteric heats of adsorption.<sup>113</sup> Adapted with authorization of Elsevier.



CO<sub>2</sub> capacity from 400 ppm air (0.96–2.05 mmol g<sup>-1</sup>, humidity-enhanced), fast kinetics (18.8 min to reach half-capacity), and, critically, full regeneration at a low temperature of 60 °C. Most significantly, COF-999 retained 100% of its performance over more than 100 cycles using ambient outdoor air, conclusively demonstrating the thermal, chemical, and cycling stability afforded by its robust covalent architecture. This study stands as a paradigm, proving that the synergistic combination of a stable porous scaffold and precisely incorporated chemisorptive sites in COFs can yield highly efficient, durable, and practical adsorbents for the most challenging capture scenarios.

**4.1.2 CMPs.** CMPs are a distinctive class of POPs that uniquely merge extended  $\pi$ -conjugated electronic structures with permanent microporosity.<sup>14,47,102,116</sup> This combination is achieved by designing rigid, planar aromatic building blocks connected through covalent bonds that allow for electron delocalization across the network, such as Sonogashira–Hagihara or Suzuki–Miyaura couplings. The rigidity of these conjugated structures prevents the collapse of the polymer network, thereby generating intrinsic and stable porosity.<sup>66,117</sup> The defining feature of CMPs is this synergistic integration of porosity and electronic properties. The conjugated backbone discriminates CMPs with unique characteristics, including tuneable optical absorption and fluorescence, as well as charge carrier mobility. This opens avenues for applications beyond simple gas storage, such as in photocatalysis and organic electronics.<sup>99</sup> For CO<sub>2</sub> capture, CMPs offer several advantageous properties. Their high surface areas and microporous volumes provide ample space for physisorption. More importantly, their electronic structure can be precisely engineered. By incorporating electron-rich aromatic units (*e.g.*, carbazoles and triphenylamines) or heteroatoms like nitrogen into the backbone, the electron density of the framework can be enhanced. This creates a polar pore environment that strengthens the quadrupole–dipole interactions with CO<sub>2</sub> molecules, thereby improving both CO<sub>2</sub> adsorption capacity and selectivity over non-polar gases like N<sub>2</sub> and CH<sub>4</sub>. The ability to fine-tune the chemical and electronic landscape within their pores, while maintaining robust stability, makes CMPs a highly versatile and functional platform for advanced carbon capture technologies.

Earlier, our team reported CMPs built from triphenylamine- and thiadiazole-containing units, showing that tuning the electronic structure of the polymer backbone strongly influences CO<sub>2</sub> uptake (Fig. 7). The TPPDA-TPA CMP, which contains more electron-rich and nucleophilic sites, exhibits nearly double the CO<sub>2</sub> adsorption capacity of the less electron-rich TPPDA-ThZ CMP, confirming that enhancing pore polarity and electron density significantly improves CO<sub>2</sub> affinity and CO<sub>2</sub>/N<sub>2</sub> selectivity. This study directly supports our argument that electron-rich aromatic units and heteroatom incorporation allow CMPs to be engineered for superior CO<sub>2</sub> capture performance.<sup>65</sup>

Furthermore, Mohamed *et al.*<sup>118</sup> demonstrated that engineering CMPs with electron-rich units and abundant heteroatoms (N and O) significantly enhances their CO<sub>2</sub> capture performance. Their Anthra-DHTP CMP, which combines

a higher BET surface area with polar phenolic OH groups and nitrogen sites, shows substantially higher CO<sub>2</sub> uptake and stronger CO<sub>2</sub> binding ( $Q_{st} = 29$  kJ mol<sup>-1</sup>) than the less electron-dense TPE-DHTP CMP. This confirms our review argument that tuning the electronic structure and heteroatom content of CMPs creates a more polar pore environment, strengthening interactions with acidic CO<sub>2</sub> and boosting both capacity and selectivity, as shown in Fig. 8.

Jia *et al.* showed that carbazole-based CMPs, which contain electron-rich aromatic units, could be precisely engineered through controlled electropolymerization to adjust their micropore size and fractional free volume. By tuning the polymerization degree, the researchers created CMP membranes with optimized microporosity and enhanced CO<sub>2</sub> transport, demonstrating how the electronic structure and packing of CMPs can be finely controlled to improve CO<sub>2</sub> affinity and separation performance. Their results strongly support our review's argument that CMPs combine tunable electronic environments with customizable microporous structures, making them powerful platforms for selective and efficient CO<sub>2</sub> capture.<sup>119</sup> By integrating polar oxygen-containing acyl groups and constructing a 3D network of aligned hollow acyl-functionalized CMPs (AC-CMPs), the material achieves both high CO<sub>2</sub> affinity through a polar pore environment and fast mass transfer through hierarchical porosity as displayed in Fig. 9. The resulting AC-CMPs show strong CO<sub>2</sub>/N<sub>2</sub> selectivity, stable performance under humidity and heat, and efficient flue-gas filtration, clearly demonstrating how the chemical tunability and structural versatility of CMPs enable advanced, selective, and robust CO<sub>2</sub> capture technologies.<sup>120</sup>

**4.1.3 CTFs.** CTFs are a prominent subclass of POPs characterized by the presence of nitrogen-rich, aromatic triazine (C<sub>3</sub>N<sub>3</sub>) rings as the fundamental building blocks of their structure.<sup>121</sup> The resulting structure is a robust, two-dimensional or three-dimensional network connected by strong covalent bonds, endowing CTFs with exceptional thermal and chemical stability.<sup>122</sup> The defining feature of CTFs—and the source of their utility in CO<sub>2</sub> capture—is their intrinsic high nitrogen content and basic character. The triazine unit is a strong Lewis base, creating a polar, electron-rich pore environment that exhibits an inherently high affinity for acidic gases like CO<sub>2</sub>. This results in a significant enhancement of CO<sub>2</sub> uptake and selectivity over non-polar gases such as N<sub>2</sub> and CH<sub>4</sub>. These frameworks are typically synthesized *via* the trimerization of aromatic nitriles under ionothermal conditions (*e.g.*, using molten ZnCl<sub>2</sub> at high temperatures) or through more modern, milder catalytic routes in the absence of any post-synthetic modification.<sup>123</sup> Beyond this intrinsic property, the structure of CTFs offers excellent tunability. By varying the geometry and size of the nitrile-containing monomer, the pore size distribution and surface area can be precisely controlled.<sup>124</sup> Furthermore, the aromatic systems within the framework facilitate  $\pi$ - $\pi$  interactions, contributing to structural stability and enabling additional guest–host interactions. The combination of high stability, inherent CO<sub>2</sub>-philicity, and synthetic design flexibility makes CTFs particularly well-suited for challenging capture scenarios, including post-combustion



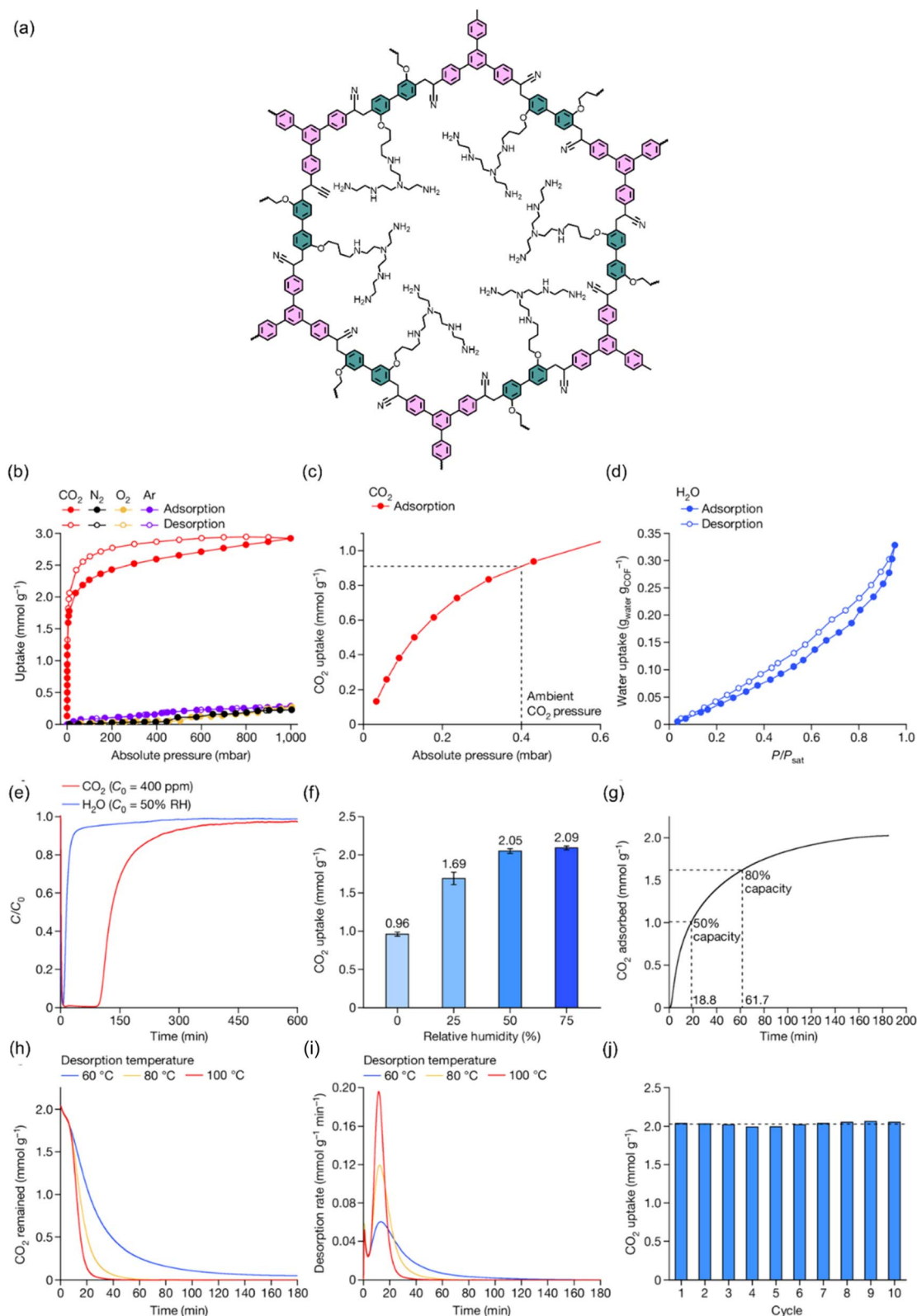
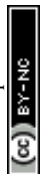


Fig. 6 (a) Structure of COF-999-NH<sub>2</sub>, (b) single-component gas adsorption isotherms at 25 °C. (c) CO<sub>2</sub> uptake at ambient pressure (0.4 mbar), (d) H<sub>2</sub>O vapor sorption isotherm at 25 °C, (e) CO<sub>2</sub>/H<sub>2</sub>O breakthrough curves under humid simulated air (400 ppm CO<sub>2</sub>, 50% RH), (f) CO<sub>2</sub> uptake at different relative humidity levels, (g) CO<sub>2</sub> adsorption kinetics under humid conditions, (h and i) CO<sub>2</sub> desorption kinetics and rates at 60–100 °C, and (j) cycling performance under humid conditions showing an average working capacity of 2.03 mmol g<sup>-1</sup>.<sup>115</sup> Adapted with authorization of Springer Nature.



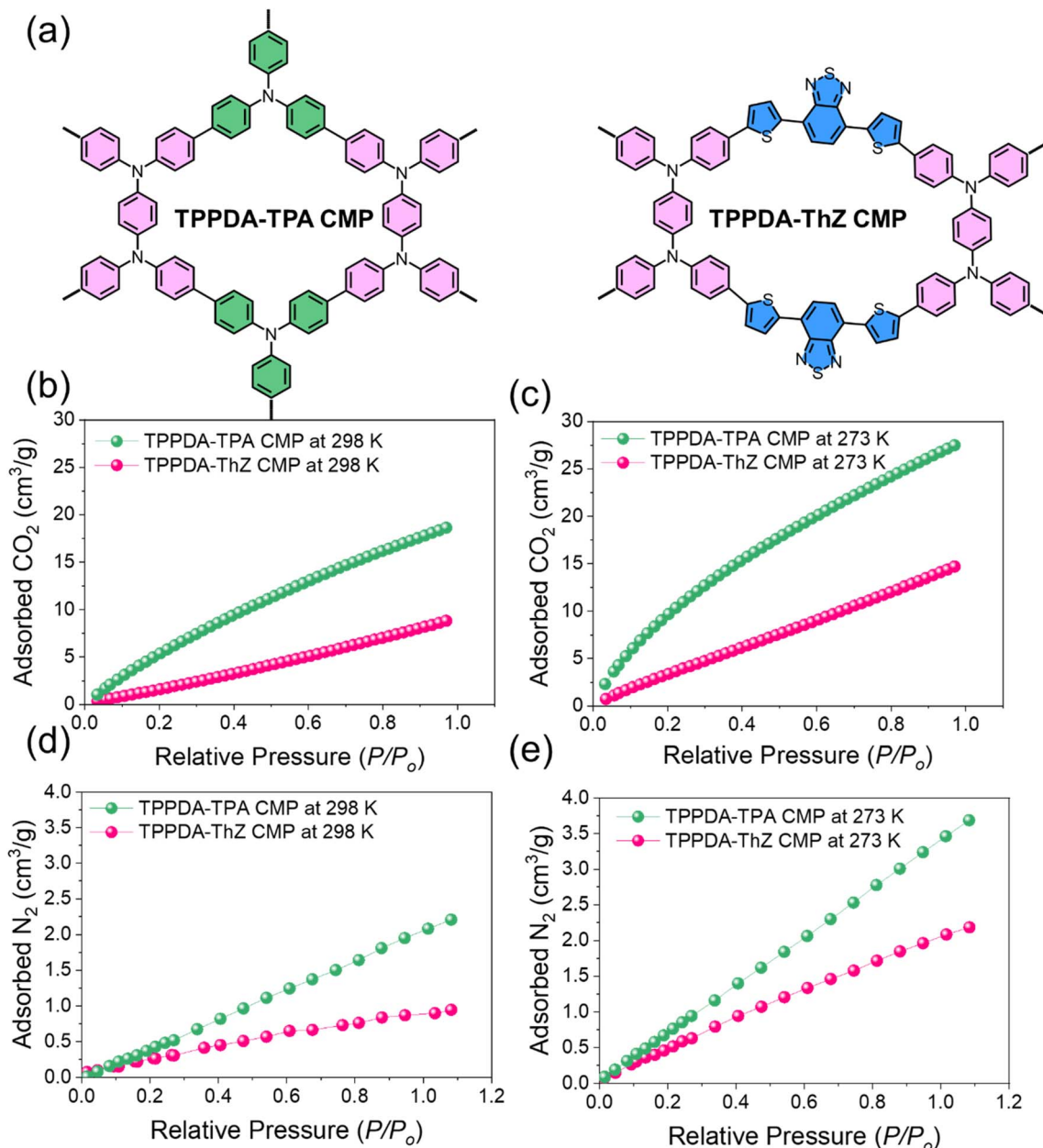


Fig. 7 (a) Molecular scheme of TPPDA-TPA and TPPDA-ThZ CMPs; CO<sub>2</sub> adsorption of TPPDA-TPA CMP and TPPDA-ThZ CMP at (b) 298 K and (c) 273 K, and their N<sub>2</sub> adsorption at (d) 298 K and (e) 273 K.<sup>65</sup> Adapted with authorization of the Royal Society of Chemistry.

flue gas treatment and the selective separation of CO<sub>2</sub> from natural gas streams.<sup>125</sup>

Maharana *et al.* developed nitrogen-rich CTFs (BMTz-CTFs) using a triazole-functionalized benzonitrile monomer, enabling a highly porous structure with abundant N sites. The optimized material (BMTz-CTF600) achieved a very high surface area (1557 m<sup>2</sup> g<sup>-1</sup>), mixed micro/mesoporosity, and partially graphitic domains that together enhance CO<sub>2</sub> affinity. As a result, it showed excellent CO<sub>2</sub> uptake (5.77 mmol g<sup>-1</sup> at 273 K, 1 bar) and high CO<sub>2</sub>/N<sub>2</sub> selectivity (IAST = 82). These nitrogen functionalities also provided strong redox activity, endowing the material with exceptional supercapacitor performance and long-term stability (Fig. 10).<sup>126</sup>

Huang *et al.*<sup>127</sup> developed the first photo-switchable CTFs for low-energy CO<sub>2</sub> capture and release. Unlike MOF-based photo-responsive adsorbents—which often suffer from poor thermal and chemical stability—the metal-free CTFs combined high porosity, strong structural stability, and tunable azobenzene photochromic groups. Light irradiation (UV/visible) allowed reversible CO<sub>2</sub> adsorption/desorption, and the switching efficiency was further improved by increasing azobenzene content or applying structural alleviation strategies. Actually, the Huang study demonstrates that CTFs can be engineered into highly stable, tuneable, and low-energy CO<sub>2</sub>-responsive materials, strongly supporting the idea of using CTFs for selective CO<sub>2</sub> capture (Fig. 11).



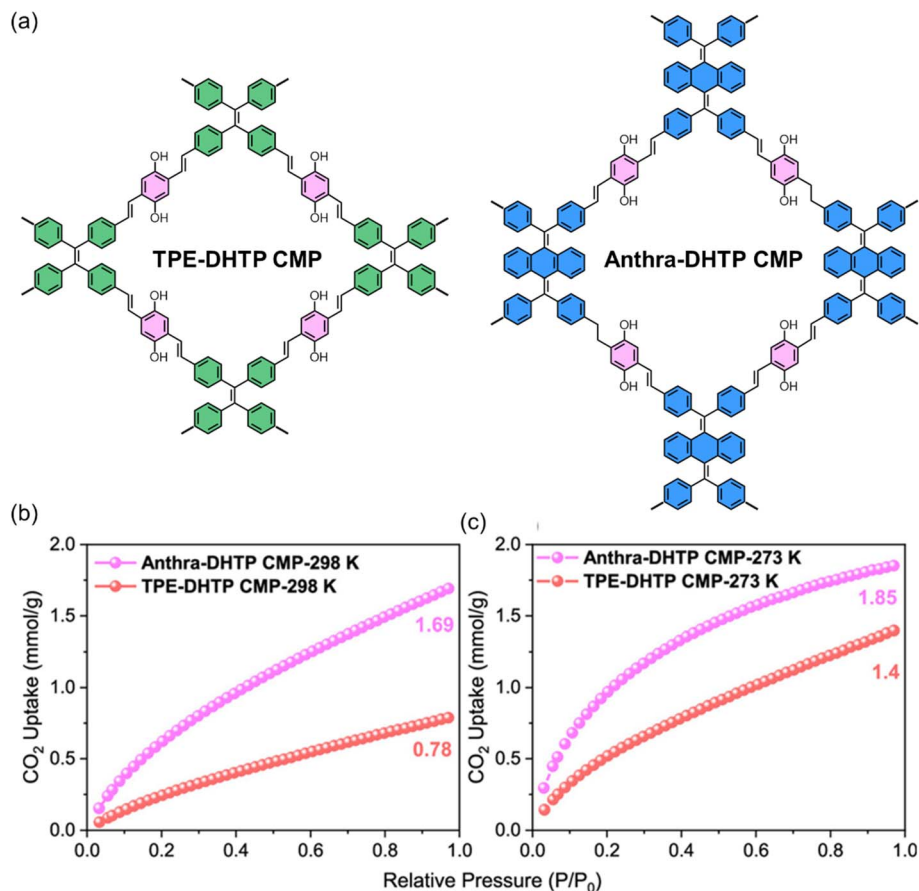


Fig. 8 (a) Molecular structures of TPE-DHTP and Anthra-DHTP CMPs and CO<sub>2</sub> adsorption performance of TPE-DHTP and Anthra-DHTP CMPs measured at (b) 298 K and (c) 273 K.<sup>118</sup> Adapted with authorization of American Chemical Society.

Earlier, we synthesized nitrogen-rich covalent triazine frameworks (ANT-CTF-10-500 and ANT-CTF-20-500) using an ionothermal method with ZnCl<sub>2</sub> at 500 °C.<sup>128</sup> These CTFs showed high thermal stability (up to 81% char yield), moderate surface areas (106–170 m<sup>2</sup> g<sup>-1</sup>), and strong CO<sub>2</sub> affinity, achieving uptake values up to 2.14 mmol g<sup>-1</sup>. Their high nitrogen content and polar triazine rings created CO<sub>2</sub>-philic pore environments, confirming that CTFs intrinsically enhance CO<sub>2</sub> adsorption without requiring post-functionalization (Fig. 12).

Further, Zhao *et al.* used DFT simulations to investigate how covalent triazine frameworks (pym-CTF) capture CO<sub>2</sub> under both dry and humid conditions. They found that CO<sub>2</sub> interacts favourably inside the pores, while in humid environments a stable seven-membered ring forms through multiple hydrogen bonds with H<sub>2</sub>CO<sub>3</sub>, showing strong affinity under both conditions. Importantly, ammoniating the CTF greatly increased the adsorption energies for CO<sub>2</sub> and H<sub>2</sub>CO<sub>3</sub>, demonstrating that chemical functionalization can significantly boost capture performance (Fig. 13).<sup>130</sup>

**4.1.4 HCPs.** HCPs represent a class of POPs renowned for their straight-forward and cost-effective synthesis, yielding materials with impressive surface areas and robust structures. Their defining characteristic is an extensively cross-linked

three-dimensional network, created through a facile one-step Friedel–Crafts alkylation or similar reactions that connect aromatic precursor units (like styrene, benzene, or triphenylmethane derivatives) with rigid cross-linkers (*e.g.*, formaldehyde dimethyl acetal or dichloroxylylene). This process creates a dense, “knitted” macromolecular structure that is permanently locked in an expanded state, preventing the collapse of the polymer chains and generating permanent porosity.<sup>128,131</sup> A key advantage of HCPs is their exceptional synthetic versatility and scalability. They could be produced from a wide range of commercially available and low-cost monomers, often without the need for precious metal catalysts.<sup>132</sup> Furthermore, they can be synthesized in a post-crosslinking fashion from pre-existing polystyrene polymers, offering a route to high surface area materials from common industrial precursors.<sup>26,100</sup> We presented a straightforward Friedel–Crafts strategy to develop TPA-CH POP from triphenylamine and chloranil-derived trihydroxy aryl units and further enhanced its CO<sub>2</sub> capture performance by functionalizing it with (3-mercaptopropyl)trimethoxysilane to form a TPA-CH POP-SH nanocomposite (Fig. 14). The MPTS-treated nanocomposite shows significantly improved properties, including higher thermal stability (char yield 71.5 wt% at 800 °C), a 2.5-fold increase in CO<sub>2</sub> uptake (48.07 cm<sup>3</sup> g<sup>-1</sup> at 273 K), and enhanced CO<sub>2</sub>/N<sub>2</sub> selectivity, attributed to stronger



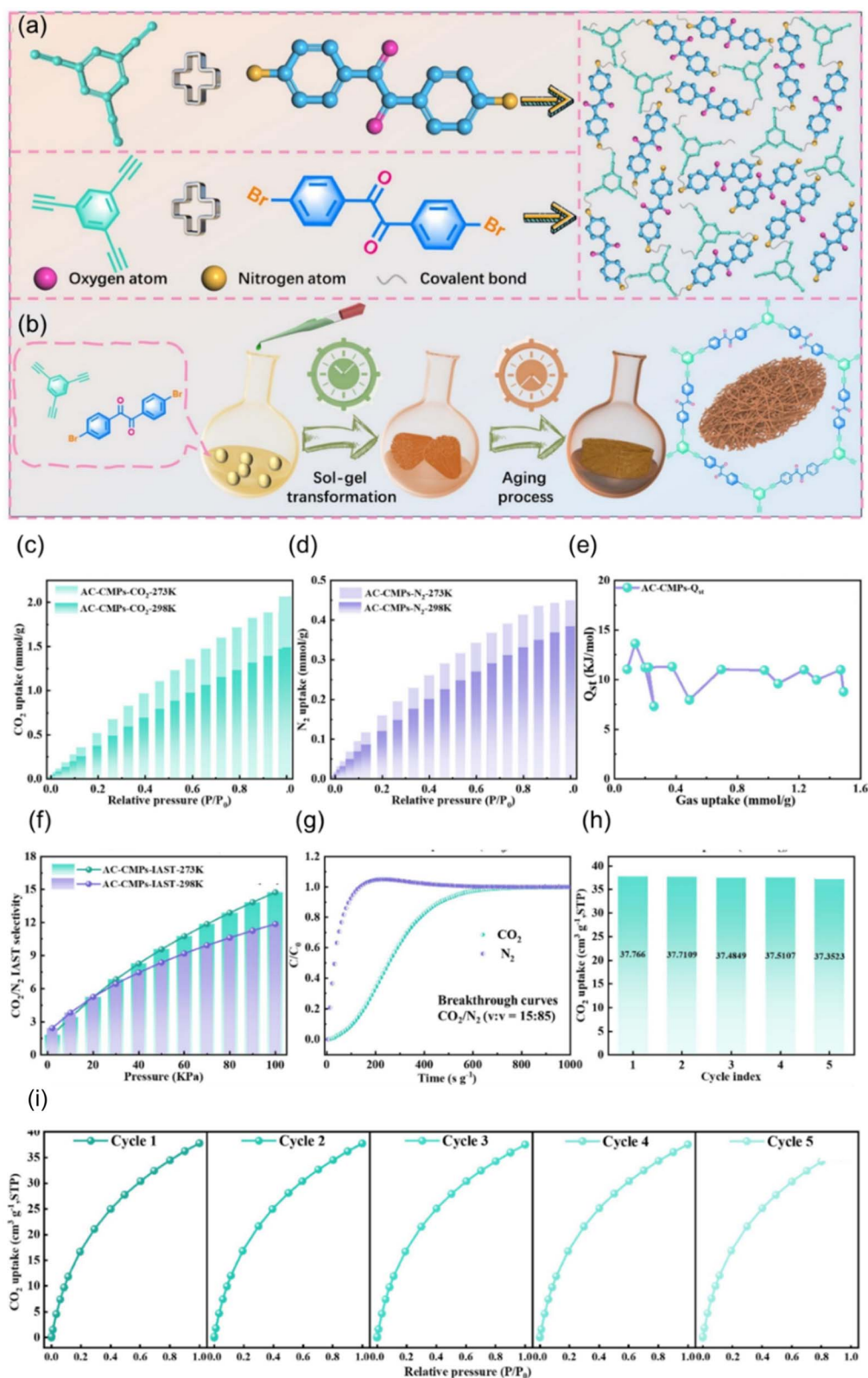


Fig. 9 (a) Formation of AC-CMP monoliths through self-assembly, (b) schematic of the AC-CMP synthesis process at various stages, (c and d)  $\text{CO}_2$  and  $\text{N}_2$  adsorption by AC-CMPs at 273 K and 298 K over 0–1.0 bar, (e) isothermic heat of  $\text{CO}_2$  adsorption calculated from 273 K isotherms using the Clausius–Clapeyron equation, (f) IAST-predicted  $\text{CO}_2/\text{N}_2$  (15 : 85 v/v) selectivity at 273 K and 298 K, (g)  $\text{CO}_2/\text{N}_2$  breakthrough curves at 298 K (flow: 10 mL min<sup>-1</sup>;  $\text{CO}_2$ : 15%, and  $\text{N}_2$ : 85%; 1 bar), (h)  $\text{CO}_2$  adsorption capacity over 5 cycles, and (i) cyclic  $\text{CO}_2$  adsorption performance.<sup>120</sup> Adapted with authorization of Elsevier.



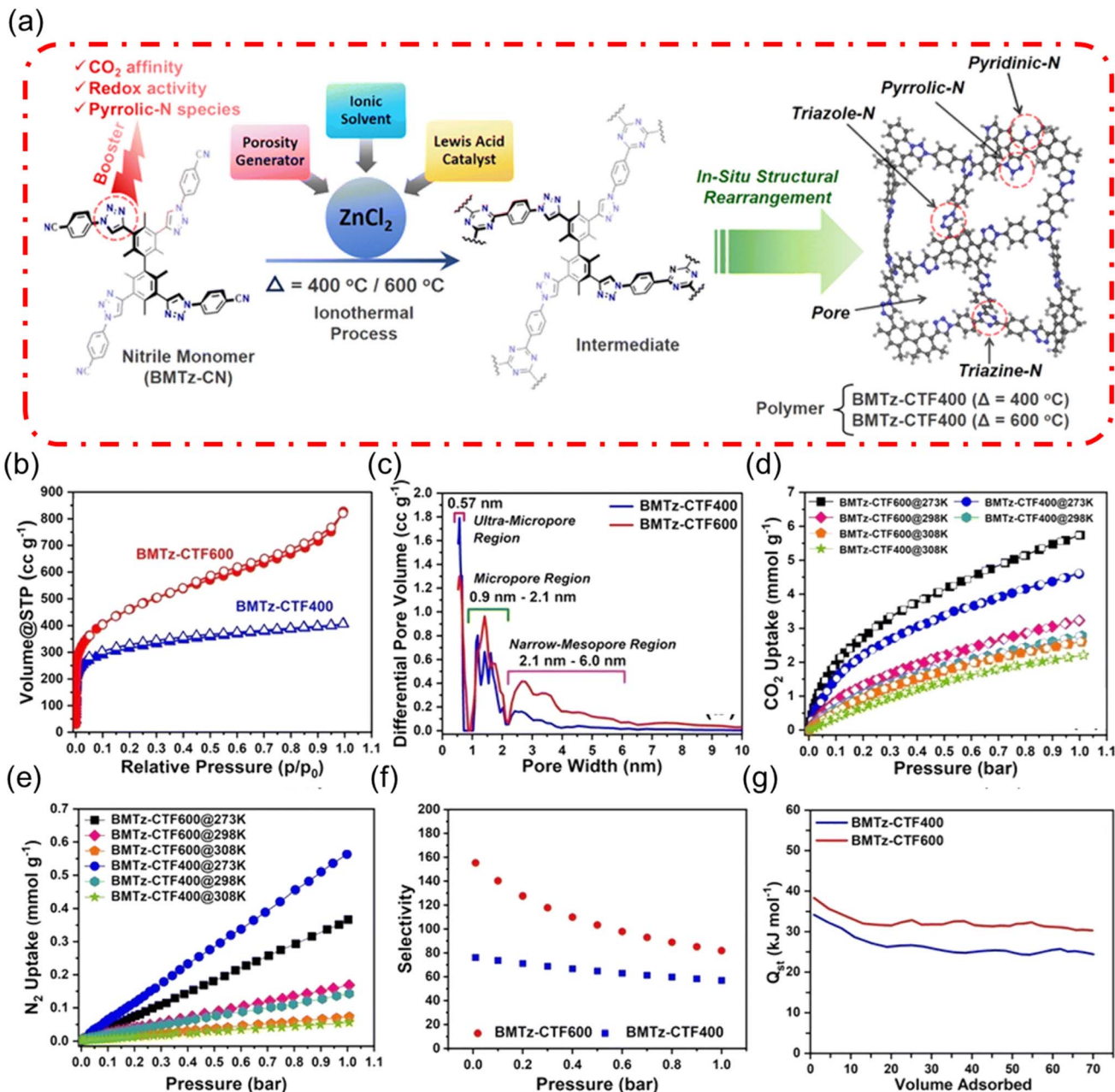


Fig. 10 (a) Synthesis route and proposed chemical structure of BMTz-CTFs, (b)  $N_2$  adsorption (filled) and desorption (open) isotherms of BMTz-CTFs at 77 K, (c) pore size distribution calculated from the 77 K  $N_2$  isotherm, (d)  $CO_2$  adsorption isotherms up to 1 bar, (e)  $N_2$  adsorption isotherms up to 1 bar, (f) IAST-predicted  $CO_2/N_2$  (15 : 85) selectivity at 298 K and (g) isosteric heat of  $CO_2$  adsorption.<sup>126</sup> Adapted with authorization of the Royal Society of Chemistry.

adsorbent- $CO_2$  interactions. These findings highlighted the effectiveness of functional group modification in boosting  $CO_2$  capture and supported the broader concept—central to HCPs—that simple, low-cost synthetic routes can produce robust, high-surface-area porous materials with tuneable adsorption properties.<sup>64</sup>

For  $CO_2$  capture, HCPs offer significant practical benefits. Their synthesis readily generates a high density of ultra-micropores (<1 nm), which are crucial for strong physisorption of  $CO_2$  at low pressures due to the overlapping potential from adjacent pore walls.<sup>133</sup> While they are

traditionally considered physisorbents, their chemical structure provides an excellent platform for post-synthetic modification.<sup>134</sup> The aromatic backbone can be easily functionalized to incorporate chemisorptive sites, thereby enhancing  $CO_2$  affinity and selectivity.<sup>135,136</sup> Combined with their high thermal stability and demonstrated recyclability, HCPs stand out as highly practical and economically viable candidates for large-scale post-combustion carbon capture applications. Alemin *et al.*<sup>136</sup> reported that the combination of porosity engineering with post-synthetic chemical modification to create HCPs can lead to both high  $CO_2$  uptake and exceptional  $CO_2/N_2$  selectivity



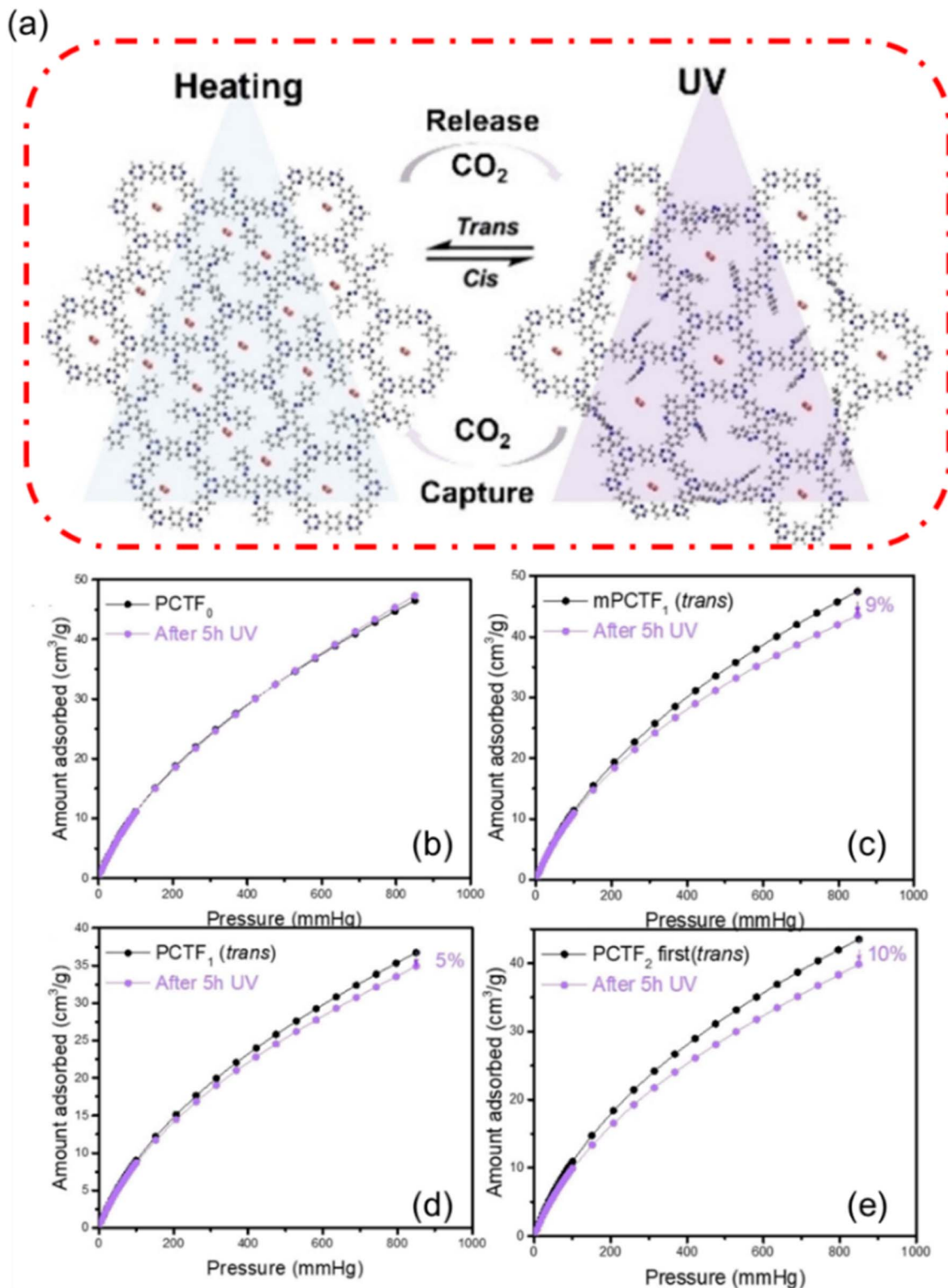


Fig. 11 (a) Schematic representation of CO<sub>2</sub> capture and release through chemical transformation (*cis/trans*), and CO<sub>2</sub> adsorption isotherms of (b) PCTF<sub>0</sub>, (c) PCTF<sub>1</sub>, (d) mPCTF<sub>1</sub>, and (e) PCTF<sub>2</sub> measured in the dark (black) and after 5 hours of UV irradiation at 273 K (purple).<sup>127</sup> Adapted with authorization of John Wiley and Sons.

(Fig. 15). By first tuning the pore structure using different cross-linkers and then introducing polar functional groups (NO<sub>2</sub> and NH<sub>2</sub>), Alemin *et al.* showed that CO<sub>2</sub> selectivity can be

dramatically improved even when the surface area decreases. In particular, converting HCP-F-NO<sub>2</sub> to HCP-F-NH<sub>2</sub> generates strong CO<sub>2</sub>-binding sites that boost CO<sub>2</sub>/N<sub>2</sub> selectivity to 100—



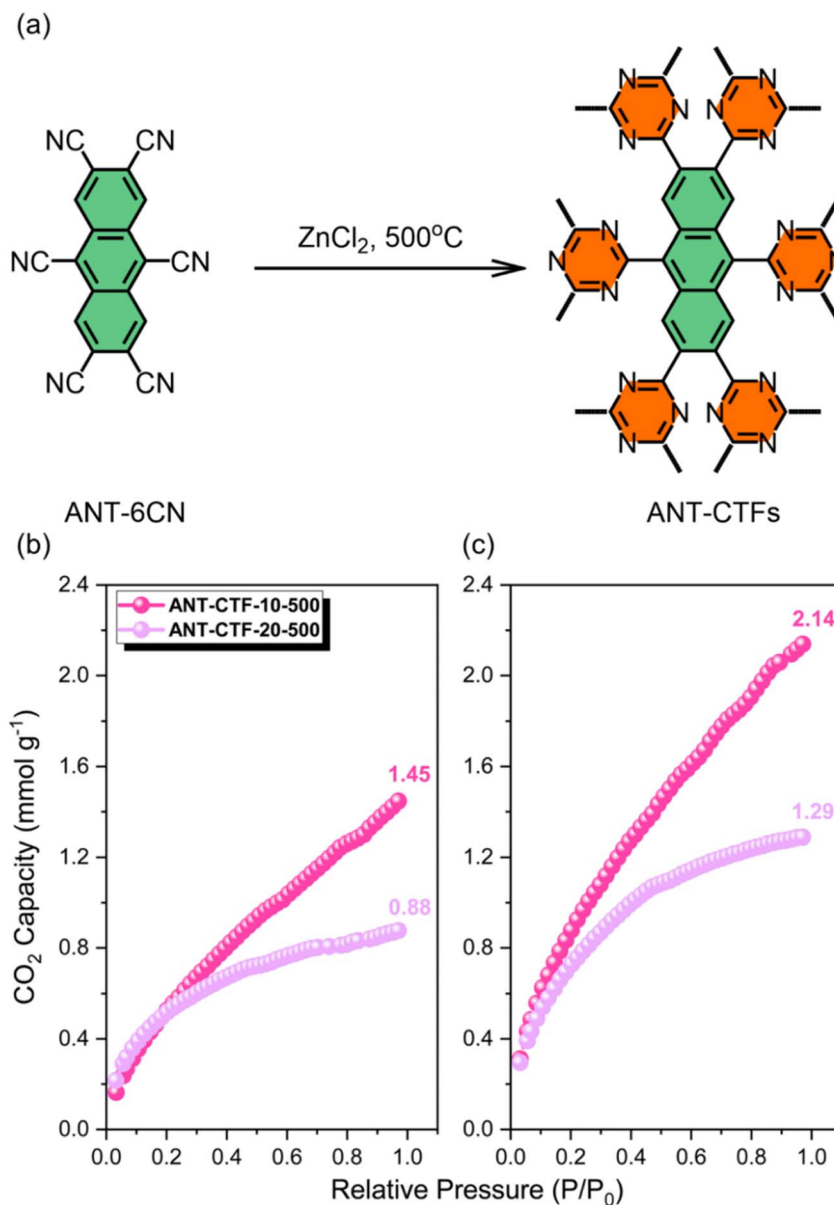


Fig. 12 (a) Synthesis protocol of ANTs-CTFs and CO<sub>2</sub> capture capacity of ANT-CTF-10-500 and ANT-CTF-20-500 at (b) 298 K and (c) 273 K.<sup>129</sup> Adapted with authorization of the Royal Society of Chemistry.

far higher than that of the unmodified framework. Breakthrough and recyclability tests further confirm practical stability.

Recently, Ma and his team *et al.*<sup>52</sup> developed a dually functionalized hyper-cross-linked polymer (HCP-A-S) that combines ultramicropores (0.34 nm) with two strong CO<sub>2</sub>-binding groups (-NH<sub>2</sub> and -SO<sub>3</sub>H). This design allows the material to precisely sieve CO<sub>2</sub> over N<sub>2</sub> and significantly enhance CO<sub>2</sub> affinity through polar interactions (Fig. 16). As a result, the polymer shows high CO<sub>2</sub> uptake, excellent CO<sub>2</sub>/N<sub>2</sub> selectivity, and low-energy regeneration, maintaining full performance over repeated cycles.

Liu *et al.*<sup>137</sup> demonstrated a pore-engineering strategy to enhance HCP performance by using Friedel-Crafts alkylation

followed by HFA etching to create hydroxyl-functionalized HCPs (HCPs-X-HFA) (Fig. 17). This treatment greatly increases surface area, pore volume, and the number of -OH groups, resulting in high CO<sub>2</sub> uptake (up to 3.41 mmol g<sup>-1</sup> at 0 °C) and improved CO<sub>2</sub>/N<sub>2</sub> selectivity. The introduced hydroxyl sites not only strengthen CO<sub>2</sub> binding through hydrogen bonding but also make the materials effective recyclable catalysts for CO<sub>2</sub> conversion into cyclic carbonates under mild conditions (60 °C, 1 bar). Liu's work demonstrates well how post-synthetic pore and functionality engineering can produce HCPs with dual CO<sub>2</sub> adsorption and catalytic capabilities, supporting their versatility in carbon capture and utilization.

**4.1.5 PAFs.** PAFs represent a family of ultra-stable POPs distinguished by their design based exclusively on strong, rigid



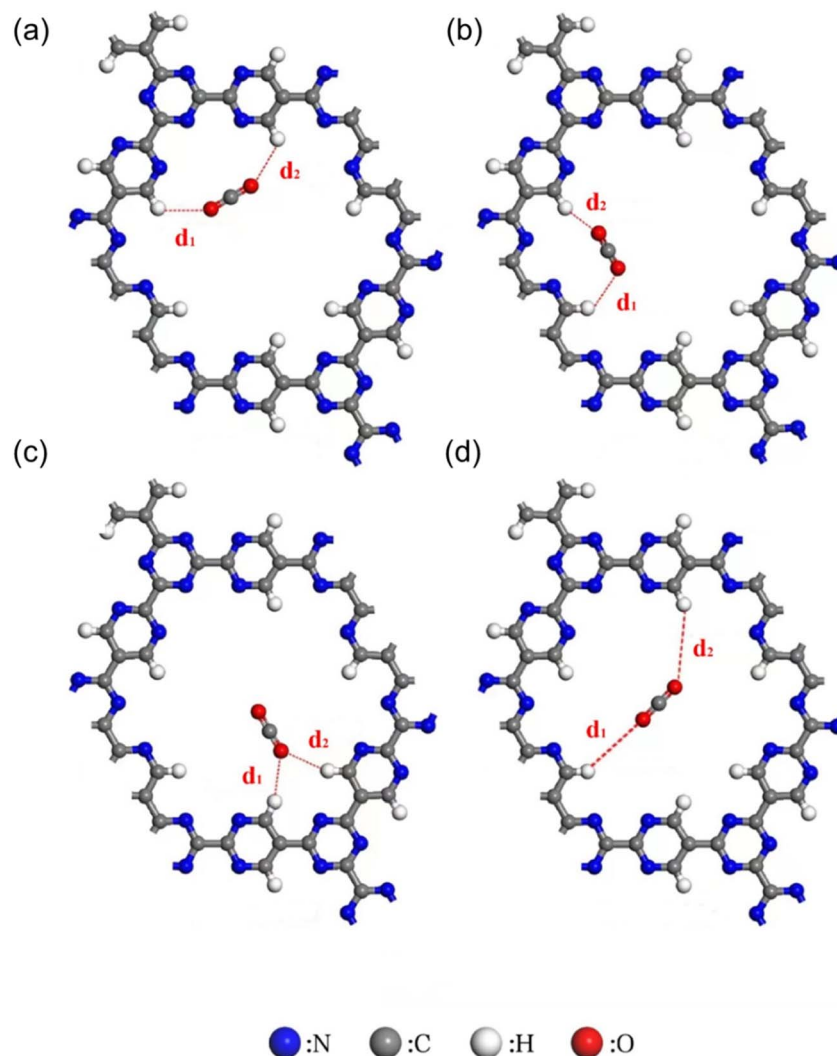


Fig. 13 Optimized CO<sub>2</sub> adsorption configurations on pym-CTF at (a) site 1, (b) site 2, (c) site 3, and (d) site 4.<sup>150</sup> Adapted with authorization of Elsevier.

carbon-carbon (C-C) bonds between aromatic building blocks.<sup>138</sup> Inspired by the structure of diamond, PAFs are constructed from tetrahedral or other multi-directional monomers (a renowned example being the tetraphenylmethane core in PAF-1) using coupling reactions like Yamamoto or Suzuki cross-coupling.<sup>139</sup> This all-carbon connectivity results in an exceptionally robust three-dimensional framework. The most salient feature of PAFs is their extraordinary physicochemical stability. The combination of strong C-C bonds and the inherent stability of aromatic rings makes them resistant to high temperatures, moisture, strong acids, bases, and even boiling organic solvents. This resilience far exceeds that of many other POPs and is a critical advantage for long-term use in harsh industrial environments.<sup>140</sup> In the protocol of CO<sub>2</sub> capture, PAFs are renowned for their record-breaking surface areas (*e.g.*, PAF-1 boasts a Langmuir surface area exceeding 7000 m<sup>2</sup> g<sup>-1</sup>), which provides a vast landscape for gas physisorption.<sup>140,141</sup> While their unfunctionalized versions exhibit high CO<sub>2</sub> storage capacity, particularly at high pressures, their true potential is

unlocked through post-synthetic modification.<sup>142</sup> The aromatic rings in the framework serve as versatile handles for introducing a wide range of functional groups, such as amines or lithium alkoxides, *via* electrophilic aromatic substitution or other reactions. This allows for the precise engineering of pore chemistry to enhance CO<sub>2</sub> affinity and selectivity without compromising the exceptional stability of the core scaffold. Consequently, PAFs are considered premier candidates for demanding carbon capture industries where long-term adsorbent integrity under aggressive conditions is paramount. In this regard, Zhang *et al.*<sup>143</sup> designed a porous aromatic framework (PAF-45DPA) using a mixed-monomer strategy, producing a material with small pores, high porosity, and strong CO<sub>2</sub> selectivity. When incorporated into polysulfone (PSF) to form hollow-fiber hybrid membranes, PAF-45DPA greatly enhanced CO<sub>2</sub> separation: CO<sub>2</sub> permeance tripled and the CO<sub>2</sub>/N<sub>2</sub> separation factor doubled (up to 24.2). The membranes remained stable and reproducible under various conditions, demonstrating that PAFs—with their tuneable structure and amine



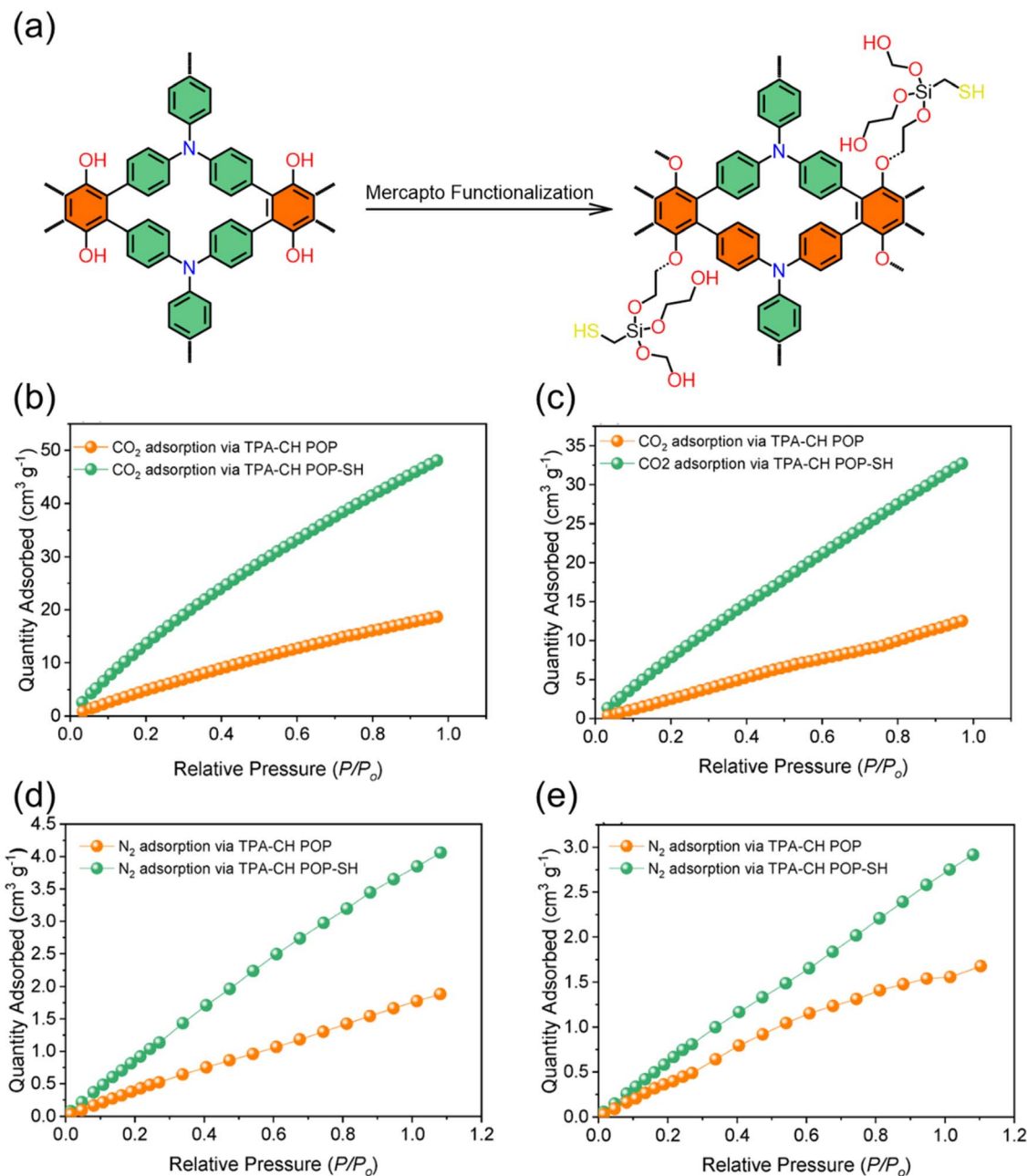


Fig. 14 (a) Mercapto functionalization of TPA-CH POP, (b and c) uptake records of CO<sub>2</sub> and (d and e) N<sub>2</sub> by the TPA-CH POP and the TPA-CH POP-SH nanocomposite, respectively, at two different temperatures of (b and d) 273 K and (c and e) 298 K.<sup>64</sup> Adapted with authorization of MDPI.

functionality—are highly promising materials for efficient and selective CO<sub>2</sub> capture and separation (Fig. 18).

**4.1.6 PIMs.** PIMs constitute a unique class of POPs whose microporosity arises not from a rigid, cross-linked network, but from the inability of their macromolecular chains to pack efficiently in the solid state.<sup>144</sup> Basically, PIMs are typically solution-processable, a property that distinguishes them from many other POPs and facilitates their fabrication into thin films and membranes—a critical advantage for practical gas separation applications.<sup>145</sup> For dynamic CO<sub>2</sub> capture, PIMs offer a compelling combination of high free volume, which grants substantial gas uptake capacity, and a tuneable chemical structure. Their

properties can be finely adjusted through post-synthetic modification or by copolymerization, allowing for the introduction of specific functional groups (such as amines or carboxylates) to enhance CO<sub>2</sub> affinity and selectivity over other gases like N<sub>2</sub>. While early PIMs were prone to physical aging and a gradual loss of free volume, recent advancements in cross-linking and the development of more rigid “PIM of Organic Soluble Networks (PIM-PONs)” have significantly improved their long-term stability, solidifying their role as a versatile platform for membrane-based and adsorptive carbon capture technologies. Rodriguez *et al.*<sup>146</sup> showed that functionalized PIMs, especially the amine-modified PIM-NH<sub>2</sub>, achieve dramatically better



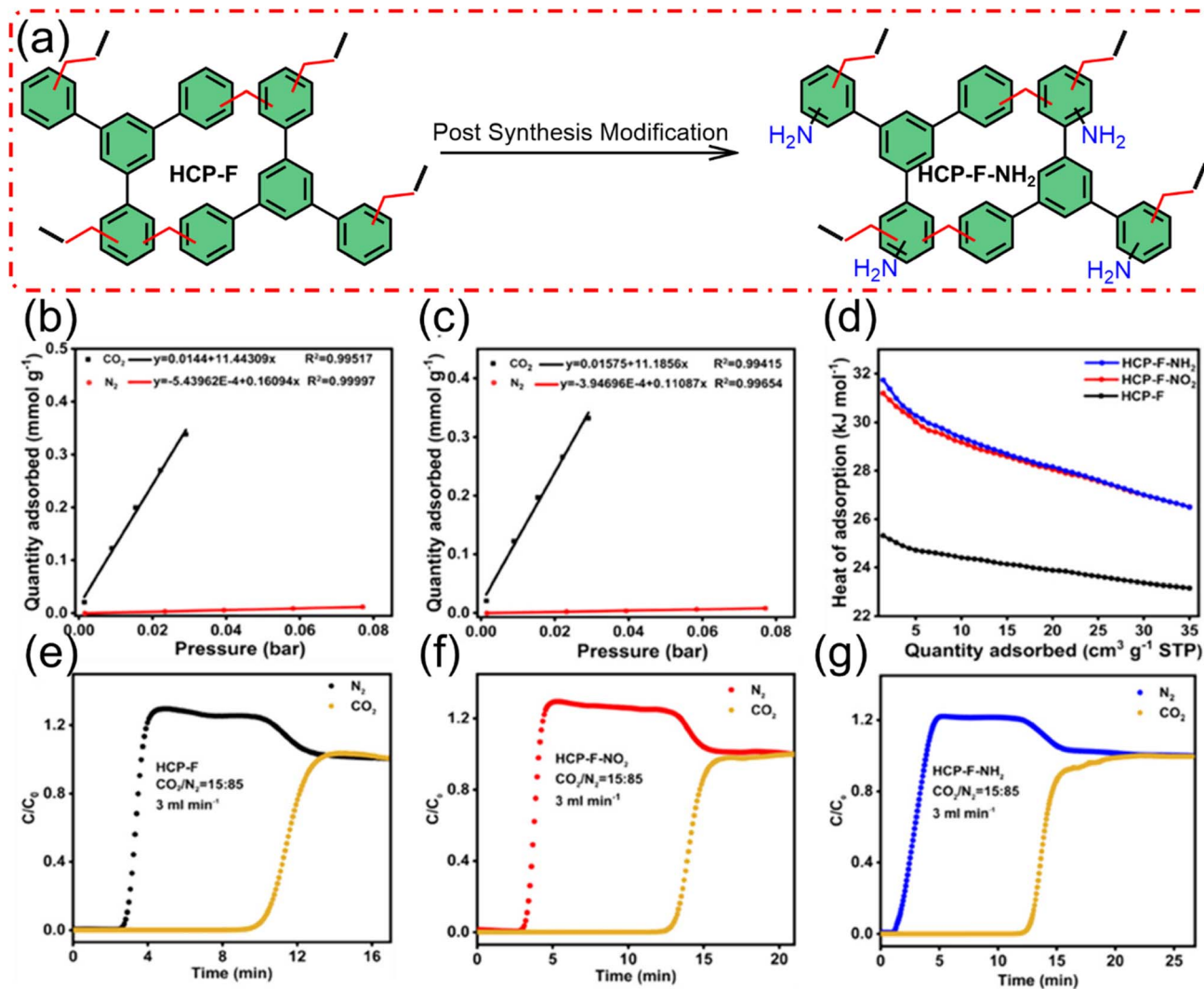


Fig. 15 (a) Post-synthetic modification of dimethoxymethane (HCP-F), (b) CO<sub>2</sub>/N<sub>2</sub> adsorption selectivity of HCP-F-NO<sub>2</sub>, (c) CO<sub>2</sub>/N<sub>2</sub> adsorption selectivity of HCP-F-NH<sub>2</sub>, (d) CO<sub>2</sub> heat of adsorption for both materials, and (e–g) selectivity was determined from the initial slope of Henry's law at 273.15 K (pressure < 0.3 bar). The heat of adsorption was calculated from CO<sub>2</sub> isotherms at 273.15 and 298.15 K. Dynamic CO<sub>2</sub>/N<sub>2</sub> (15 : 85 v/v) breakthrough curves at 298 K and 3 mL min<sup>-1</sup> for HCP-F, HCP-F-NO<sub>2</sub>, and HCP-F-NH<sub>2</sub>, respectively.<sup>136</sup> Adapted with authorization of John Wiley and Sons.

mixed-gas CO<sub>2</sub> separation than that predicted from pure-gas tests, thanks to competitive sorption that strengthens CO<sub>2</sub> selectivity and offsets plasticization (Fig. 19). PIM-NH<sub>2</sub> delivered exceptional improvements in CO<sub>2</sub>/CH<sub>4</sub> and CO<sub>2</sub>/N<sub>2</sub> permselectivity (up to 250%) and maintained high performance even at high pressures, demonstrating strong CO<sub>2</sub> affinity, structural stability, and resistance to plasticization. These findings support our claim that PIMs, with their tunable chemistry and ability to incorporate CO<sub>2</sub>-philic functional groups, form a versatile and high-performing platform for membrane-based carbon capture.

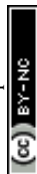
To provide clear guidance for the field, we present a quantitative benchmarking of representative POP subclasses (Table 1), comparing key metrics including CO<sub>2</sub> capacity, selectivity, heat of adsorption, stability, and synthesis complexity. This analysis reveals distinct performance trade-offs that inform material

selection for specific capture scenarios and highlights opportunities for future innovation.

## 4.2 Structure–property relationships in POPs

The performance of POPs in CO<sub>2</sub> capture is not a product of chance but is directly governed by their molecular-level architecture.<sup>147</sup> Understanding the structure–property relationship is fundamental to the rational design of next-generation adsorbents. These relationships can be analyzed in terms of the interplay among the building blocks, the resulting porous network, and the chemical functionality.

**4.2.1 Building block geometry and rigidity.** The choice of units directly dictates the topology and stability of the POP. In general, monomers with rigid, multi-armed geometries (e.g., tetrahedral and trigonal) are essential for creating permanent, well-defined porosity.<sup>148,149</sup> Furthermore, the geometry of the



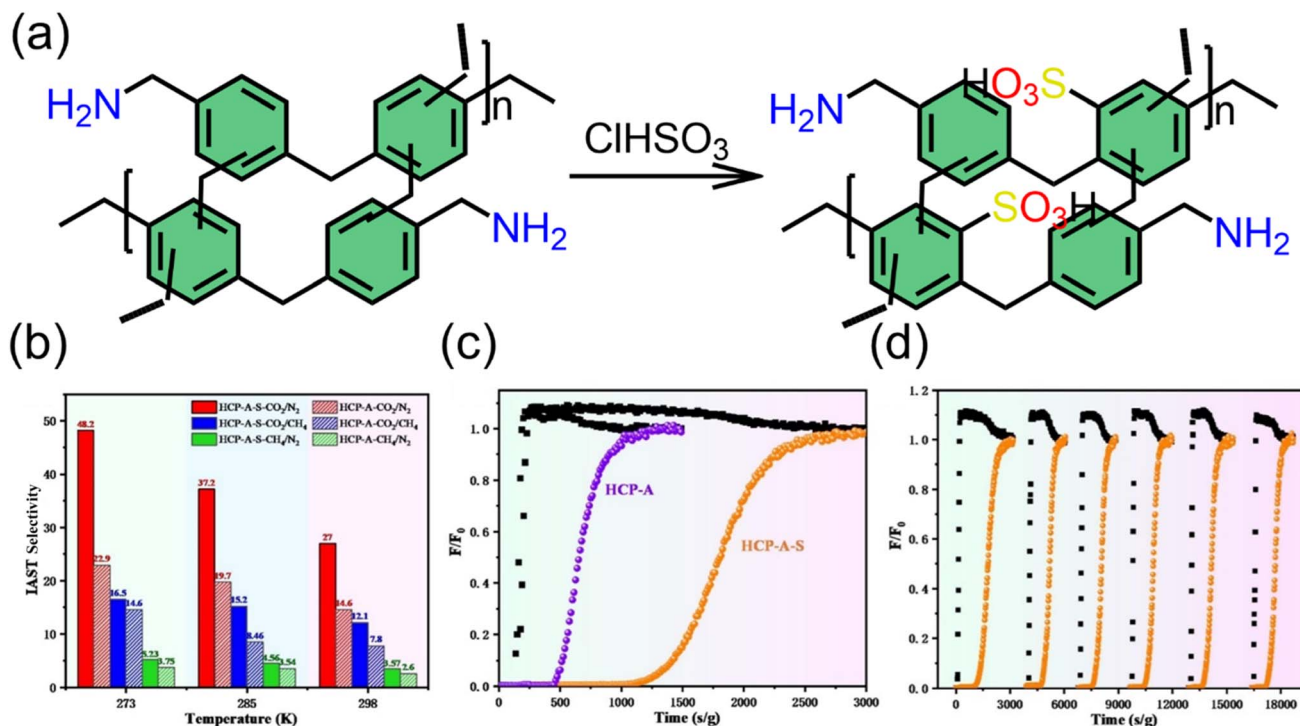


Fig. 16 (a) Sulphonation of HCP-A, CO<sub>2</sub>/N<sub>2</sub>; (b) selectivity of HCP-A-S and HCP-A, dynamic CO<sub>2</sub> capture at 298 K and 1 bar; (c) breakthrough curves for N<sub>2</sub> (black), HCP-A (purple), and HCP-A-S (orange); (d) CO<sub>2</sub> adsorption stability over six adsorption–regeneration cycles using helium.<sup>52</sup> Adapted with authorization of Elsevier.

building block controls the framework topology. For instance, linear linkers form two-dimensional layers in COFs, while tetrahedral monomers create three-dimensional diamondoid structures in PAFs, which often yield higher surface areas and more robust networks.<sup>20,150</sup>

**4.2.2 Pore architecture: surface area, volume, and size.** The connection of rigid building blocks generates the porous structure, characterized by the following key parameters.

**4.2.2.1 Surface area.** The high BET surface area provides a greater number of adsorption sites, generally correlating with higher gas uptake capacity, particularly for physisorption.<sup>151</sup> Liao *et al.*<sup>152</sup> developed hydroxyl-functionalized ionic hyper-cross-linked polymers using a one-step Friedel–Crafts method, achieving very high surface areas (560–1480 m<sup>2</sup> g<sup>-1</sup>) and rich microporosity. These structural features, combined with ionic sites, resulted in exceptionally high and reversible CO<sub>2</sub> uptake, reaching 157.5 mg g<sup>-1</sup> at 273 K and 1 bar—surpassing many reported ionic polymers. The materials also served as efficient, recyclable catalysts for CO<sub>2</sub> conversion due to synergistic effects from hydroxyl groups. This study clearly demonstrates that maximizing BET surface area significantly enhances available adsorption sites and directly boosts CO<sub>2</sub> capture performance, reinforcing the importance of high-surface-area porous polymers in selective CO<sub>2</sub> adsorption (Fig. 20).

**4.2.2.2 Pore size.** Actually, this is a critical parameter for selectivity as ultra-micropores (<0.8 nm) exert a strong van der Waals potential on confined CO<sub>2</sub> molecules (kinetic diameter ~0.33 nm), leading to high adsorption energy and excellent molecular sieving for separations such as CO<sub>2</sub>/N<sub>2</sub>. In this

context, He *et al.*<sup>153</sup> demonstrated that both intrinsic defects and precise pore size control are critical for maximizing CO<sub>2</sub> adsorption in porous carbons. Their combined experimental and multiscale simulation study showed that defects distort graphene layers, creating more micropores and additional high-energy adsorption sites that strengthen CO<sub>2</sub> binding. Through slit-pore simulations, they identified an optimal pore size of ~7 Å, where CO<sub>2</sub> forms a stable monolayer with the highest adsorption energy; larger pores lead to weaker bilayer adsorption. Defect-rich activated carbons (VAC700 and VAC900) also generated more ultramicropores, further enhancing CO<sub>2</sub> uptake.

### 4.3 Chemical functionality and binding energy

The chemical composition of the pore walls dictates the strength of the CO<sub>2</sub>–framework interaction.

**4.3.1 Physisorption POPs.** Pristine frameworks with non-polar walls rely on van der Waals forces and the quadrupole moment of CO<sub>2</sub>. Their performance is primarily a function of their ultra-microporous surface area.<sup>58</sup>

**4.3.2 Chemisorptive POPs.** The incorporation of Lewis basic sites, most notably amine groups (–NH<sub>2</sub>) but also nitrogen-rich heterocycles (triazine in CTFs and azo groups), introduces specific, strong chemisorptive interactions. This dramatically increases  $Q_{\text{st}}$  and CO<sub>2</sub> selectivity, particularly at low partial pressures (*e.g.*, post-combustion and DAC), but often at the cost of higher regeneration energy. Yang *et al.*<sup>154</sup> synthesized a series of amine-functionalized POPs using primary, secondary, and tertiary amine monomers to understand how



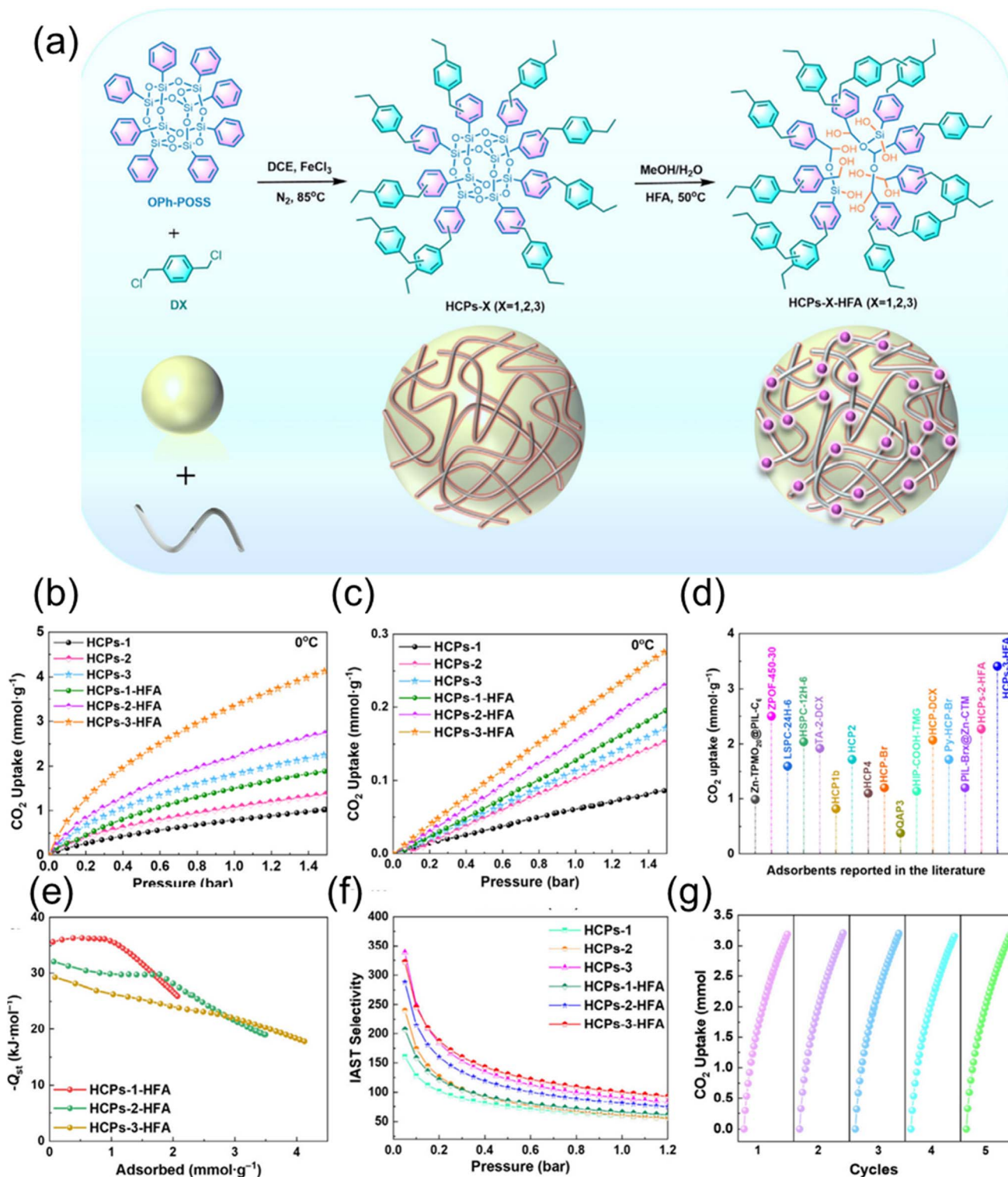


Fig. 17 (a) Synthesis of HCPs-X-HFA ( $X = 1, 2$ , or  $3$ ) using OPh-POSS and DX in the following ratios:  $1 : 6$  ( $X = 1$ ),  $1 : 9$  ( $X = 2$ ), and  $1 : 12$  ( $X = 3$ ), (b)  $\text{CO}_2$  and (c)  $\text{N}_2$  adsorption isotherms of HCPs at  $0^\circ\text{C}$ , (d) comparison of  $\text{CO}_2$  uptake at  $0^\circ\text{C}$  and 1 bar with top-performing materials, (e)  $\text{CO}_2$  isosteric heat of adsorption ( $Q_{\text{st}}$ ) for HCPs, (f) IAST-predicted  $\text{CO}_2/\text{N}_2$  (15 : 85 v/v) selectivity at  $0^\circ\text{C}$ , and (g)  $\text{CO}_2$  adsorption cycling performance of HCPs-2-HFA.<sup>137</sup> Adapted with authorization of American Chemical Society.

the amine type affects  $\text{CO}_2$  adsorption. Among them, the ethylenediamine-modified POP (POP-3), containing both primary and secondary amines, showed the strongest chemisorptive interaction with  $\text{CO}_2$ , achieving the highest adsorption

heat ( $54.8 \text{ kJ mol}^{-1}$ ) and outstanding selectivity (IAST = 202). Breakthrough experiments confirmed excellent  $\text{CO}_2/\text{N}_2$  and  $\text{CO}_2/\text{CH}_4$  separation and stable cycling performance (Fig. 21).



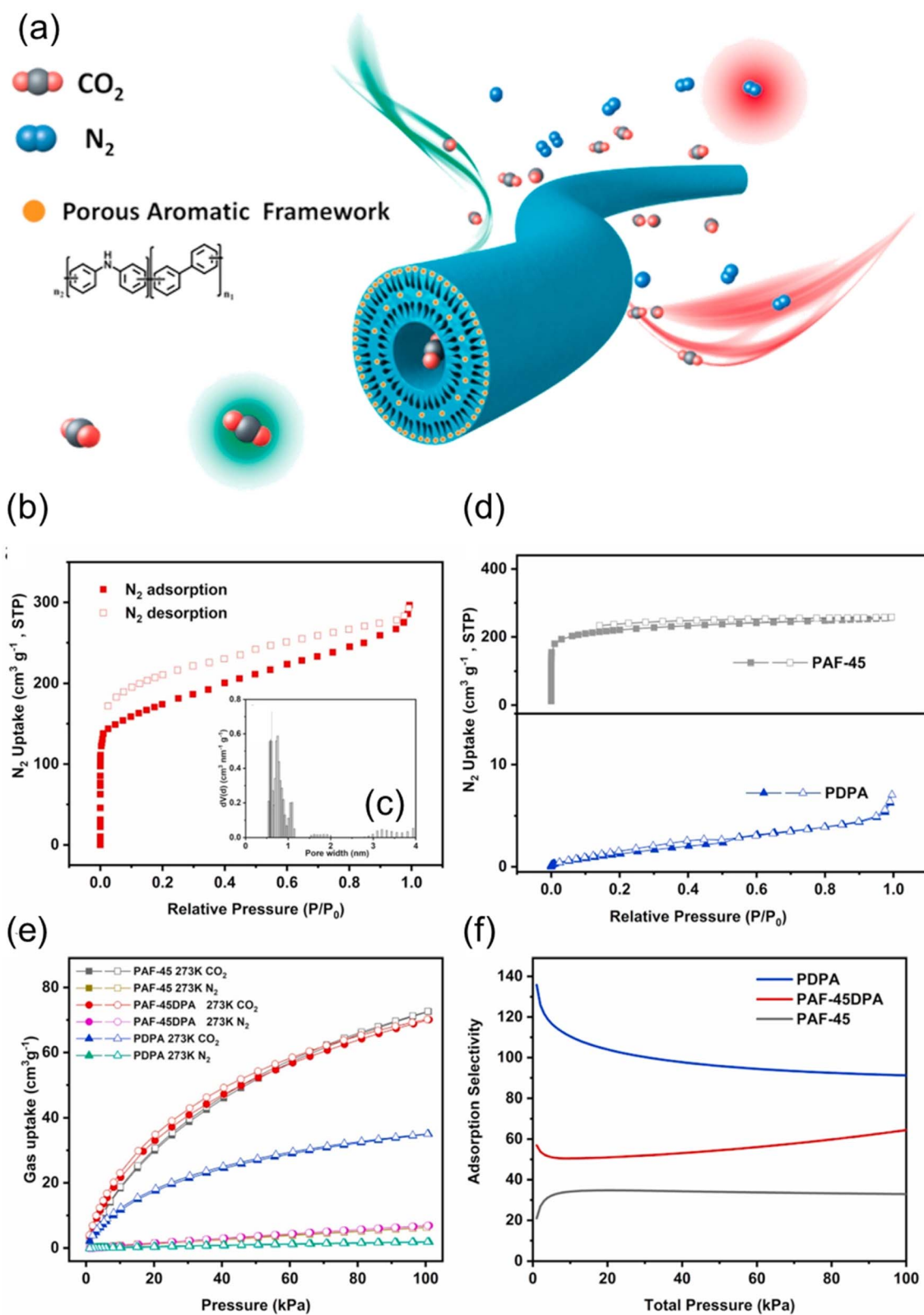


Fig. 18 (a) Schematic representation of CO<sub>2</sub> capture and separation over PAF-45DPA, (b) N<sub>2</sub> adsorption-desorption isotherms of PAF-45DPA at 77 K, (c) pore size distribution from QSDFT analysis, (d) N<sub>2</sub> adsorption-desorption isotherms of PAF-45 and PDPA, (e) CO<sub>2</sub> and N<sub>2</sub> adsorption-desorption isotherms of PAF-45, PAF-45DPA, and PDPA at 273 K, and (f) IAST-predicted CO<sub>2</sub>/N<sub>2</sub> selectivity at 273 K for PAF-45DPA, PDPA, and PAF-45.<sup>143</sup> Adapted with authorization of Elsevier.



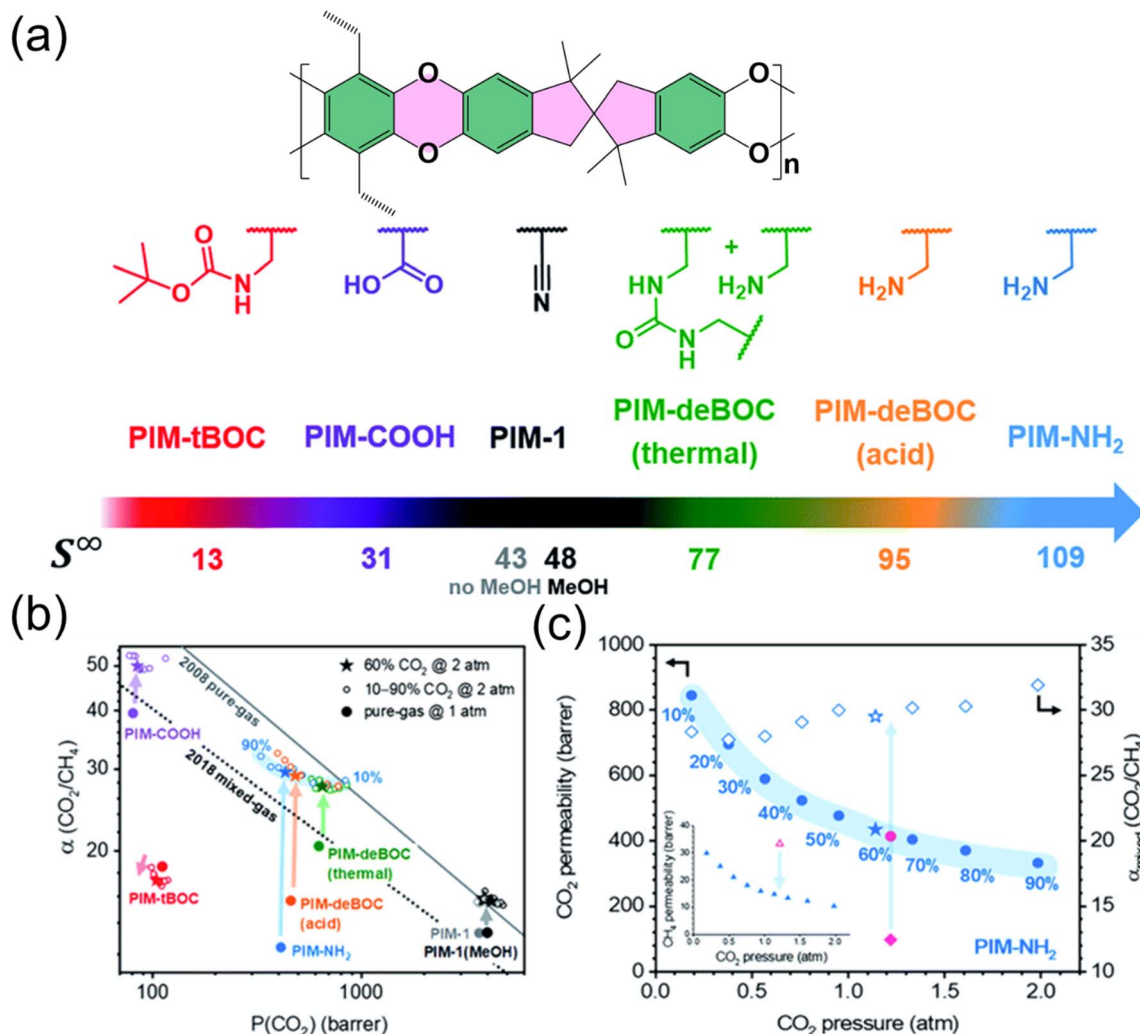


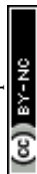
Fig. 19 (a) Structures of PIM-1 and its functionalized derivatives with their infinite-dilution sorption coefficients, (b) Robeson plot comparing pure- and mixed-gas  $\text{CO}_2/\text{CH}_4$  separation performance of aged PIMs, and (c) mixed-gas  $\text{CO}_2$  permeability and  $\text{CO}_2/\text{CH}_4$  selectivity of PIM- $\text{NH}_2$  as a function of  $\text{CO}_2$  fraction, with corresponding  $\text{CH}_4$  permeabilities.<sup>146</sup> Adapted with authorization of the Royal Society of Chemistry.

Table 1 Quantitative benchmarking of representative POPs for  $\text{CO}_2$  capture

POP subclass	Representative material	$\text{CO}_2$ (mmol $\text{g}^{-1}$ ) at 1 bar	$Q_{\text{st}}$ ( $\text{kJ mol}^{-1}$ )	Selectivity ( $\text{CO}_2/\text{N}_2$ , IAST)	Selectivity ( $\text{CO}_2/\text{CH}_4$ )	Stability (cycles)	Regeneration temperature ( $^\circ\text{C}$ )	Synthesis complexity	Ref.
COFs	TaTp-COF	5.0 at 273 K	35	233 (15 : 85)	NA	Excellent (>10 cycles)	Not specified	Moderate	113
CMPs	AC-CMPs	2.07 at 273 K	13	15 (15 : 85)	NA	Excellent (>5 cycles)	60 $^\circ\text{C}$	Moderate	120
CTFs	BMTz-CTFs-600	5.77 at 273 K	38	82 (50 : 50)	NA	Not specified	Not specified	High	126
HCPs	HCPs-3-HFA	3.41 at 273 K	29.2	65 (15 : 85)	NA	75% (>7 cycles)	Not specified	Low	137
PAF	PAF-45DPA/PSF	3.55 mmol $\text{g}^{-1}$	32.7	63 (15 : 85)	N/A	79 GPU 10-day period	Not specified	Simple	143
PIMs	PIM-1	—	—	N/A	$13.5 \pm 0.8$	N/A	N/A	Moderate	146

The most effective POPs for  $\text{CO}_2$  capture are designed by synergistically combining these elements. An ideal adsorbent might feature a rigid 3D scaffold to ensure stability, a high density of ultra-micropores for strong physisorption, and a strategic distribution of amine groups for enhanced

selectivity. This allows for the optimization of the trade-off between high capture capacity (governed by porosity) and strong affinity (governed by chemistry), while maintaining the structural integrity required for long-term recyclability.



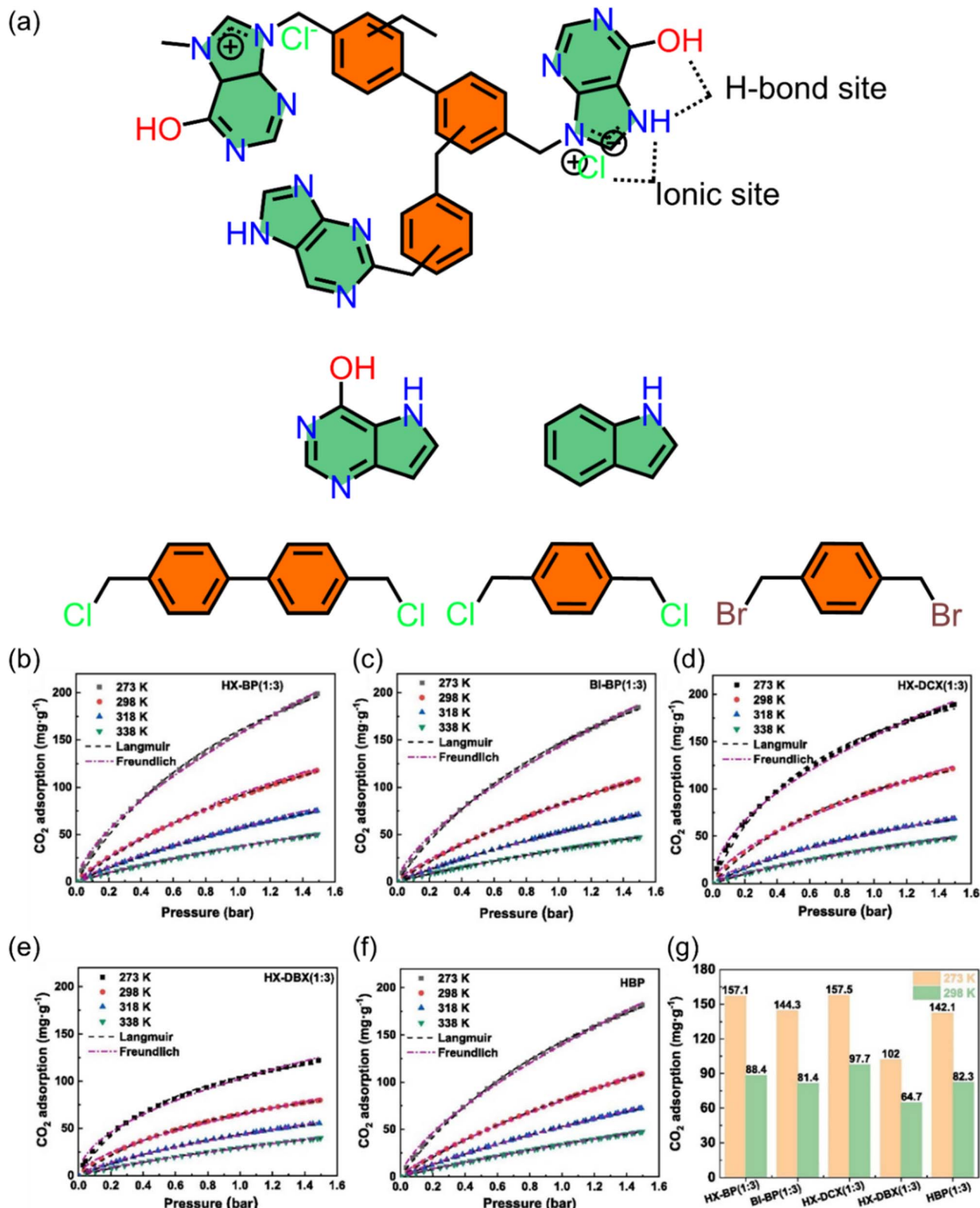


Fig. 20 (a) Molecular representation of the rational design of ionic HCPs, (b–f) CO<sub>2</sub> adsorption isotherms of HCPs measured from 273 to 338 K, and (g) comparison of CO<sub>2</sub> uptake among the different HCPs.<sup>152</sup> Adapted with authorization of Elsevier.

#### 4.4 Computational insights and predictive modelling

Molecular dynamics (MD) simulations provide a powerful computational lens through which researchers can observe and

understand the dynamic behaviour of CO<sub>2</sub> molecules within the porous landscapes of POPs. Unlike static models, MD simulates the motions of atoms and molecules over time under specified



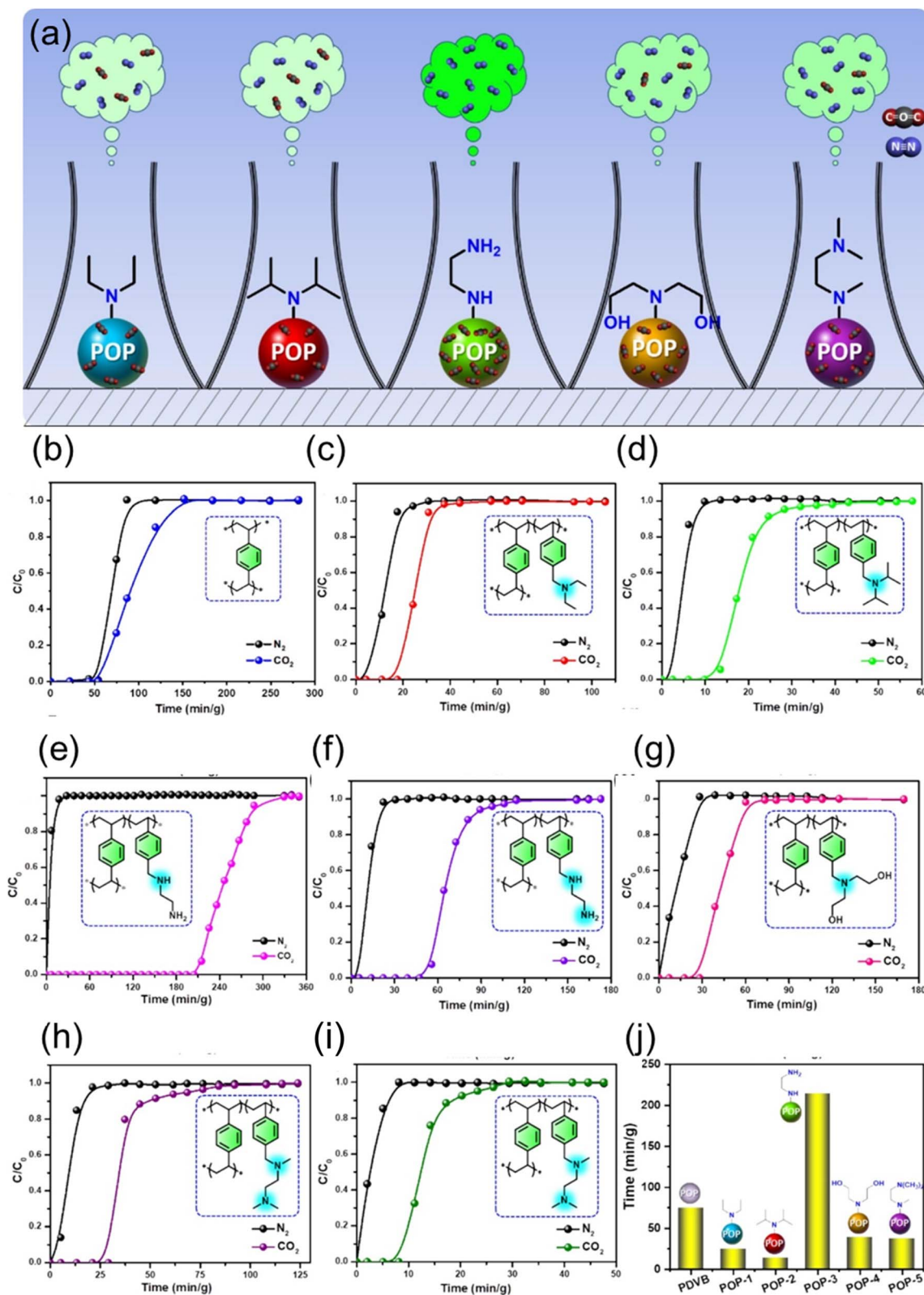


Fig. 21 (a) Tuneable amine functionalized POPs utilized for CO<sub>2</sub> capture, dynamic CO<sub>2</sub>/N<sub>2</sub> (15/85 v/v) breakthrough curves for amino-functionalized POPs at 298 K and 1.0 bar (flow rate: 0.5 mL min<sup>-1</sup>): (b) PDVB, (c) POP-1, (d) POP-2, (e) POP-3, (f) POP-3, (g) POP-4, (h) POP-5, and (i) POP-5, and (j) comparison of breakthrough performance for PDVB and all amino-functionalized POPs.<sup>154</sup> Adapted with authorization of Elsevier.



conditions of temperature and pressure, governed by a force field that describes interatomic interactions. This approach offers unique, time-resolved insights that are often inaccessible through experimentation alone. The primary strength of MD simulations in CO<sub>2</sub> capture research lies in elucidating transport phenomena and dynamic adsorption processes.

**4.4.1 Diffusion kinetics.** MD simulations can quantify the self-diffusion coefficient of CO<sub>2</sub> and other gas molecules (*e.g.*, N<sub>2</sub> and CH<sub>4</sub>) within the pore network. This reveals how quickly gas molecules can move through the material, which is critical for determining adsorption/desorption cycle times in practical applications. Simulations can identify diffusion bottlenecks and show how pore size, shape, and functionalization influence molecular mobility.

**4.4.2 Adsorption mechanism and dynamics.** While Grand Canonical Monte Carlo (GCMC) often predicts equilibrium uptake, MD shows how this uptake is achieved. It can visualize the filling process of pores, the preferential adsorption sites, and the residence time of CO<sub>2</sub> molecules at specific functional groups, providing a molecular-level movie of the capture event.

**4.4.3 Mixture separation and selectivity.** By simulating gas mixtures, MD can reveal competitive diffusion and adsorption between different components. For instance, it can demonstrate why CO<sub>2</sub> might preferentially occupy certain ultra-micropores over N<sub>2</sub> or how water vapor might interact with and potentially block amine functional groups, providing insights into selectivity and stability under realistic, humid conditions.

**4.4.4 Framework flexibility.** Many POPs are not perfectly rigid. MD simulations can account for framework flexibility, showing how the polymer backbone might swell, contract, or dynamically adjust in response to guest molecules, which can significantly impact adsorption capacity and diffusion pathways.<sup>28</sup>

Jeong *et al.*<sup>155</sup> developed nitrogen-rich POPs and incorporated them into mixed-matrix membranes to enhance CO<sub>2</sub>/N<sub>2</sub> separation. MD simulations, combined with experiments, showed that these POP fillers improve CO<sub>2</sub> separation by increasing both CO<sub>2</sub> solubility and diffusivity within the membrane—effects directly linked to the nitrogen-functionalized porous structure. MD played a key role in revealing how CO<sub>2</sub> molecules move through the POP-filled membrane, identifying faster CO<sub>2</sub> transport pathways and stronger CO<sub>2</sub>–polymer interactions compared with N<sub>2</sub> (Fig. 22). Consequently, MD simulations bridge the gap between the static structure of a POP and its dynamic performance. By providing atomistic-level details on gas motion and host–guest interactions, they serve as an indispensable tool for interpreting experimental results, validating hypotheses, and guiding the design of next-generation POPs with optimized pore geometries and surface chemistries for fast and selective CO<sub>2</sub> capture.

## 5 Performance under real-world conditions

### 5.1 Effect of humidity and water vapor

The performance of POPs under real-world flue gas or ambient air conditions is critically dependent on their interaction with

water vapor, which is a major and ubiquitous component. The presence of humidity can have complex and often competing effects on CO<sub>2</sub> capture performance, ranging from cooperative enhancement to detrimental competition, making it a paramount consideration for practical implementation.<sup>156</sup>

**5.1.1 Competitive adsorption and site blocking.** For many physisorptive POPs, particularly those that rely on non-polar or weakly polar surfaces, water vapor acts as a strong competitor. Water molecules can preferentially adsorb in the ultra-micropores that are essential for strong CO<sub>2</sub> physisorption, effectively blocking access and leading to a significant decrease in CO<sub>2</sub> capacity. This is a major challenge for materials like some activated carbons and purely aromatic frameworks.<sup>157</sup>

**5.1.2 Cooperative enhancement for chemisorbents.** Conversely, for amine-functionalized POPs that rely on chemisorption, a certain level of humidity is often essential for the capture mechanism. The reaction between CO<sub>2</sub> and amines to form ammonium carbamates requires the presence of water. In these cases, humidity can significantly boost the CO<sub>2</sub> capture capacity and kinetics. However, an excess of water can lead to the formation of a water layer that dilutes the amine sites and creates a diffusion barrier for CO<sub>2</sub> and in extreme cases can cause hydrolytic degradation of the polymer framework or leaching of functional groups.<sup>158</sup> Wang *et al.*<sup>159</sup> developed an amine-functionalized polyHIPE adsorbent with a high surface area and abundant branched amine groups, enabling strong chemisorptive interaction with CO<sub>2</sub>. Their results showed that the presence of moisture enhanced CO<sub>2</sub> uptake, with the adsorption capacity increasing from 2.40 mmol g<sup>-1</sup> (dry) to 3.25 mmol g<sup>-1</sup> (humid) at 0.1 atm CO<sub>2</sub>. This improvement occurs because water facilitates the formation of ammonium carbamate/bicarbonate species, accelerating CO<sub>2</sub>–amine reaction pathways. At the same time, while moderate humidity boosts capacity and kinetics, excessive water could potentially block pores or dilute amine sites (Fig. 23).

### 5.2 Presence of co-adsorbates (SO<sub>2</sub>, NO<sub>x</sub>, and O<sub>2</sub>)

Real-world flue gas is a complex mixture containing not only CO<sub>2</sub> and N<sub>2</sub> but also trace acidic and oxidative impurities, primarily sulfur oxides (SO<sub>x</sub>), nitrogen oxides (NO<sub>x</sub>), and oxygen (O<sub>2</sub>). The presence of these co-adsorbates poses a significant challenge to the long-term performance and stability of POPs, as they can compete for adsorption sites, react irreversibly with the framework, and lead to permanent degradation.

**5.2.1 Competitive and irreversible adsorption.** SO<sub>2</sub> and NO<sub>2</sub> are highly reactive acidic gases with a stronger affinity for basic sites than CO<sub>2</sub>.<sup>160</sup> In amine-functionalized POPs, these molecules will competitively and often irreversibly bind to the amine sites, forming stable sulfates, sulfites, or nitrates. This process, known as fouling, permanently removes these sites from participating in CO<sub>2</sub> capture, leading to a continuous and irreversible decline in capacity over multiple cycles. Even in non-functionalized POPs, SO<sub>2</sub> can strongly physisorb in ultra-micropores, blocking access for CO<sub>2</sub>.<sup>98,161</sup>

**5.2.2 Oxidative degradation.** The presence of O<sub>2</sub>, especially at elevated temperatures during regeneration, can lead to the



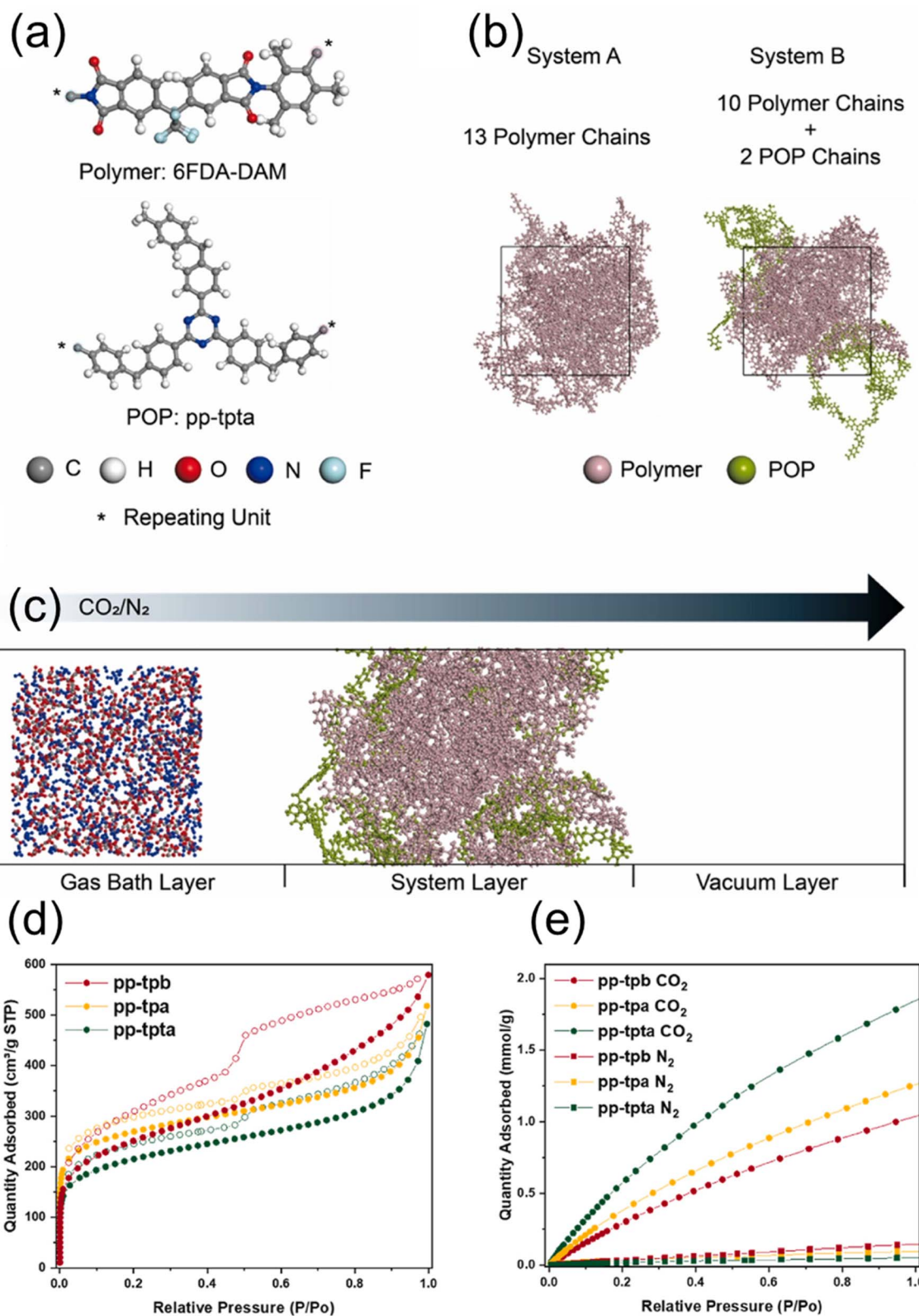


Fig. 22 (a) Molecular structures of the polymer (6FDA-DAM) and the POP (POP, pp-tpta), (b) equilibrated models of system A (pure polymer) and system B (polymer/POP blend), including system details, (c) NEMD simulation setup showing the gas bath, membrane layer, and vacuum region, where a mixture of 200  $\text{CO}_2$  and 800  $\text{N}_2$  molecules diffuses along the z-axis, (d)  $\text{N}_2$  physisorption isotherms of POPs at 77 K, and (e)  $\text{CO}_2$  and  $\text{N}_2$  adsorption isotherms of POPs at 25 °C.<sup>155</sup> Adapted with authorization of Elsevier.



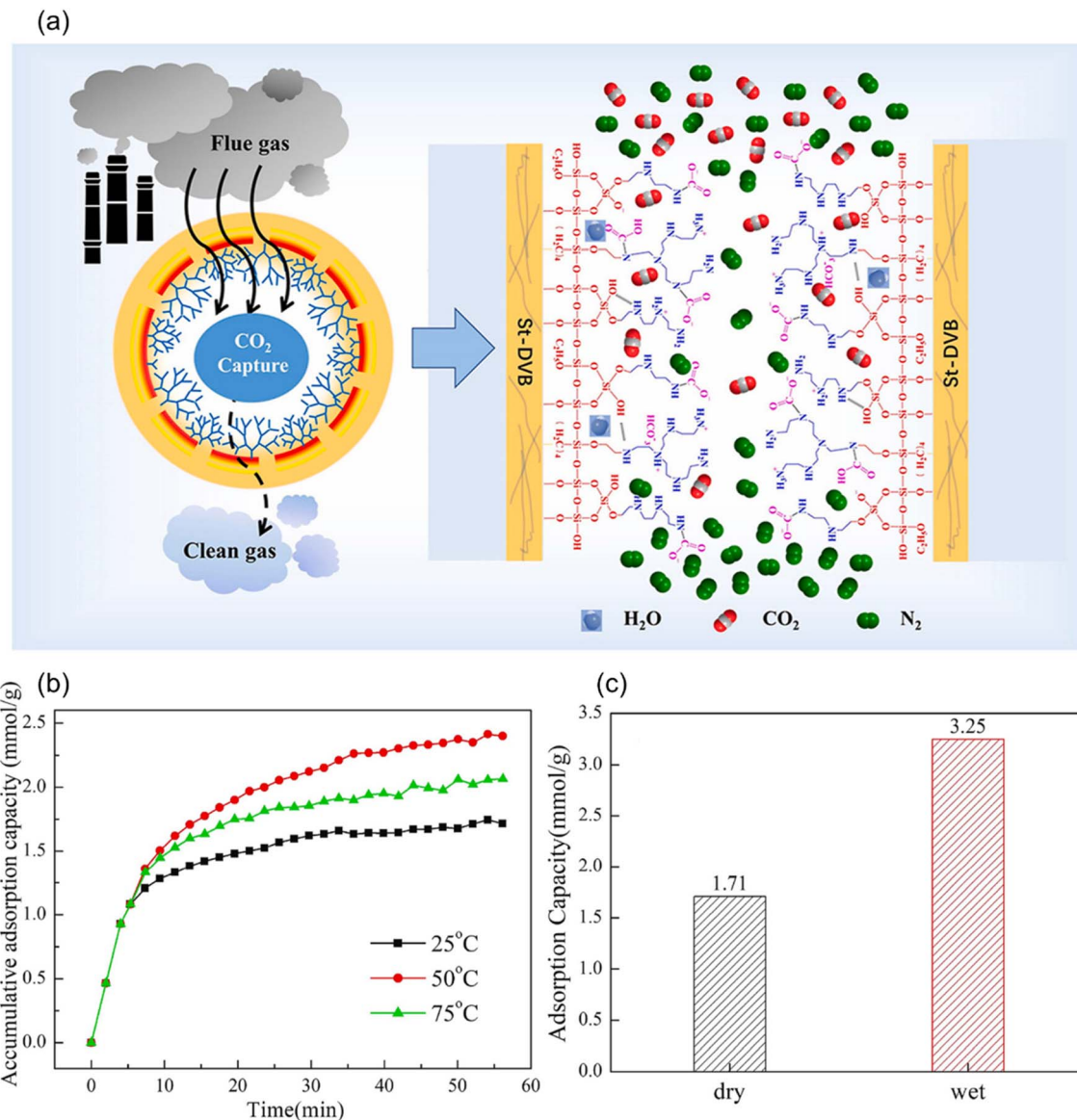


Fig. 23 (a) CO<sub>2</sub> capture over the hierarchically porous amine moiety, (b) effect of temperature and (c) effect of humidity on the CO<sub>2</sub> adsorption capacity of polyHIPE-V1T2-HCP-NH.<sup>159</sup> Adapted with authorization of Elsevier.

oxidative degradation of the polymer framework.<sup>162</sup> This is a particular concern for POPs with vulnerable functional groups. For instance, amine groups can be gradually oxidized to nitro groups or other species, diminishing their CO<sub>2</sub> capture efficiency. The conjugated backbones of CMPs and the organic linkers in other POPs can also undergo oxidation, potentially compromising the structural integrity and porosity of the material over time.<sup>102,163</sup>

**5.2.3 Synergistic damaging effects.** The combination of some impurities can lead to synergistic effects. For example, the co-presence of NO<sub>2</sub> and O<sub>2</sub> can accelerate oxidative degradation. Similarly, SO<sub>2</sub> in the presence of water vapor can form sulfuric acid, leading to acid-catalyzed hydrolysis of sensitive chemical linkages within the POP, such as imine or boronate ester bonds.<sup>164,165</sup>

### 5.3 Temperature and pressure variations

The performance of POPs in CO<sub>2</sub> capture is not static but is profoundly influenced by the operational temperature and pressure of the gas stream. Understanding these dependencies is crucial for selecting the appropriate adsorbent for a given capture scenario and for designing an efficient adsorption-desorption cycle.

**5.3.1 The influence of temperature.** Adsorption is an exothermic process; therefore, temperature is a primary lever controlling adsorption capacity and kinetics. As temperature increases, the capacity of a POP for CO<sub>2</sub> typically decreases significantly.<sup>64</sup> This is because higher thermal energy allows well adsorbed molecules to overcome the energy of the adsorption site, favouring desorption.<sup>166</sup> This principle is harnessed in Temperature Swing Adsorption (TSA) cycles, where



adsorption occurs at a lower temperature (*e.g.*, near flue gas temperature of 40–60 °C) and regeneration is achieved by raising the temperature (*e.g.*, 100–120 °C) to desorb the captured CO<sub>2</sub>. Conversely, higher temperatures increase the diffusion rate of gas molecules within the pore network, potentially leading to faster uptake kinetics. This creates a trade-off: higher temperature speeds up the rate at which capacity is reached but lowers the ultimate capacity.<sup>167</sup> Therefore, the regeneration temperature must be carefully chosen to fall within the thermal stability window of the POP. Exceeding this limit can lead to decomposition, degradation of functional groups (*e.g.*, amines), or collapse of the porous structure. Elsayed *et al.*<sup>168</sup> showed that CO<sub>2</sub> adsorption in LTA-type zeolites is highly temperature-dependent, confirming the general principle that adsorption decreases as temperature increases (Fig. 24). Their thermodynamic data clearly demonstrate this as the process is exothermic ( $\Delta H = -44.04 \text{ kJ mol}^{-1}$ ), spontaneous at low temperature, and becomes less favourable as temperature rises (Gibbs free energy shifts from  $-9.68$  to  $-1.03 \text{ kJ mol}^{-1}$  between 298 and 373 K). They also observed that higher temperatures increase CO<sub>2</sub> diffusion rates, even though the total adsorption capacity drops—exactly matching the trade-off described for POPs.

**5.3.2 The influence of pressure.** Adsorption capacity generally increases with pressure, as described by the adsorption isotherm, but the relationship is highly dependent on the capture technology as we ascribed above.

**5.3.2.1 Post-combustion capture (low pressure).** At the near-ambient pressures of flue gas, the performance of a POP hinges on its uptake in the low-pressure region of the isotherm (0–1 bar). Materials must be engineered for strong affinity (*e.g.*, ultra-micropores and amines) to achieve meaningful capacity under these dilute conditions.<sup>169</sup>

**5.3.2.2 Pre-combustion capture (high pressure).** In high-pressure syngas streams (tens of bars), the POP's performance is determined by its high-pressure capacity. Here, a high surface area and large pore volume are critical to maximize the amount of CO<sub>2</sub> that can be stored *via* physisorption. The working capacity for a Pressure Swing Adsorption (PSA) cycle is the difference in uptake between the high adsorption pressure and the low desorption pressure.<sup>133</sup>

## 5.4 Long-term stability and degradation

The transition of POPs from laboratory marvels to industrially viable adsorbents is contingent upon their long-term stability under continuous operation. This encompasses the material's ability to retain its structural integrity, porosity, and chemical functionality over thousands of adsorption–desorption cycles in the presence of real flue gas constituents. Degradation, the irreversible loss of performance, can occur through several distinct but often interconnected mechanisms.

**5.4.1 Chemical degradation.** This involves the breaking of covalent bonds within the polymer framework or functional groups.

**5.4.1.1 Hydrolytic degradation.** Sensitive chemical linkages, such as boronate esters, some imines, or esters, can be

susceptible to cleavage in the presence of heat and moisture, leading to a collapse of the porous network.<sup>170</sup>

**5.4.1.2 Oxidative degradation.** Trace oxygen O<sub>2</sub> in the flue gas, especially at elevated regeneration temperatures, can gradually oxidize the polymer. This is particularly detrimental to amine functionalities, which can be converted to nitro groups or other oxidized species, losing their ability to chemisorb CO<sub>2</sub>. The conjugated backbones of CMPs are also vulnerable.<sup>171,172</sup>

**5.4.1.3 Acidic gas attack.** The presence of SO<sub>x</sub> NO<sub>x</sub> can cause irreversible chemical poisoning. These strongly acidic gases form stable salts (sulfates and nitrates) with basic sites like amines, permanently removing them from the adsorption pool.<sup>173,174</sup>

**5.4.2 Physical degradation.** This refers to changes in the physical structure and porosity without necessarily breaking primary covalent bonds. Over time, and especially upon exposure to steam during regeneration, some amorphous polymers may undergo a slow relaxation or compaction, reducing their surface area and micropore volume—a phenomenon often observed as physical aging.<sup>175,176</sup> Further, in fluidized-bed or moving-bed reactor systems, the POP particles are subject to mechanical stress and abrasion, which can cause them to fracture into fine powders, leading to increased pressure drop and material loss.<sup>177</sup>

**5.4.3 Thermal degradation.** Prolonged exposure to the high temperatures required for regeneration (*e.g.*, 100–120 °C for amine-sorbents) can induce decomposition if the material's thermal stability is exceeded. This can involve the breakdown of functional groups or even the main polymer scaffold.

**5.4.4 Assessing and ensuring stability.** Long-term stability is evaluated through accelerated aging tests, involving extended multi-cycle adsorption–desorption experiments with simulated flue gas. A stable POP will show a minimal decline in its CO<sub>2</sub> working capacity over hundreds of cycles.<sup>178</sup> The design of stable POPs, therefore, focuses on using hydrolytically and oxidatively robust building blocks and linkages (*e.g.*, C–C bonds in PAFs and triazine rings in CTFs) and functional groups that are resistant to poisoning and degradation. Without demonstrated long-term stability, even the most high-performing POP in initial tests will be impractical for industrial implementation.<sup>63</sup>

## 5.5 From powder to product: shaping, cost, and technology readiness of POPs

For POPs to move from the research laboratory into real industrial applications, they must be transformed from fine powders into practical forms that can be used in large-scale equipment. The as-synthesized POPs are typically fine powders that would cause a high-pressure drop and handling difficulties if used directly in an industrial column, so they must be shaped into larger, robust forms such as pellets, beads, or monoliths. The most common method is binder-assisted granulation, where the POP powder is mixed with a binder material like clay or another polymer and then pressed or extruded into pellets. Choosing the right binder is a balancing act: while a small amount can significantly increase pellet strength, too much binder or the pressing process itself can



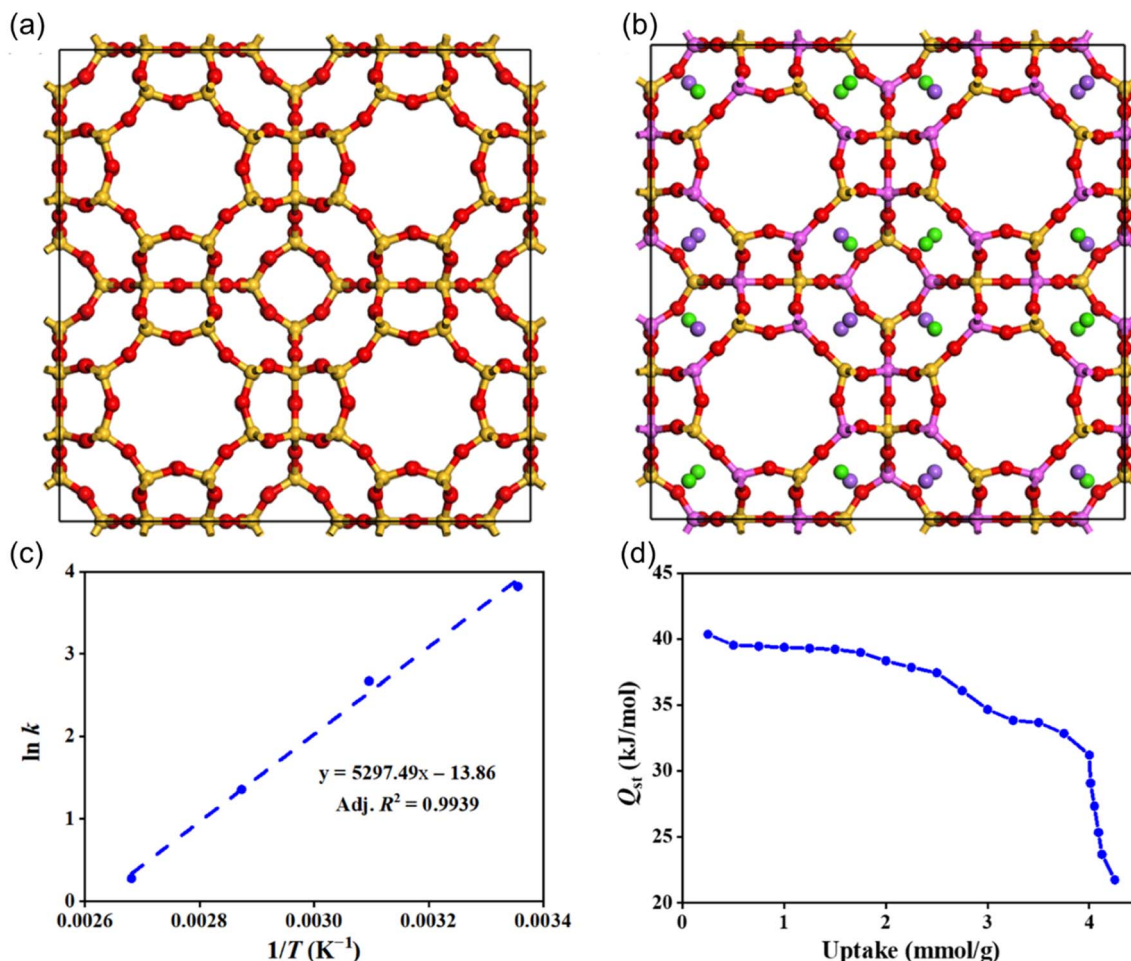


Fig. 24 Molecular visualizations of (a) ITQ-29 and (b) zeolite 5A. Atom colors: Si (yellow), O (red), Al (pink), Na (purple), and Ca (green). Lattice parameters: ITQ-29,  $a = b = c = 23.70 \text{ \AA}$ ; zeolite 5A,  $a = b = c = 24.84 \text{ \AA}$ . (c) van't Hoff plot of CO<sub>2</sub> adsorption on zeolite 5A, with the negative slope indicating an exothermic process, and (d) isosteric heat of adsorption ( $Q_{st}$ ) versus CO<sub>2</sub> uptake, showing a decrease with higher loading due to the gradual filling of lower-energy adsorption sites.<sup>168</sup> Adapted with authorization of MDPI.

block the POP's pores and reduce its CO<sub>2</sub> capture capacity. A more advanced approach is monolith fabrication, where the material is shaped into a honeycomb-like structure with straight, open channels that allow gas to flow through with very little resistance, making them ideal for fast cycling processes. Once shaped, mechanical strength is essential for long-term use. Inside an adsorption column, pellets and monoliths must withstand constant gas pressure, temperature changes during regeneration, and the weight of the material itself without cracking or crumbling. Researchers have shown that optimized pellets can withstand pressures, while emerging monolithic POP structures demonstrate good resilience by bouncing back after compression. The cost of the final shaped product is another major factor in commercial viability. Key cost drivers include the price of starting materials, where using cheap, widely available chemicals like common diamines can potentially bring material costs down. The synthesis method itself matters too—traditional routes using toxic solvents and high temperatures add cost, while greener methods using benign solvents like ethanol at room temperature have already

been scaled to produce sub-kilogram quantities. The shaping process also adds its own cost, which must be factored into the final price. To measure where this technology stands, researchers use the TRL scale from 1 (basic research) to 9 (proven in operation). Most POP research currently sits at TRL 2–3, where concepts are proven in the lab. Reaching the next levels will require scaling up synthesis to produce kilograms of material, proving that shaped pellets or monoliths can withstand thousands of capture-and-release cycles using real flue gas containing water and impurities and successfully testing the material in small pilot-scale reactor systems.<sup>179</sup>

## 6 Emerging trends and future directions

### 6.1 Machine learning and AI-driven design

The field of porous material discovery is undergoing a paradigm shift with the integration of Machine Learning (ML) and AI, moving away from reliance on intuition towards a predictive, data-driven design cycle for POPs. This approach leverages



computational power to uncover complex, non-linear relationships between a POP's chemical structure, its synthesis conditions, and its resulting properties, thereby dramatically accelerating the development of next-generation materials for CO<sub>2</sub> capture.

## 6.2 High-throughput screening approaches

Complementing AI-driven design, high-throughput screening (HTS) represents a powerful experimental paradigm for rapidly evaluating vast libraries of POPs. This approach adapts methodologies from pharmaceutical and materials science to systematically synthesize and test numerous POP variants in parallel, dramatically accelerating the empirical discovery and optimization process. By miniaturizing and automating synthesis and characterization, HTS enables a comprehensive exploration of the multi-dimensional parameter space governing POP performance.

## 6.3 Multi-functional POPs

Moving beyond their role as passive adsorbents, a frontier in POPs research is the design of multi-functional materials that not only capture CO<sub>2</sub> but also actively transform it or perform additional valuable tasks within a single integrated platform. This approach enhances the economic viability and utility of carbon capture by creating systems that do more than just sequester CO<sub>2</sub>, potentially enabling a circular carbon economy. The development of multi-functional POPs represents a shift from a singular focus on adsorption metrics towards a holistic design of "smart" materials that integrate capture, sensing, and conversion. This model not only addresses the challenge of CO<sub>2</sub> emissions but also adds value to the capture process, creating a more compelling and sustainable pathway for its implementation.

## 6.4 DAC applications

The application of POPs in DAC represents one of the most challenging yet potentially transformative directions for this polymer class. DAC requires the selective extraction of CO<sub>2</sub> from the ultra-dilute atmosphere, a task with unique thermodynamic and kinetic demands that push the limits of adsorbent design. POPs, with their unparalleled synthetic tunability, are at the forefront of developing next-generation solid sorbents for this critical negative emissions technology.

## 6.5 Next-generation synthesis methods

The pursuit of commercially viable POPs for CO<sub>2</sub> capture is driving innovation not only in molecular design but also in every method used to create them. Next-generation synthesis aims to exceed the limitations of traditional solvothermal routes, focusing on principles of scalability, sustainability, and precision to enable the practical production of advanced POPs. These emerging methodologies seek to make the synthesis faster, greener, and more amenable to industrial manufacturing.

The pursuit of sustainable POPs can be guided by recent advances in biomass-derived carbons. For example, phosphorus-doped carbons from lotus petiole waste using sodium phytate as a green activating agent achieve notable CO<sub>2</sub> uptake (2.51 mmol g<sup>-1</sup>) through a one-step, environmentally friendly process.<sup>180</sup> Similarly, the use of sodium metaborate tetrahydrate (NaBO<sub>2</sub>·4H<sub>2</sub>O) as a non-corrosive alternative to KOH or ZnCl<sub>2</sub> for activating water chestnut shells represents a significant step towards greener activation chemistry.<sup>181,182</sup> These examples demonstrate that high performance and sustainability can be synergistically achieved.

Importantly, the future of sustainable CO<sub>2</sub> capture lies in the convergence of performance with green chemistry. For POPs, this translates directly into several of our actionable research directions, including prioritizing bio-based monomers (*e.g.*, from lignin, vanillin, tannins, or other renewable resources) over petrochemical-derived building blocks; adopting solvent-free (mechanochemical) or aqueous-based methods and replacing toxic or precious-metal catalysts with earth-abundant or organocatalysts; and moving beyond performance metrics (capacity and selectivity) to systematically evaluate the environmental footprint of the entire material life cycle using Life Cycle Assessment (LCA) tools.

By embedding these principles into the design pipeline, the next generation of POPs can achieve not only high efficiency but also true environmental sustainability, ensuring that they contribute positively to the net-zero goal they are intended to serve.

# 7 Challenges and opportunities

## 7.1 Current limitations

Despite their considerable promise, the widespread deployment of POPs for CO<sub>2</sub> capture faces several significant challenges that must be addressed to transition from laboratory excellence to industrial relevance.

## 7.2 Scalability barriers

A primary obstacle is the difficulty in synthesizing many high-performance POPs on a kilogram-to-ton scale. Actually, the intricate, multi-step synthesis of organic building units is often cost-prohibitive and resource-intensive at large scales. Further, many protocols rely on extended reaction times (days), high temperatures and pressures, and air-sensitive catalysts, which pose significant engineering and safety challenges for scale-up. Furthermore, the use of large volumes of toxic, high-boiling-point solvents generates substantial waste, and the energy-intensive purification (*e.g.*, Soxhlet extraction) becomes impractical commercially. Most importantly, processing the synthesized powder into mechanically robust, shaped bodies for use in industrial reactors without losing porosity or performance remains a non-trivial challenge.

## 7.3 Stability issues

Long-term operational stability under real flue gas conditions is a critical concern. Firstly, polymer frameworks, particularly



those with hydrolytically sensitive linkages (*e.g.*, boronate esters and some imines), can decompose in the presence of heat and moisture. Furthermore, functional groups like amines are susceptible to oxidative degradation by O<sub>2</sub> or irreversible poisoning by SO<sub>x</sub> and NO<sub>x</sub>. Secondly, over multiple adsorption–desorption cycles, some amorphous POPs can undergo physical aging and pore collapse, especially when exposed to steam during regeneration, leading to a permanent loss of surface area and capacity. Thirdly, in dynamic reactor systems, POP particles must resist abrasion and fragmentation to prevent powdering and increased pressure drop.

#### 7.4 Cost competitiveness

The overall cost of CO<sub>2</sub> capture using POPs must be competitive with established technologies like amine scrubbing. Notably, the combined cost of complex monomers, precious metal catalysts, and solvent management often results in a prohibitively high price for the final adsorbent. Moreover, while – in many reported cases – some POPs offer lower regeneration energy than amines, this advantage must be substantial enough to offset their potentially higher initial cost. The energy required for compression and vacuum pumping also contributes to the operational expense. On the other hand, a short operational lifespan due to chemical or physical degradation necessitates frequent sorbent replacement, severely impacting the leveled cost of capture. A material with a high initial capacity but poor stability is ultimately not economically viable.

#### 7.5 Opportunities for innovation

The challenges and knowledge gaps facing POPs simultaneously delineate a rich landscape for transformative innovation. By addressing these hurdles through creative scientific and engineering approaches, POPs have the potential to redefine the economics and efficiency of carbon capture.

**7.5.1 Molecular-level precision design.** The synthetic versatility of POPs offers an unparalleled opportunity to move beyond simple functionalization to the precise engineering of binding sites. This involves designing frameworks with cooperative effects, where a combination of functional groups (*e.g.*, an amine adjacent to a polar aromatic system) works together to bind CO<sub>2</sub> with optimal energy—strong enough for high selectivity but weak enough for low-energy regeneration. The emerging integration of machine learning and AI will be pivotal in navigating this vast design space to identify such high-performing structures.

**7.5.2 Advanced manufacturing and scalable synthesis.** There is a significant opportunity to develop next-generation, cost-effective synthesis routes. This includes designing novel polymerization reactions that use earth-abundant catalysts and benign solvents, pioneering continuous flow manufacturing processes for consistent quality and scale, and creating *in situ* methods for forming POPs into monolithic structures or directly depositing them on supports, thus avoiding the costly powder-shaping step.

**7.5.3 Multi-functional polymer platforms.** Innovation can shift the paradigm from passive adsorbents to active, multi-

functional systems. Opportunities include designing POPs that integrate capture with conversion, acting as catalysts to transform captured CO<sub>2</sub> into valuable chemicals or fuels directly within their pores. Furthermore, the development of “smart” POPs that change colour or conductivity upon CO<sub>2</sub> saturation could enable real-time process monitoring and optimized regeneration cycles, enhancing overall system efficiency.

**7.5.4 Tailored POPs for specific niches.** Instead of a one-size-fits-all approach, there is a major opportunity to design POPs for specific, high-value capture applications. This includes creating ultra-stable, water-tolerant materials for humid DAC, highly selective POPs for CO<sub>2</sub> removal from natural gas (purification), or robust frameworks for capturing CO<sub>2</sub> from industrial processes with unique gas compositions. By seizing these opportunities, the field can overcome current limitations and unlock the full potential of POPs. The goal is to transition from creating materials that are merely scientifically interesting to engineering robust, scalable, and economically viable solutions that can make a tangible impact on global carbon emissions.

## 8 Conclusions and outlook

This review has detailed the significant progress in engineering POPs for CO<sub>2</sub> capture, establishing them as a formidable class of materials due to their exceptional tunability, high surface area, and robust frameworks. Our review demonstrates that the strategic design of pore architecture is paramount for achieving strong physisorption and high selectivity, while chemical functionalization, particularly amine grafting and heteroatom doping, dramatically enhances CO<sub>2</sub> affinity and selectivity in low-pressure scenarios such as post-combustion capture and direct air capture. Furthermore, the stability of the covalent bonds within the framework is a critical differentiator, with materials featuring C–C, triazine, and other robust linkages demonstrating superior resistance to harsh operational conditions compared to more labile counterparts. While performance in idealized laboratory settings is promising, real-world viability is contingent upon performance under realistic conditions, including the presence of moisture, trace oxidants, and acidic gases, which can lead to competitive adsorption and degradation. To transition POPs from academic interest to industrial reality, future research must focus on several concrete and actionable directions. First, targeted pore engineering should move beyond surface area maximization to focus on the precise design of ultra-micropores (<0.8 nm) with narrow size distributions tailored for specific CO<sub>2</sub> partial pressures, achieved through molecular building blocks with fixed geometries that lock in optimal pore dimensions, while hierarchical pore architectures integrating mesopores can enhance adsorption kinetics. Second, advanced heteroatom functionalization should explore cooperative binding sites—such as amine–hydroxyl pairs or amine–triazine combinations—that work synergistically to achieve an enthalpy of adsorption in the “Goldilocks zone” (50–70 kJ mol<sup>−1</sup>), balancing strong selectivity with low-temperature regeneration (≤80 °C), while



systematically investigating doping density and spatial distribution to maximize site utilization without pore blocking. Third, scalable and green synthesis must prioritize solvent-free or aqueous-based routes using earth-abundant, low-cost monomers derived from biomass or commodity chemicals, replacing precious metal catalysts with organocatalysts or recyclable heterogeneous catalysts and transitioning from batch to continuous flow manufacturing for consistent, large-scale production with reduced environmental footprints. Fourth, the development of hybrid and composite materials—including POP-polymer mixed-matrix membranes, POP-metal nanoparticle composites for integrated capture and conversion, and POP-ionic liquid hybrids—offers untapped potential for multifunctional performance. Fifth, dedicated studies on long-term stability under realistic conditions are needed to elucidate molecular degradation mechanisms, guiding the design of self-healing or protective frameworks and the development of accelerated aging protocols that reliably predict multi-year performance. Sixth, data-driven discovery and validation require the creation of open-access, standardized databases to train robust machine learning models for high-throughput virtual screening and inverse design, predicting exact monomer combinations and topologies required to meet specific performance targets before experimental validation. Finally, application-specific design must tailor POPs for individual capture scenarios: ultra-microporous, hydrolytically stable frameworks with moderate amine density for post-combustion capture; ultra-high surface area materials with large pore volumes for pre-combustion capture; frameworks with hydrophobic pore environments that exclude water while hosting optimized amine sites for DAC; and size-selective pores for CO<sub>2</sub>/CH<sub>4</sub> separation with minimal methane loss for natural gas upgrading. By systematically addressing these concrete research directions—moving from broad statements to targeted, actionable strategies—POPs are poised to transition from academic curiosity to a cornerstone technology in the global effort to achieve a net-zero future.

## Author contributions

Mohammed G. Kotp: writing – review & editing, writing – original draft, visualization, investigation, data curation, conceptualization. Shiao-Wei Kuo: review & editing, resources, project administration.

## Conflicts of interest

There are no conflicts to declare.

## Data availability

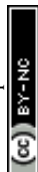
No primary research results, software or code have been included and no new data were generated or analysed as part of this review.

## Acknowledgements

The study was supported by the National Science and Technology Council, Taiwan (NSTC 114-2223-E-110-001).

## References

- Q. Ge, Y. Liu, W. You, Y. Li, W. Wang, L. Yang, L. Xie, K. Li, L. Wang and M. Ma, *Sci. Adv.*, 2025, **11**, eadx5714.
- B. Shao, Y. Jiang, S. Li, Z. Xie, Z.-Q. Wang, S. Dai, H. Liu, F. Qian and J. Hu, *ACS Catal.*, 2025, **15**, 18315–18325.
- Y.-S. Chang, M.-Y. Ho, C.-W. Wu and Y.-J. Chang, *Process Saf. Environ. Prot.*, 2025, **200**, 107419.
- S. R. Pacella, C. A. Brown, R. G. Labiosa, B. Hales, T. C. Mochon Collura, W. Evans and G. G. Waldbusser, *J. Geophys. Res., Oceans*, 2024, **129**, e2023JC020313.
- A. P. Schurer, M. E. Mann, E. Hawkins, S. F. Tett and G. C. Hegerl, *Nat. Clim. Change*, 2017, **7**, 563–567.
- S. I. Seneviratne, J. Rogelj, R. Séférian, R. Wartenburger, M. R. Allen, M. Cain, R. J. Millar, K. L. Ebi, N. Ellis and O. Hoegh-Guldberg, *Nature*, 2018, **558**, 41–49.
- M. Meinshausen, J. Lewis, C. McGlade, J. Gütschow, Z. Nicholls, R. Burdon, L. Cozzi and B. Hackmann, *Nature*, 2022, **604**, 304–309.
- Y. Kumar and J. Sangwai, *Energy Fuels*, 2025, **39**, 5007–5033.
- S. A. Ali, S. N. Shah, M. A. Karim, S. A. M. Hashmi, F. Ahmad, K. Habib, A. Sami and M. Abdullah, *Energy Fuels*, 2025, **39**, 9285–9315.
- P. Stierne, A. Verdin, N. Johnsson, A. Jaworski, D. Prietzel, N. Hedin and J. Yuan, *ACS Appl. Mater. Interfaces*, 2025, **17**, 60400–60410.
- H. Qiu, Q. Long, Y. Bai, X. Fu, C. Liu, G. Jing, Z. Zhou and B. Lv, *Chem. Eng. J.*, 2025, **520**, 165388.
- P.-Y. Liu, Y.-F. Lu, Y.-C. Kuo and Y.-J. Lin, *Ind. Eng. Chem. Res.*, 2025, **64**, 24779–24796.
- Y. Song, J. Li, D. Chi, Z. Xu, J. Liu, M. Chen and Z. Wang, *Chem. Commun.*, 2025, **61**, 15972–16001.
- M. G. Mohamed, M. G. Kotp, A. Osama Mousa, Y.-S. Li and S.-W. Kuo, *ACS Appl. Energy Mater.*, 2025, **4**, 2389–2402.
- C.-W. Hsiao, A. M. Elewa, M. G. Mohamed, M. G. Kotp, M. M.-C. Chou and S.-W. Kuo, *Colloids Surf., A*, 2024, **699**, 134658.
- M. M. Ayad, W. A. Amer and M. G. Kotp, *Mol. Catal.*, 2017, **439**, 72–80.
- Y.-C. Kao, P.-H. Chen, C.-Y. Chen, H.-W. Chen, W.-C. Chen, M. Ejaz, M. G. Kotp, M. G. Mohamed, H. Karim and S.-W. Kuo, *Polymer*, 2025, **338**, 129041.
- M. G. Kotp, S.-W. Kuo and A. F. M. EL-Mahdy, *Colloids Surf., A*, 2024, **685**, 133210.
- M. Hussain, A. S. Ali, T. Kousar, F. Mahmood, A. Haruna, Z. U. Zango, H. Adamu, M. G. Kotp, I. A. Abdulganiyyu and B. E. Keshta, *Sustain. Chem. One World*, 2025, **5**, 100047.
- M. G. Kotp, J. Lüder, S.-W. Kuo and A. F. M. EL-Mahdy, *Mater. Adv.*, 2024, **5**, 4142–4150.
- M. G. Kotp, A. F. M. EL-Mahdy, T.-L. Yang and S.-W. Kuo, *Microporous Mesoporous Mater.*, 2022, **331**, 111669.



- 22 M. G. Kotp, A. F. M. EL-Mahdy and S.-W. Kuo, *Polym. Chem.*, 2025, **16**, 422–432.
- 23 M. M. Ayad, W. A. Amer, M. G. Kotp, I. M. Minisy, A. F. Rehab, D. Kopecký and P. Fitl, *RSC Adv.*, 2017, **7**, 18553–18560.
- 24 M. G. Kotp, C.-L. Chang and A. F. M. EL-Mahdy, *J. Water Process Eng.*, 2023, **53**, 103675.
- 25 M. G. Kotp, S. U. Sharma, J.-T. Lee, A. F. M. EL-Mahdy and S.-W. Kuo, *J. Taiwan Inst. Chem. Eng.*, 2022, **134**, 104310.
- 26 M. Ejaz, M. G. Mohamed, M. G. Kotp, A. M. Elewa and S.-W. Kuo, *Colloids Surf., A*, 2025, **722**, 137239.
- 27 M. G. Kotp, N. L. Torad, H. Nara, W. Chaikittisilp, J. You, Y. Yamauchi, A. F. M. EL-Mahdy and S.-W. Kuo, *J. Mater. Chem. A*, 2023, **11**, 15022–15032.
- 28 M. G. Kotp, M. G. Mohamed, P.-T. Wang, A. E. Hassan, A. M. Elewa and S.-W. Kuo, *ACS Polym. Au*, 2025, **5**, 379–393.
- 29 H. Kumar, O. A. Britto, M. Thamizharasan, G. Arthanareeswaran and M. R. Viswanathan, *Mater. Chem. Front.*, 2026, **10**, 184–205.
- 30 X. Zhang, H. Zhang, S. Gu, J. Tang and G. Yu, *ACS Appl. Mater. Interfaces*, 2025, **17**, 42530–42540.
- 31 C. F. Martin, E. Stöckel, R. Clowes, D. J. Adams, A. I. Cooper, J. J. Pis, F. Rubiera and C. Pevida, *J. Mater. Chem.*, 2011, **21**, 5475–5483.
- 32 D. R. Kumar, C. Rosu, A. R. Sujana, M. A. Sakwa-Novak, E. W. Ping and C. W. Jones, *ACS Sustain. Chem. Eng.*, 2020, **8**, 10971–10982.
- 33 G. T. Rochelle, *Carbon Capture Sci. Technol.*, 2024, **11**, 100192.
- 34 M. H. Nawaz, S. Santhoshkumar, T. H. Ho, B. Arumugam, M. G. Mohamed, T. V. Vu, Y. M. Nabil, M. G. Kotp, L.-W. Tu and H.-D. Yang, *Chem. Eng. J.*, 2025, **527**, 171521.
- 35 A. Aslani, H. Masoumi and A. Ghaemi, *CO<sub>2</sub> Adsorbents: Advances in Materials, Technologies, and Applications for a Sustainable Future*, 2025.
- 36 M. G. Mohamed, T.-C. Chen and S.-W. Kuo, *Macromolecules*, 2021, **12**, 5866–5877.
- 37 I. Ul Hassan, S. A. Hussien, R. Sathyamurthy, U. Zahid, U. Ahmed, V. M. Reddy and A. G. Abdul Jameel, *Energy Fuels*, 2025, **39**, 13931–13968.
- 38 M. Shen, W. Guo, L. Tong, L. Wang, P. K. Chu, S. Kawi and Y. Ding, *Chem. Soc. Rev.*, 2025, **54**, 2762–2831.
- 39 K. Atsonios, K. Panopoulos, A. Doukelis, A. Koumanakos and E. Kakaras, *Energy*, 2013, **53**, 106–113.
- 40 F. Raganati and P. Ammendola, *Energy Fuels*, 2024, **38**, 13858–13905.
- 41 S. Nandi, J. Rother, D. Chakraborty, R. Maity, U. Werner-Zwanziger and R. Vaidhyanathan, *J. Mater. Chem. A*, 2017, **5**, 8431–8439.
- 42 Y. Wang, F. Gao, Y. Niu, J. Zhang, K. Chen, Y. Zhou, X. Tang, S. Zhao and H. Yi, *J. Mater. Chem. A*, 2025, **13**, 23323–23353.
- 43 M. Vorokhta, M. I. M. Kusdhany, M. Švábová, M. Nishihara, K. Sasaki and S. M. Lyth, *Sep. Purif. Technol.*, 2025, **354**, 129054.
- 44 D. Chakraborty, R. Chatterjee, S. Mondal, S. K. Das, V. Amoli, M. Cho and A. Bhaumik, *ACS Appl. Mater. Interfaces*, 2023, **15**, 48326–48335.
- 45 Y. Wang, J. Guo, L. Qu, P. Webley, H. Ding and G. K. Li, *Chem Catal.*, 2025, **5**, 101254.
- 46 R. Norouzbeigi, *CO<sub>2</sub> Adsorbents: Advances in Materials, Technologies, and Applications for a Sustainable Future*, 2025, p. 125.
- 47 T.-L. Lee, A. M. Elewa, M. G. Kotp, H.-H. Chou and A. F. M. EL-Mahdy, *Chem. Commun.*, 2021, **57**, 11968–11971.
- 48 M. G. Kotp, M. G. Mohamed, A. O. Mousa and S.-W. Kuo, *Eur. Polym. J.*, 2025, **227**, 113786.
- 49 Y. Du, T. Gao, G. T. Rochelle and A. S. Bhowan, *Int. J. Greenhouse Gas Control*, 2021, **111**, 103473.
- 50 F. Xia, Z. Yang, A. Adeosun, A. Gopan, B. M. Kumfer and R. L. Axelbaum, *Fuel*, 2016, **181**, 1170–1178.
- 51 M. De Joannon, A. Chinnici, P. Sabia and R. Ragucci, *Chem. Eng. J.*, 2012, **211**, 318–326.
- 52 P. Ma, W. Zhou, C. Yu, Z. Liu, Q. Chen, S.-P. Sun and X. Wang, *Sep. Purif. Technol.*, 2025, **380**, 135242.
- 53 B. Ma, N. Qin, Q.-Q. Yan, S. Zhang, X. Wang, L. Bao and X. Lu, *Digital Discovery*, 2026, **5**, 523–547.
- 54 H. Xu, Y. Chen and Z. He, *Sep. Purif. Technol.*, 2025, **382**, 136054.
- 55 S. Pal, E. P. Roberts, M. Trifkovic and G. Natale, *Commun. Mater.*, 2025, **6**, 130.
- 56 P. D. Raju, A. R. Sujatha, S. Krishnan and C. V. Suneesh, *Nanoscale*, 2025, **17**, 22100–22121.
- 57 Y. Zhou, S. Li, Y. Bai, B. Ji, X. Kong, B. Hu and J. Zhang, *Energy Fuels*, 2024, **39**, 626–637.
- 58 D. Wu, M. Yang, J. Yu, M. Dyballa, P. Yang, M. Li, G. Hou, M. Hunger and W. Dai, *Chem. Soc. Rev.*, 2025, **54**, 9192–9244.
- 59 L. Jiang, F. Bao, Y. Peng, Z. Zhao, Y. Wang, Y. Song, J. Li, K. Lv, J. Zhang and K. Yuan, *Microporous Mesoporous Mater.*, 2025, **381**, 113338.
- 60 S. Raza, A. Abid, I. Areej, S. Nazeer, A. K. Qureshi and B. Tan, *ACS Appl. Polym. Mater.*, 2024, **6**, 6843–6851.
- 61 H. Zhang, H. Wang, T. Gao, S. Pan, C. Liu, C. Li and X. Tao, *Carbon*, 2025, **234**, 120004.
- 62 M. Abdalla, M. Essalhi, M. H. Elsayed, A. Sabbah, M. G. Mohammed, I. H. Aljundi and M. M. Abdelnaby, *ACS Appl. Polym. Mater.*, 2025, **7**, 8731–8742.
- 63 A. Mollahosseini, M. N. Dafchahi, S. K. Salestan, J. W. Chew, M. Mozafari, M. Soroush, S. Hrapovic, U. D. Hemraz, R. Giro and M. B. Steiner, *Energy Environ. Sci.*, 2025, **18**, 5025–5092.
- 64 M. G. Kotp and S.-W. Kuo, *Polymers*, 2024, **13**, 1759.
- 65 M. G. Kotp, A. F. M. EL-Mahdy, M. M. Chou and S.-W. Kuo, *New J. Chem.*, 2024, **48**, 14435–14443.
- 66 P. N. Singh, M. G. Mohamed, M. G. Kotp, T. Mondal, S. V. Chaganti, M. Ibrahim, S. U. Sharma, Y. Ye and S.-W. Kuo, *ACS Appl. Polym. Mater.*, 2025, **7**, 3324–3336.
- 67 J. R. Serrano, P. Piqueras, E. J. Sanchis and F. J. García, *Energy Convers. Manage.*, 2025, **342**, 120034.
- 68 H. Pal, A. Karmakar, A. Sadhukhan, K. Koner, S. Karak, R. K. Sharma, M. Ghosh, K. K. Dey, B. Pathak and S. Kundu, *Adv. Funct. Mater.*, 2024, **34**, 2408255.
- 69 J. Zhou, M. Deissenroth-Uhrig and M. Gallei, *Adv. Funct. Mater.*, 2025, e20959.



- 70 Y. Song and S. Ma, *Chem. Sci.*, 2025, **16**, 11740–11767.
- 71 M. K. Wong, J. J. Foo, J. Y. Loh and W. J. Ong, *Adv. Energy Mater.*, 2024, **14**, 2303281.
- 72 C. Y. Chuah, Y. L. Ho, A. M. H. Syed, K. G. K. Thiyvalakshmi, E. Yang, K. Johari, Y. Yang and W. C. Poon, *Ind. Eng. Chem. Res.*, 2025, **64**, 4117–4147.
- 73 X. Wang, Y. Chen, A. Lindbråthen, Z. Waris and L. Deng, *Chem. Eng. J.*, 2025, **512**, 162377.
- 74 S. Zhao, Y. Zhang, L. Li, J. Feng, W. Qiu, Y. Ning, Z. Huang and H. Lin, *Sep. Purif. Technol.*, 2025, **354**, 129586.
- 75 M. G. Kotp and S.-W. Kuo, *Mater. Today Chem.*, 2024, **41**, 102299.
- 76 M. Joshi, X. Ren, T. Lin and R. Joshi, *Small*, 2025, **21**, 2406706.
- 77 L. Joos, K. Lejaeghere, J. M. Huck, V. Van Speybroeck and B. Smit, *Energy Environ. Sci.*, 2015, **8**, 2480–2491.
- 78 G. Cui, J. Wang and S. Zhang, *Chem. Soc. Rev.*, 2016, **45**, 4307–4339.
- 79 A. Chamoun-Farah, L. M. Cañada, J. F. Brennecke and B. D. Freeman, *J. Membr. Sci.*, 2025, **727**, 124081.
- 80 R. Krishna and J. M. van Baten, *Sep. Purif. Technol.*, 2025, **362**, 131757.
- 81 S. A. Khan, S. Ahmed, S. Ali and F. Altaf, *Carbon Neutrality*, 2025, **4**, e70063.
- 82 V. Ramar, X. Zhang, H. Zhang, H. Tan and Y. Zhao, *Small Methods*, 2025, **9**, e00717.
- 83 E. Pérez-Botella, S. Valencia and F. Rey, *Chem. Rev.*, 2022, **122**, 17647–17695.
- 84 M. Zhang, J. Huang, F. Meng, C. Zhang and Z. Zhang, *Dalton Trans.*, 2025, **54**, 17383–17399.
- 85 M. Ejaz, M. G. Mohamed and S.-W. Kuo, *Polym. Chem.*, 2023, **14**, 2494–2509.
- 86 A. Kumari, K. Kaushik, A. Shankar, R. Aneja, A. Chauhan and V. K. Saini, *Fuel*, 2025, **399**, 135651.
- 87 G. Li, H. Yu, D. Ji, C. Zhu, K. Thu and T. Miyazaki, *Energy*, 2025, **328**, 136506.
- 88 M. G. Mohamed, Y.-C. Kao, B.-X. Su, H. Karim and S.-W. Kuo, *Sep. Purif. Technol.*, 2025, **387**, 136692.
- 89 C. A. Trickett, A. Helal, B. A. Al-Maythaly, Z. H. Yamani, K. E. Cordova and O. M. Yaghi, *Nat. Rev. Mater.*, 2017, **2**, 17045.
- 90 H. Lyu, O. I.-F. Chen, N. Hanikel, M. I. Hossain, R. W. Flaig, X. Pei, A. Amin, M. D. Doherty, R. K. Impastato and T. G. Glover, *J. Am. Chem. Soc.*, 2022, **144**, 2387–2396.
- 91 R. W. Flaig, T. M. Osborn Popp, A. M. Fracaroli, E. A. Kapustin, M. J. Kalmutzki, R. M. Altamimi, F. Fathieh, J. A. Reimer and O. M. Yaghi, *J. Am. Chem. Soc.*, 2017, **139**, 12125–12128.
- 92 G. Lee and S. H. Jhung, *Fuel*, 2025, **394**, 135143.
- 93 K. Klemenčič, A. Krajnc, A. Puškarić, M. Huš, D. Marinič, B. Likozar, N. Z. Logar and M. Mazaj, *Angew. Chem.*, 2025, **137**, e202424747.
- 94 W. Song, Y. Wen, Y. Cho, X. Zhang, D. Kang, E. Shin, D. G. Yu, G. Li, Y. Liao and I. D. Kim, *Adv. Mater.*, 2025, e13138.
- 95 K. Patra, S. Dey, C. Solanki, A. Sengupta and V. K. Mittal, *ACS Appl. Eng. Mater.*, 2025, **3**, 1130–1165.
- 96 J. He, D. Wen, Y. Wang, Y. Qian, J. Guo, Z. Yun and W. Yang, *Appl. Catal., A*, 2025, **708**, 120604.
- 97 Y. Wu, Y. Wu, Y. Sun, W. Zhao and L. Wang, *Adv. Mater.*, 2024, **36**, 2312460.
- 98 A. K. Sekizkardes, P. Wang, J. Hoffman, S. Budhathoki and D. Hopkinson, *Mater. Adv.*, 2022, **3**, 6668–6686.
- 99 M. G. Kotp, M. G. Mohamed and S.-W. Kuo, *Chem. Sci.*, 2025, **16**, 20718–20754.
- 100 M. G. Kotp and S.-W. Kuo, *Electrochim. Acta*, 2025, **531**, 146440.
- 101 M. G. Kotp, I. M. Minisy, B. Al-Saida and S.-W. Kuo, *Carbohydr. Polym.*, 2025, **356**, 123399.
- 102 M. G. Kotp, N. L. Torad, J. Lüder, A. El-Amir, W. Chaikittisilp, Y. Yamauchi and A. F. M. EL-Mahdy, *J. Mater. Chem. A*, 2023, **11**, 764–774.
- 103 M. G. Mohamed, C.-C. Chen and S.-W. Kuo, *React. Funct. Polym.*, 2025, **214**, 106286.
- 104 M. G. Mohamed, A. F. M. EL-Mahdy, M. G. Kotp and S.-W. Kuo, *Mater. Adv.*, 2022, **3**, 707–733.
- 105 A. F. M. EL-Mahdy, C.-H. Kuo, A. Alshehri, C. Young, Y. Yamauchi, J. Kim and S.-W. Kuo, *J. Mater. Chem. A*, 2018, **6**, 19532–19541.
- 106 A. F. M. EL-Mahdy, C. Young, J. Kim, J. You, Y. Yamauchi and S.-W. Kuo, *ACS Appl. Mater. Interfaces*, 2019, **11**, 9343–9354.
- 107 M. G. Mohamed, E. C. Atayde Jr, B. M. Matsagar, J. Na, Y. Yamauchi, K. C.-W. Wu and S.-W. Kuo, *J. Taiwan Inst. Chem. Eng.*, 2020, **112**, 180–192.
- 108 A. F. EL-Mahdy, Y.-H. Hung, T. H. Mansoure, H.-H. Yu, Y.-S. Hsu, K. C. Wu and S.-W. Kuo, *J. Taiwan Inst. Chem. Eng.*, 2019, **103**, 199–208.
- 109 M. E. Tohidi and A. Amiri, *Adv. Mater.*, 2025, **38**, e11083.
- 110 C. Qian and X. Zhao, *Acc. Chem. Res.*, 2025, **58**, 1192–1209.
- 111 L. Yang, H. Yang, H. Wu, L. Zhang, H. Ma, Y. Liu, Y. Wu, Y. Ren, X. Wu and Z. Jiang, *J. Mater. Chem. A*, 2021, **9**, 12636–12643.
- 112 Y.-C. Kao, K.-T. Yeh, M. G. Mohamed, H. Karim, W.-H. Su and S.-W. Kuo, *Sep. Purif. Technol.*, 2025, **375**, 133827.
- 113 F. Zhao, F. Xu, H. García and J. Yu, *J. Colloid Interface Sci.*, 2025, **700**, 138532.
- 114 H. Daglar, Z. Zhou, R. Zhu, P. Parihar, J. I. Siepmann, O. M. Yaghi and L. Gagliardi, *J. Am. Chem. Soc.*, 2025, **1**, 1614–1622.
- 115 Z. Zhou, T. Ma, H. Zhang, S. Chheda, H. Li, K. Wang, S. Ehrling, R. Giovine, C. Li, A. H. Alawadhi, M. M. Abduljawad, M. O. Alawad, L. Gagliardi, J. Sauer and O. M. Yaghi, *Nature*, 2024, **635**, 96–101.
- 116 M. G. Kotp, A. M. Elewa, A. F. M. EL-Mahdy, H.-H. Chou and S.-W. Kuo, *ACS Appl. Energy Mater.*, 2021, **4**, 13140–13151.
- 117 Y. W. Ahmed, A. Loukanov and H. C. Tsai, *Adv. Healthcare Mater.*, 2025, **14**, 2403743.
- 118 M. G. Mohamed, C.-C. Chen, M. Ibrahim, A. Osama Mousa, M. H. Elsayed, Y. Ye and S.-W. Kuo, *JACS Au*, 2024, **4**, 3593–3605.
- 119 Y. Jia, Y. Lu, H. Yang, Y. Chen, F. Hillman, K. Wang, C. Z. Liang and S. Zhang, *Adv. Funct. Mater.*, 2024, **34**, 2407499.



- 120 B. Chai, S. Wang, Z. Li, Y. Jiang, X. Liu, M. Cui, X. Yu, Y. Xu, Y. Lei and L. Zhao, *Fuel*, 2024, **369**, 131776.
- 121 Y. Ren, S. Yang and Y. Xu, *Acc. Chem. Res.*, 2025, **58**, 474–487.
- 122 C. Lin, P. Feng, P. Geng, S. Zhang, Y. Chen, Y. Shen and Y. Zheng, *Chem. Commun.*, 2025, **61**, 16354–16371.
- 123 Y. Chen, X. Hu, J. Guo, Z. Guo, H. Zhan and S. Du, *Eur. Polym. J.*, 2022, **171**, 111215.
- 124 T. Guo, J. Chen, Y. Zhang and A. H. Bedane, *Sep. Purif. Technol.*, 2025, **359**, 130794.
- 125 R. Kishan, P. Rani, S. Kumar and C. Nagaraja, *Energy Fuels*, 2025, **39**, 18586–18596.
- 126 A. K. Maharana, S. K. Sarkar, S. Mukherjee, R. Sarkar, G. Rambabu, K. Sugamata and S. Das, *J. Mater. Chem. A*, 2025, **13**, 11717–11731.
- 127 Q. Huang, Z. Zhan, R. Sun, J. Mu, B. Tan and C. Wu, *Angew. Chem.*, 2023, **135**, e202305500.
- 128 W. Song, Y. Wen, Z. Wang, H. Xu, Q. Liao, Y. Tang, D.-G. Yu and I. Kim, *Langmuir*, 2024, **40**, 16670–16689.
- 129 M.-C. Lin, S.-W. Kuo and M. G. Mohamed, *Mater. Adv.*, 2024, **5**, 6222–6233.
- 130 Y. Zhao, Y. Hu, Y. Ma, L. Ding, S. Zhang, Y. Fu and X. Wang, *Appl. Surf. Sci.*, 2025, **685**, 161963.
- 131 M. Ejaz, M. G. Mohamed, Y.-T. Chen, K. Zhang and S.-W. Kuo, *J. Energy Storage*, 2024, **78**, 110166.
- 132 Y. Gu, S. U. Son, T. Li and B. Tan, *Adv. Funct. Mater.*, 2021, **31**, 2008265.
- 133 S. Ullah, J. Hu, S. Manzoor and B. Tan, *J. Mater. Chem. A*, 2025, **13**, 35082–35112.
- 134 S. Krishnan and C. V. Suneesh, *Mater. Today Commun.*, 2021, **27**, 102251.
- 135 H. Ouyang, K. Song, J. Du, Z. Zhan and B. Tan, *Chem. Eng. J.*, 2022, **431**, 134326.
- 136 Y. Alemin, J. Hu, P. Xie, X. Wang, H. Gao and B. Tan, *Macromol. Rapid Commun.*, 2025, **46**, 2500020.
- 137 P. Liu, F. Zhao, Z. Xu, Q. Liao, C. Yang, X. Hu, P. Chen and T. Zhao, *ACS Sustain. Chem. Eng.*, 2025, **13**, 9903–9912.
- 138 Y. Tian, F. Cui, Z. Bian, X. Tao, H. Wang, N. Zhang and G. Zhu, *Acc. Chem. Res.*, 2024, **57**, 2130–2143.
- 139 M. Li, H. Ren, F. Sun, Y. Tian, Y. Zhu, J. Li, X. Mu, J. Xu, F. Deng and G. Zhu, *Adv. Mater.*, 2018, **30**, 1804169.
- 140 H. Ali, Y. Orooji, A. Y. A. Alzahrani, H. M. Hassan, Z. Ajmal, D. Yue and A. Hayat, *ACS Nano*, 2025, **19**, 7482–7545.
- 141 T. Ben, Y. Li, L. Zhu, D. Zhang, D. Cao, Z. Xiang, X. Yao and S. Qiu, *Energy Environ. Sci.*, 2012, **5**, 8370–8376.
- 142 T. Ben, C. Pei, D. Zhang, J. Xu, F. Deng, X. Jing and S. Qiu, *Energy Environ. Sci.*, 2011, **4**, 3991–3999.
- 143 S. Zhang, J. Li, J. Liu, S. Jiang, X. Chen, H. Ren, T. X. Liu, X. Zou and G. Zhu, *J. Membr. Sci.*, 2021, **632**, 119372.
- 144 N. B. McKeown, *Curr. Opin. Chem. Eng.*, 2022, **36**, 100785.
- 145 T. H. Lee, P. A. Dean, J. Y. Yeo and Z. P. Smith, *Adv. Mater.*, 2025, e13892.
- 146 K. M. Rodriguez, F. M. Benedetti, N. Roy, A. X. Wu and Z. P. Smith, *J. Mater. Chem. A*, 2021, **9**, 23631–23642.
- 147 Z. Zhong, X. Wang and B. Tan, *Chem.–Eur. J.*, 2025, **31**, e202404089.
- 148 S. Fajal, S. Dutta and S. K. Ghosh, *Mater. Horiz.*, 2023, **10**, 4083–4138.
- 149 D. Luo, M. Li, Q. Ma, G. Wen, H. Dou, B. Ren, Y. Liu, X. Wang, L. Shui and Z. Chen, *Chem. Soc. Rev.*, 2022, **51**, 2917–2938.
- 150 V. Guillermin and M. Eddaoudi, *Acc. Chem. Res.*, 2021, **54**, 3298–3312.
- 151 Y. Zhi, J. Shao, C. Liu, Q. Xiao, M. Demir, M. K. Al Mesfer, M. Danish, L. Wang and X. Hu, *Sep. Purif. Technol.*, 2025, **361**, 131253.
- 152 Q. Liao, Y. Yuan and J. Cao, *J. Colloid Interface Sci.*, 2024, **665**, 958–968.
- 153 M. He, H. Zhao, J. Jia, W. Zhou, Z. Wang, K. An, Y. Jiao, X. Yang, X. Zhang and T. Fan, *Environ. Res.*, 2025, **267**, 120701.
- 154 X. Yang, N. Zhou, X. Xie, Z. Dai, B. T. Goh, Z. Chen and Y. Xiong, *Sep. Purif. Technol.*, 2025, **361**, 131257.
- 155 Y. Jeong, Y. Kim, W. Jeong, H. L. Choi, J. Kim and T.-H. Bae, *J. Membr. Sci.*, 2025, **738**, 124749.
- 156 B. Ray, S. R. Churipard and S. C. Peter, *J. Mater. Chem. A*, 2021, **9**, 26498–26527.
- 157 L. Yang, Y. Sheng and D. Liu, *Dalton Trans.*, 2026, **55**, 1515–1547.
- 158 C. Zhang, S. Sun, S. Xu and C. Wu, *Biomass Bioenergy*, 2022, **166**, 106608.
- 159 S. Wang, X. Qiu, Y. Chen and S. Chen, *Microporous Mesoporous Mater.*, 2022, **330**, 111585.
- 160 A. Kuang, M. Kuang, H. Yuan, G. Wang, H. Chen and X. Yang, *Appl. Surf. Sci.*, 2017, **410**, 505–512.
- 161 N. MacDowell, N. Florin, A. Buchard, J. Hallett, A. Galindo, G. Jackson, C. S. Adjiman, C. K. Williams, N. Shah and P. Fennell, *Energy Environ. Sci.*, 2010, **3**, 1645–1669.
- 162 P. Bollini, S. Choi, J. H. Drese and C. W. Jones, *Energy Fuel*, 2011, **25**, 2416–2425.
- 163 J. S. Carneiro, G. Innocenti, H. J. Moon, Y. Guta, L. Proaño, C. Sievers, M. A. Sakwa-Novak, E. W. Ping and C. W. Jones, *Angew. Chem., Int. Ed.*, 2023, **62**, e202302887.
- 164 S. S. Hamid, L. Kerber and A. B. Clarke, *Nat. Commun.*, 2025, **16**, 8923.
- 165 M. Debruyne, V. Van Speybroeck, P. Van Der Voort and C. V. Stevens, *Green Chem.*, 2021, **23**, 7361–7434.
- 166 W. Zhang, G. Li, H. Yin, K. Zhao, H. Zhao and T. An, *Environ. Sci.: Nano*, 2022, **9**, 81–104.
- 167 Y. Ran, K. Peng, Z. Li, X. Guo, H. Chen, S. Cai, L. Su, M. Niu, D. Lu and H. Wang, *Chem. Eng. J.*, 2025, **514**, 163149.
- 168 M. A. Elsayed, S. Zhou, X. Zhao, G. W. Manggada, Z. Chen, F. Wang and Z. Tang, *Nanomaterials*, 2025, **15**, 1077.
- 169 S. Podder, H. Jungi and J. Mitra, *Chem.–Eur. J.*, 2025, **31**, e202500865.
- 170 Y.-C. Su, G. Chen, Y.-J. Lai, G.-Z. Song, T.-L. Wu and Y.-C. Yeh, *Chem. Soc. Rev.*, 2026, **55**, 819–868.
- 171 S. A. Bedell, *Energy Procedia*, 2009, **1**, 771–778.
- 172 A. P. Hallenbeck and J. R. Kitchin, *Ind. Eng. Chem. Res.*, 2013, **52**, 10788–10794.
- 173 S. I. Matsumoto, Y. Ikeda, H. Suzuki, M. Ogai and N. Miyoshi, *Appl. Catal., B*, 2000, **25**, 115–124.



- 174 M. Gómez-García, V. Pitchon and A. Kiennemann, *Environ. Int.*, 2005, **31**, 445–467.
- 175 Z.-X. Low, P. M. Budd, N. B. McKeown and D. A. Patterson, *Chem. Rev.*, 2018, **118**, 5871–5911.
- 176 D. Cangialosi, V. M. Boucher, A. Alegría and J. Colmenero, *Soft Matter*, 2013, **9**, 8619–8630.
- 177 M. Meier, E. John, D. Wieckhusen, W. Wirth and W. Peukert, *Powder Technol.*, 2009, **188**, 301–313.
- 178 X. Lin, S. Kim, M. Abdallah and R. J. Farrauto, *Appl. Catal., A*, 2025, **709**, 120659.
- 179 R. Bonné, Industrial Production Of Porous Materials, in *Handbook of Porous Materials*, World Scientific, 2020.
- 180 Y. Zhi, J. Shao, J. Wang, X. Liu, Q. Xiao, M. Demir, U. B. Simsek, L. Wang and X. Hu, *Molecules*, 2025, **30**, 3990.
- 181 J. Shao, Y. Wang, M. Che, Q. Xiao, M. Demir, M. K. Al Mesfer, L. Wang, X. Hu and Y. Liu, *J. Energy Inst.*, 2025, 102273.
- 182 J. Wang, Y. Wang, X. Liu, Q. Xiao, M. Demir, M. K. Almesfer, S. G. Colak, L. Wang, X. Hu and Y. Liu, *Molecules*, 2025, **30**, 2564.

